

**MAY 24, 1999**

# **WIRE ANOMALY INVESTIGATION REPORT**

**This report documents the results of the JPL Team investigation into the loss of the WIRE Science Mission**

**A. Acord  
J. Clawson  
J. Kievit, JPL Retired  
M. Landano  
G. Macala  
T. Nguyen (ad-hoc circuit specialist)  
R. Ross  
D. Swenson  
M. Underwood**

## JPL WIRE ANOMALY INVESTIGATION REPORT OUTLINE

- I) Executive Summary
- II) WIRE Anomaly Summary
- III) Team Charter
- IV) Description Overview
- V) Identification of possible causes (functional and fish-bone diagram)
- VI) Ground/Flight key data analysis
  - Timeline overview, including FLT/GND command timing
  - Attitude control position/rate data, etc.
  - Cryostat/thermal data
  - Power bus current, pyro monitor data
  - Qualification Verification
  - Functional Verification
- VII) Troubleshooting analyses and test results
- VIII) Conclusions
- IX) Primary and contributory causes
- X) Causes/Lessons Learned/corrective actions

## Acknowledgment

The cooperation and effort by the WIRE Project Management and the Engineering staff at GSFC, JPL and SDL were essential to the timely understanding of the anomaly. The entire management and staff were open and forthcoming in providing design and process information that greatly aided this investigation.

## EXECUTIVE SUMMARY

I.) The conclusions of the WIRE Anomaly Board are:

- Premature cover ejection was the cause of the Mission failure.
- Premature cover ejection was due to faulty pyro electronics design.
- Excessive Sun/Earth heating into the telescope caused excessive solid hydrogen "boil-off".
- Venting due to "boil-off" exceeded the capability of the S/C attitude control system to maintain attitude causing total loss of the science mission.
- JPL Management/Development Team did not penetrate the electronic design of the pyro electronics box.

II.) The WIRE anomaly board presents the following findings:

- The pyro design did not appropriately consider power turn-on transient effects (See Figures 6 and 7).
- Fault containment was not adequately considered.
- Detailed reviews were not held for the pyro electronics.
- No end-to-end pyro functional test was performed in full flight configuration with the flight mission sequence and effective pyro device simulation.
- Testing to find anomalous pyro box operational behavior was ineffective due to the deficiencies of test configurations and instrumentation.

- There was no design requirement for explicit, real-time telemetry for important, irreversible functions.
- There was little early consideration for the Attitude Control System (ACS) to handle worst-case venting torques. ACS did not have control authority to handle worst case torques.
- A factor of 100 error was made in the late-performed analysis which incorrectly showed the attitude control could handle worst-case venting torques.
- The design of the cryo tank vent outlet was insufficient to ensure torque balance in a worst case venting situation. These characteristics prevented timely control of spacecraft attitude subsequent to the anomaly, and essentially prevented any possible productive efforts to save the mission.

III.) These problems could have been mitigated by:

- Holding a detailed peer review of the pyro electronics design.
- Employing power turn-on transient timed lock-out circuitry or independent, separate inhibits in each pyro interface.
- Using an effective pyro energy monitor in the ground support equipment rather than one ohm resistors to simulate the pyro squib.
- Testing in the end-to-end flight configuration using a "hard" power source (battery) with relay switch to accomplish turn-on of the pyro electronics and use of flight mission sequence.
- Early review of the system design considering both expected and potentially catastrophic worst-case operational scenarios.

## WIRE ANOMALY SUMMARY

The primary cause of the WIRE instrument failure was the premature ejection of the instrument aperture cover prior to spacecraft attitude stabilization following venting. The early ejection of the cover caused continuous venting of the solid hydrogen due to large Sun/Earth heat loads into the instrument. The rapid venting maintained a high torque that prevented the spacecraft attitude control system from stabilizing the S/C attitude until venting completed and mission was lost.

A large number of failure scenarios were evaluated to determine the root cause of the cover ejection encompassing prelaunch, launch, powered flight, separation, software, operations, design and component reliability faults. Based on comprehensive, systematic review of data, it was determined the cover was most likely ejected at the time the WIRE Pyro Electronics box was turned on due to a transient condition that exists in the pyro electronics during startup. This transient condition is the direct result of the non-deterministic initialization of a Field-Programmable Gate Array (FPGA) that controls both the arming and firing circuits in the pyro electronics.

Although some design attention was given to the startup behavior of the FPGA, the design contained un-analyzed idiosyncrasies that triggered the cover ejection. The system design did not contain sufficient start-up lock-out protection or independent provisions to prevent the FPGA startup operation from propagating to the firing circuits.

The project did not hold a detailed peer review of the pyro electronics. At the time of the instrument electronics review, the pyro electronics was not yet designed and no further review was held.

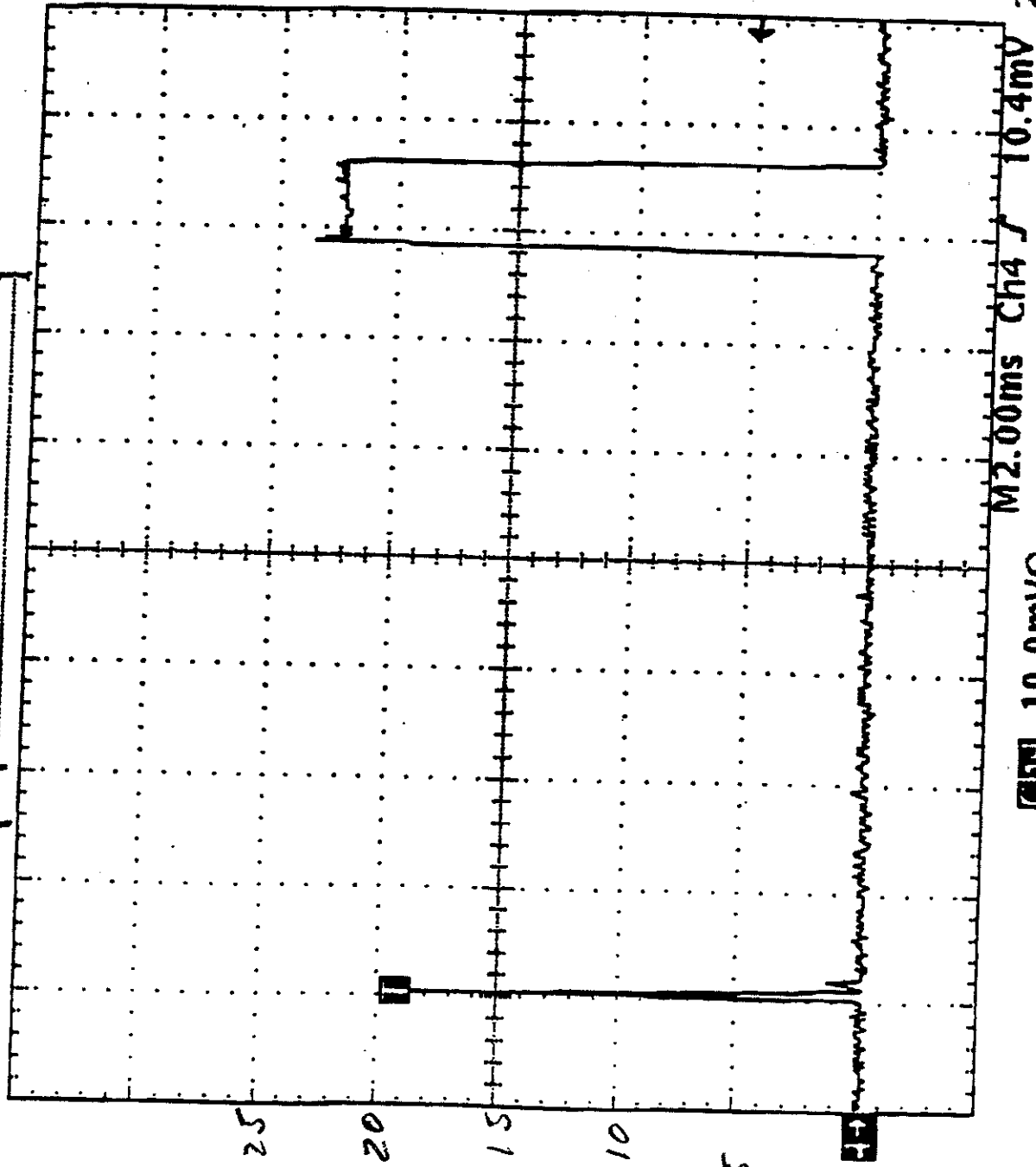
The anomalous characteristics of the pyro electronics unit were not detected during subsystem or system functional testing due to the limited fidelity and detection capabilities of the electrical ground support equipment. Circuit analyses have predicted the existence of the anomaly and it has been confidently reproduced using engineering model hardware. The capability of the startup phenomena to cause the cover ejection could have been exacerbated by feedback of transients caused by actual pyro firing to the electronics.

A major contributor to the WIRE failure was the failure of the JPL development/management team to penetrate the electronic design of the pyro electronics box. While it appears that the design was completed late, and that there was little time for its implementation does not excuse the lack of technical attention, either at a peer review or other reviews JPL had with its contractor. It is also not clear that an existing, flight proven design was sought in lieu of the implementation that was eventually flown. It is the JPL Anomaly Team's assessment that a peer review, held by appropriately knowledgeable people would have identified the turn-on characteristic which led to the failure.

## WIRE ANOMALY SUMMARY (Cont'd)

It is pointed out that while flight telemetry data electronic analyses and test all point to cover ejection immediately prior to secondary vent firing, analysis of the cryostat suggests the cover may have come off much earlier. Based on vent blow down analysis (see R. Ross' inputs), the predicted time of cover ejection could have occurred approximately 1450 sec prior to secondary event opening, corresponding to a time near spacecraft-launch vehicle separation. However, because of uncertainty in the thrust vector direction and behavior of venting gas due to the partially blocked thrust neutralizer, this ejection time must be viewed with a critical eye and be interpreted within the total body of evidence. No credible opportunity was found to exist for cover ejection prior to the time of pyro box power application. It is important to note uncertainty in cover ejection time, based on cryostat analyses does not in any way alter the conclusion that cover ejection occurred at pyro electronics first power turn-on.

Tek Stopped: 3 Acquisitions



5A/DIV  
A SIDE POWER  
INPUT - ETU  
PYRO BOX

26 Apr 1999  
14:21:57

Figure 7 ETU TRANSIENT

**JET PROPULSION LABORATORY**

**INTEROFFICE MEMORANDUM**

March 5, 1999

**TO:** Charles Elachi  
**FROM:** Larry Dumas  
**SUBJECT:** Formation of Review Board for the Wide-Field Infrared Explorer (WIRE) Anomaly of March 4/5, 1999  
**REFERENCE:** JPL Policy: Special Review Boards; Dated: October 14, 1996

In accordance with the reference JPL Policy, a Review Board for the WIRE anomaly experienced on March 4-5, 1999 is appointed.

The JPL members of the review board are:

Matthew Landano, Chairman  
Glenn Macala, S/C Attitude Control/Dynamics  
James Clawson, Mission Assurance  
David Swenson, SESPD Chief, Secretary

Mark Underwood, Power/Pyro  
John Kievit, JPL Retired, Devices  
Arden Acord, ATLO  
Ronald Ross, Cryo

The Review Board will:

Determine the root cause of the anomaly and identify steps that should be taken in the future to prevent similar occurrences.

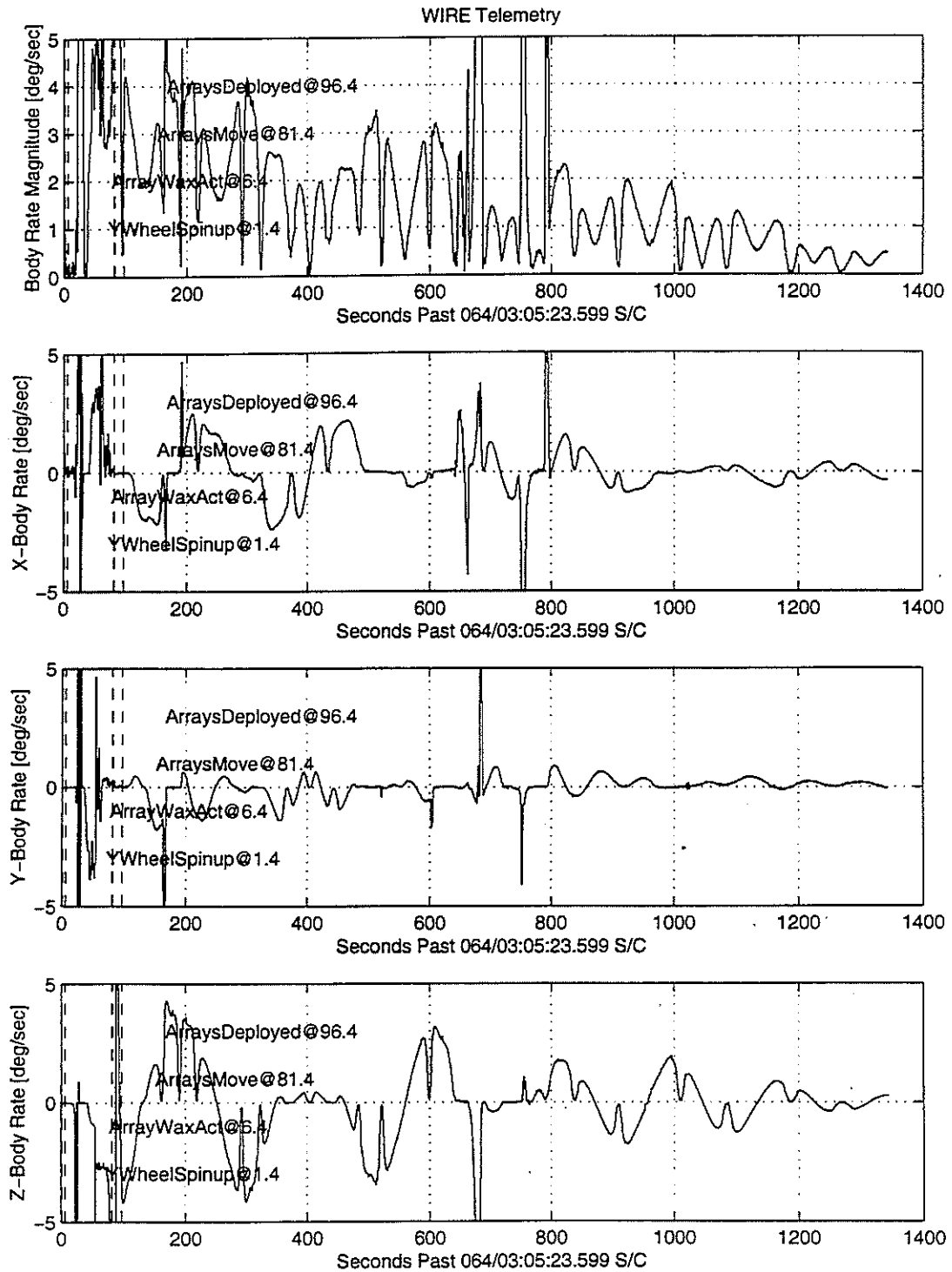
The review board is instructed to begin operation on March 8, 1999. The board should focus on the root cause of the problem as a first priority. Other aspects of the review should be worked in parallel only to the extent necessary to support the root cause conclusions. The review board report should be completed by June 8.

The WIRE Project is part of the Small Explorer Program Office at the Goddard Space Flight Center (GSFC) and the mission is being conducted at GSFC. It is important that the JPL Review Board interact and support any GSFC activities being conducted in relation to the WIRE anomaly.

cc:  
M. Devirian  
A. Diaz, GSFC  
T. Gavin  
R. Ploszaj  
E. Stone  
W. Townsend, GSFC  
W. Weber  
Review Board

The sun sensor data was processed in a variety of ways in an attempt to extract S/C rate. Due to the coarseness of the data, telemetry dropouts, and various other operational aspects of the sun sensors, the resulting rates are very noisy and contain many artifacts that are not believed to truly indicate rates. Figure 4.B.2 shows a representative set of derived S/C angular rates expressed in S/C body coordinates. The time span covered here is also from S/C separation until just prior to pyro box turn on.

The top plot in the figure shows the magnitude of the total rate vector. One can see that the initial tip-off rates and y-axis wheel spin-up caused about a 3 to 4 deg/sec tumble. However, the rates were slowly being damped out over this time period.

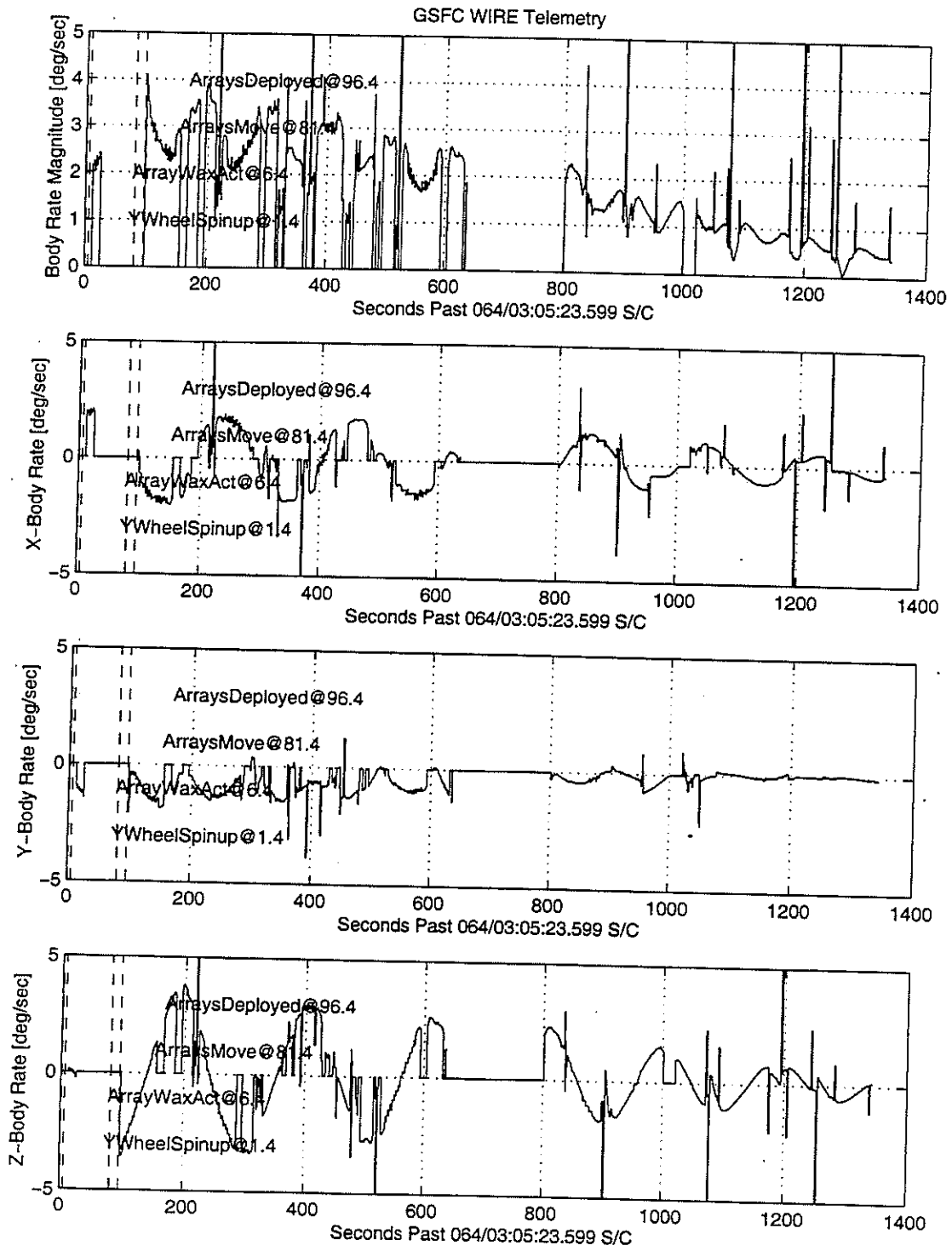


G.A. Macala 30-Apr-1999, 10:23

Figure 4.B.2 Sun Sensor Derived S/C Angular Rates

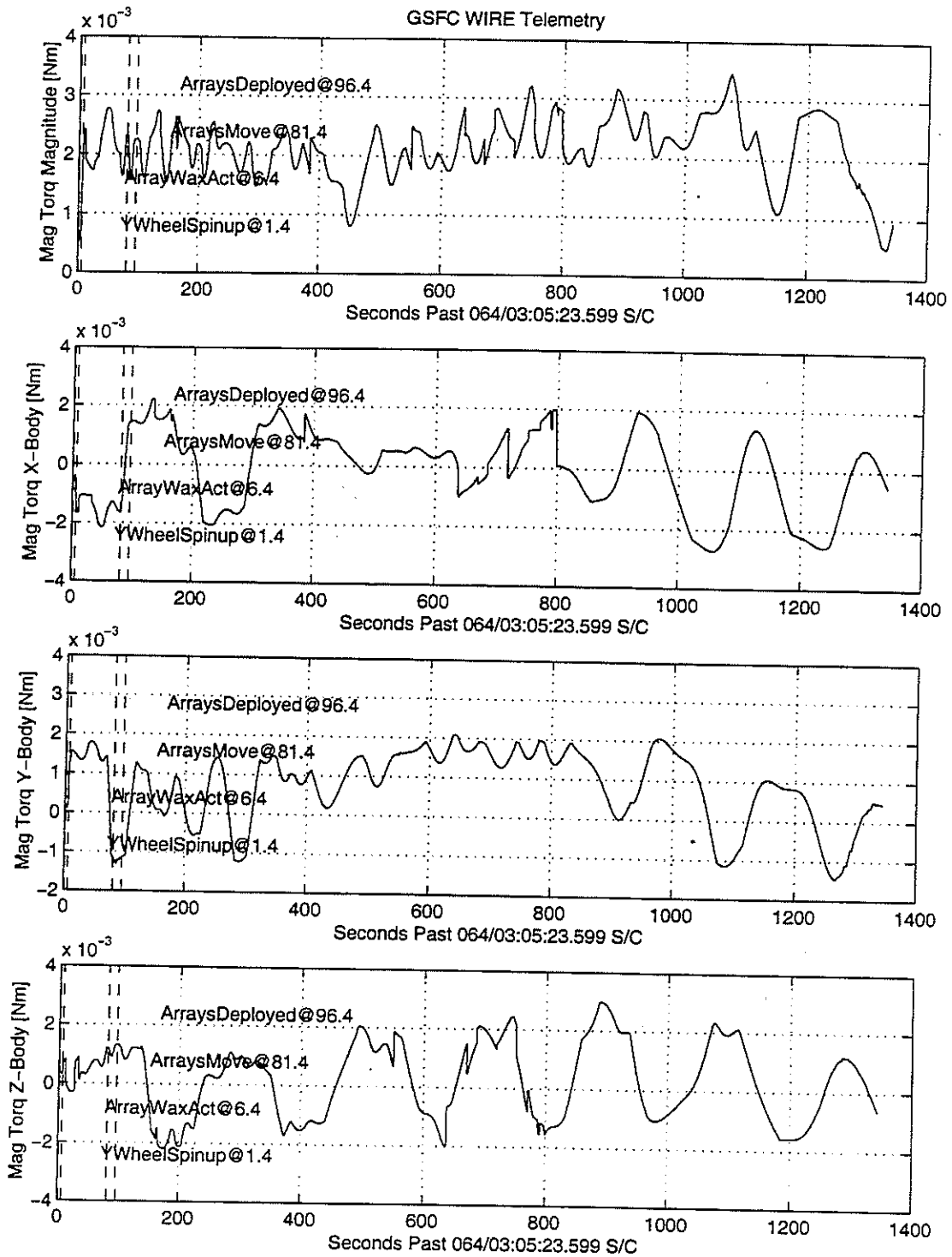
The coarse sun sensor, fine sun sensor, magnetometer, and magnetorquer outputs were processed at Goddard Space Flight Center by Tom Correll to remove "questionable" telemetry values. Figures 4.B.3 & 4 show the GSFC processed data for derived S/C angular rate and the values of the magnetic torque that the torque rods were applying to damp out the rates.

Note that the rates are very similar to those derived using the raw data from the coarse sun sensors. Also note from the signs of the magnetic torques that the magnetic torquers were applying torques opposing sensed rates. In other words, the control system was working as expected in reducing S/C rates.



G.A. Macala 30-Apr-1999, 10:15

Figure 4.B.3 GSFC Derived S/C Rates



G.A. Macala 30-Apr-1999, 10:09

Figure 4.B.4 Magnetic Torque Rod Applied Torques

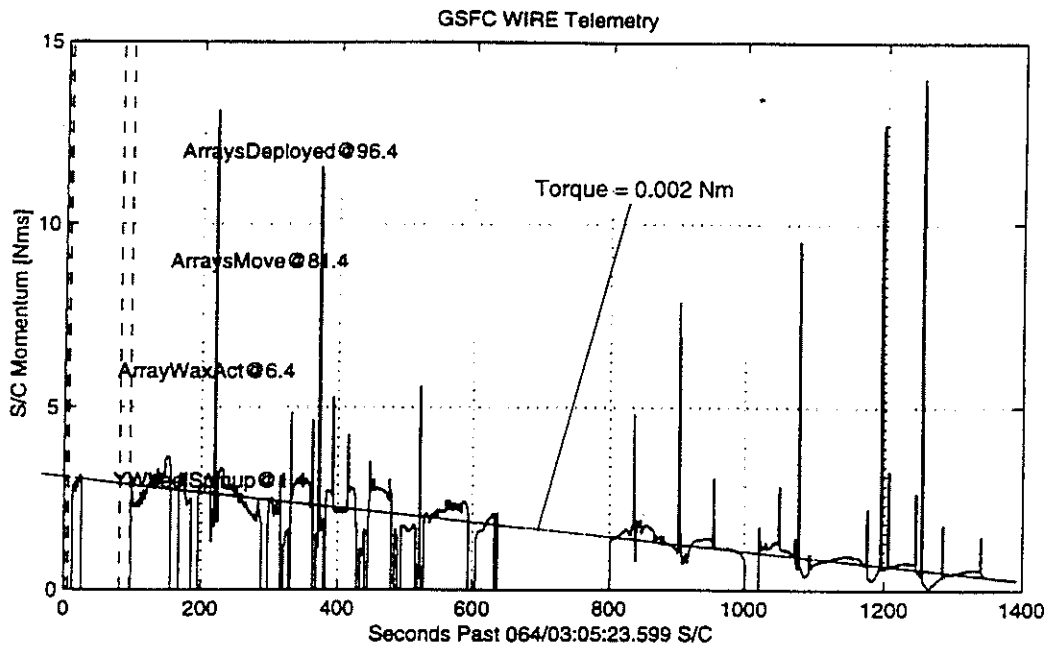
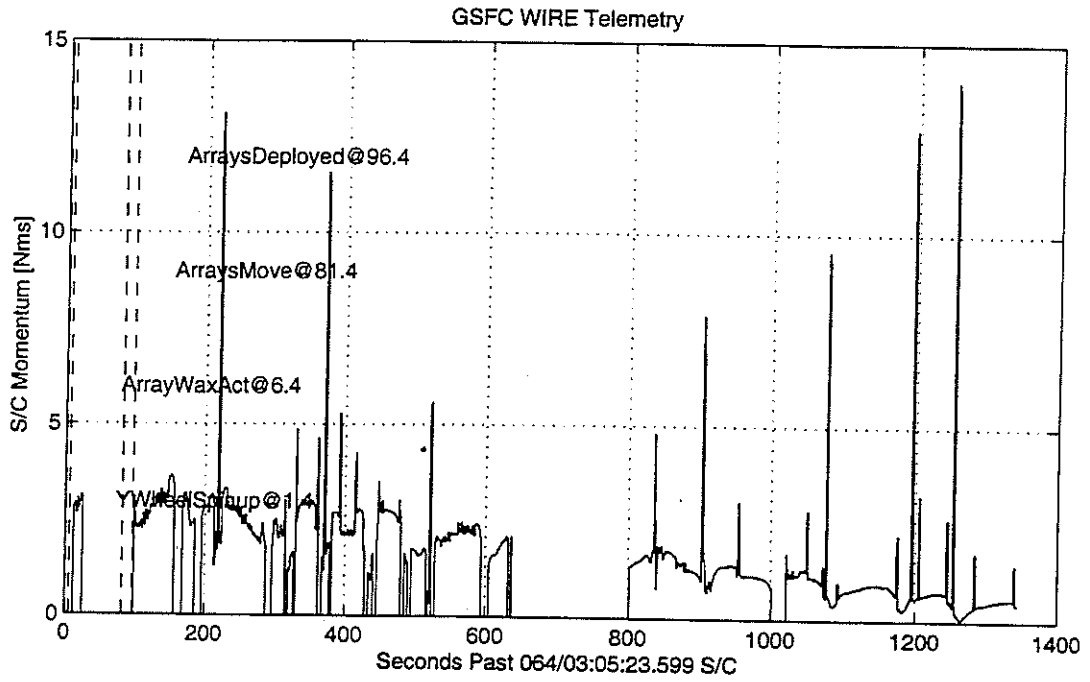
Figure 4.B.5 illustrates that S/C momentum was being driven to zero. The S/C rates derived by GSFC were multiplied by the S/C inertia tensor to provide S/C momentum:

$$H = I \omega$$

where  $I$  is the 3x3 inertia tensor, in this case approximated by using 75 kg-m<sup>2</sup> for the  $I_{xx}$  and  $I_{yy}$  terms and 35 kg-m<sup>2</sup> for the  $I_{zz}$  term, and  $\omega$  is the 3x1 angular rate vector. The products of inertia are assumed to be negligible. Also, for this purpose we ignore the contribution of the Y-axis momentum wheel which simply adds 1.8 Nms to the Y-axis direction.

The upper plot in the figure is the raw magnitude of  $H$  and the lower plot represents a filtered version using a 20<sup>th</sup> order moving average filter.

Note that  $H$  is reducing as expected. Also note that a straight line fit to the filtered data indicates that the slope of  $H$ ,  $dH/dt$ , which roughly corresponds to average applied torque, is approximately -0.001 Nm. This agrees roughly with the torque values seen in the previous figure and is about the capability of the magnetorquers.



Measured decay in spacecraft momentum due to torque rod operation after L/V separation.

G.A. Macala 30-Apr-1999, 10:16

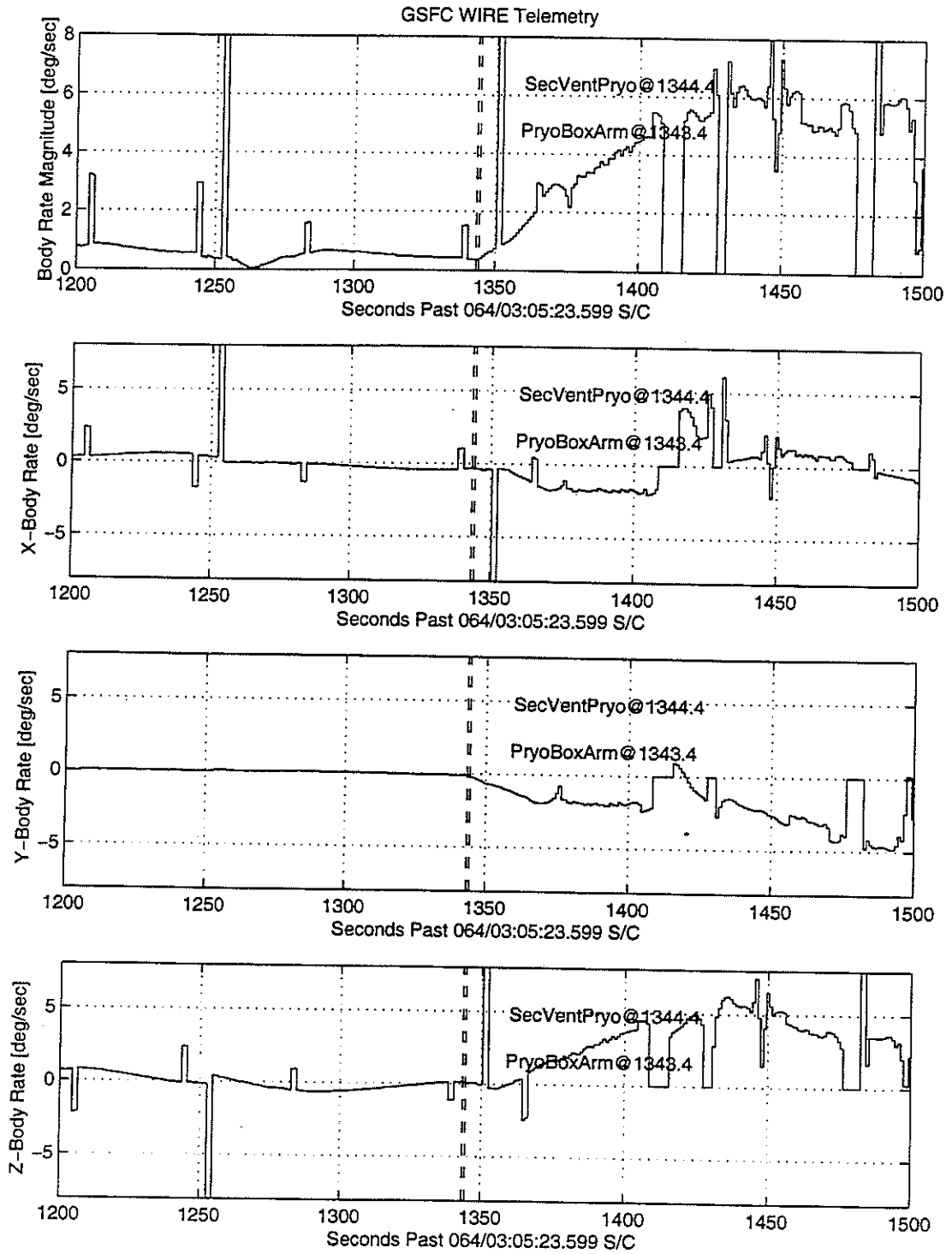
Figure 4.B.5 Derived Raw and Filtered S/C Momentum

### Rates and Torques at the "Event"

The telemetry evaluated so far seems to be nominal: the y-axis wheel is at its commanded rate; S/C tip-off rates have been damped to less than 1 deg/sec; all these events have taken place in the expected amount of time.

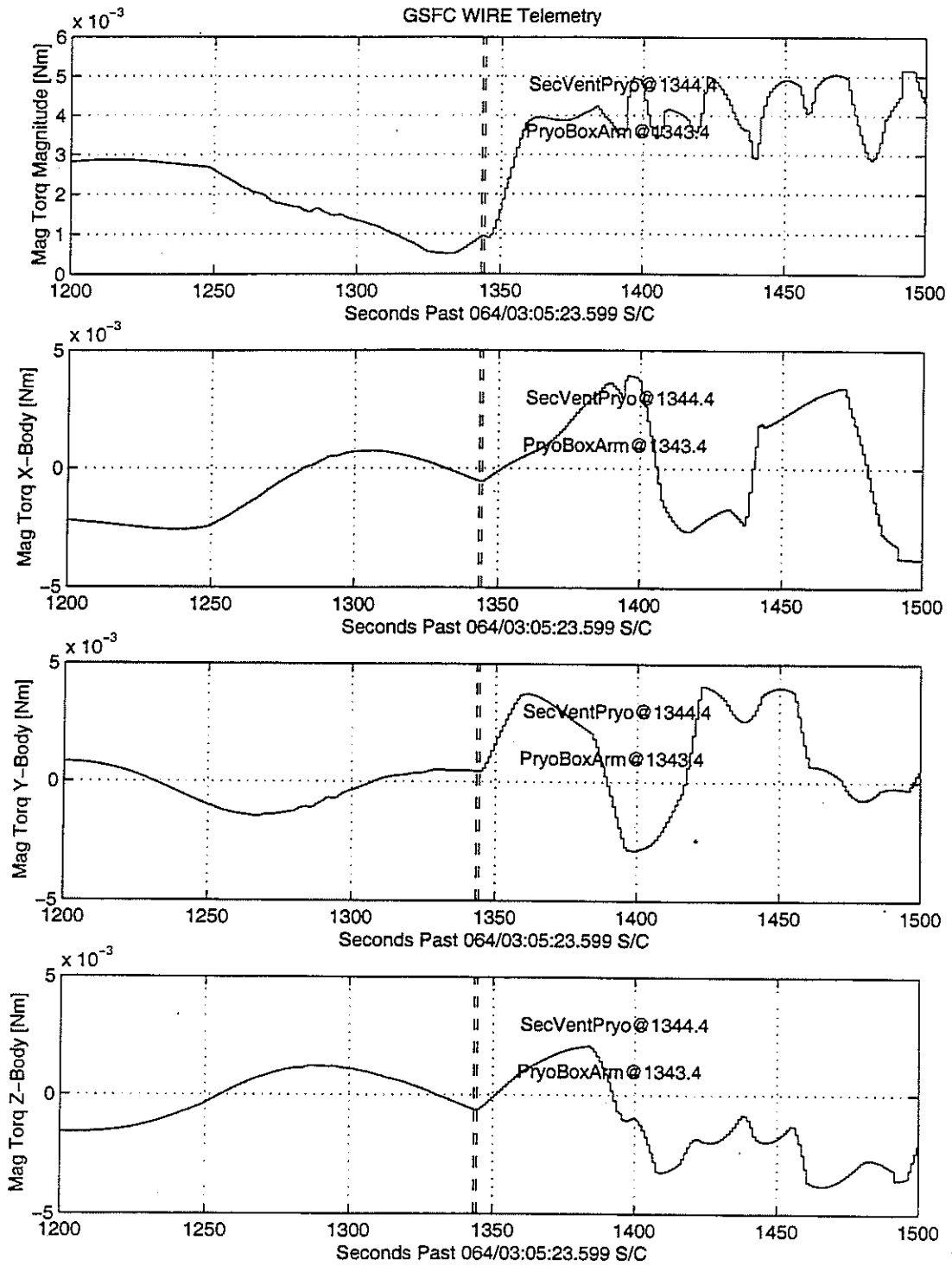
The next actions scheduled to take place were to power on the pyro electronics box and then fire the secondary hydrogen vent pyro. The expectation was that a "puff" of thrust would occur that could spin the S/C back up to about the rates experienced at tip-off from the launch vehicle. The magnetorquers would then despin the S/C again and ACS would proceed to place the S/C in a thermally safe attitude. A few days later, the pyros on the telescope cover would be fired and the cover would be ejected.

Figure 4.B.6 and Figure 4.B.7 show the derived S/C rates just before and just after the turn on of the pyro electronics box and the firing of the secondary vent pyro. Note that these events took place only 1 second apart.



G.A. Macala 30-Apr-1999, 14:27

Figure 4.B.6 GSFC Derived S/C Rates



G.A. Macala 30-Apr-1999, 14:27

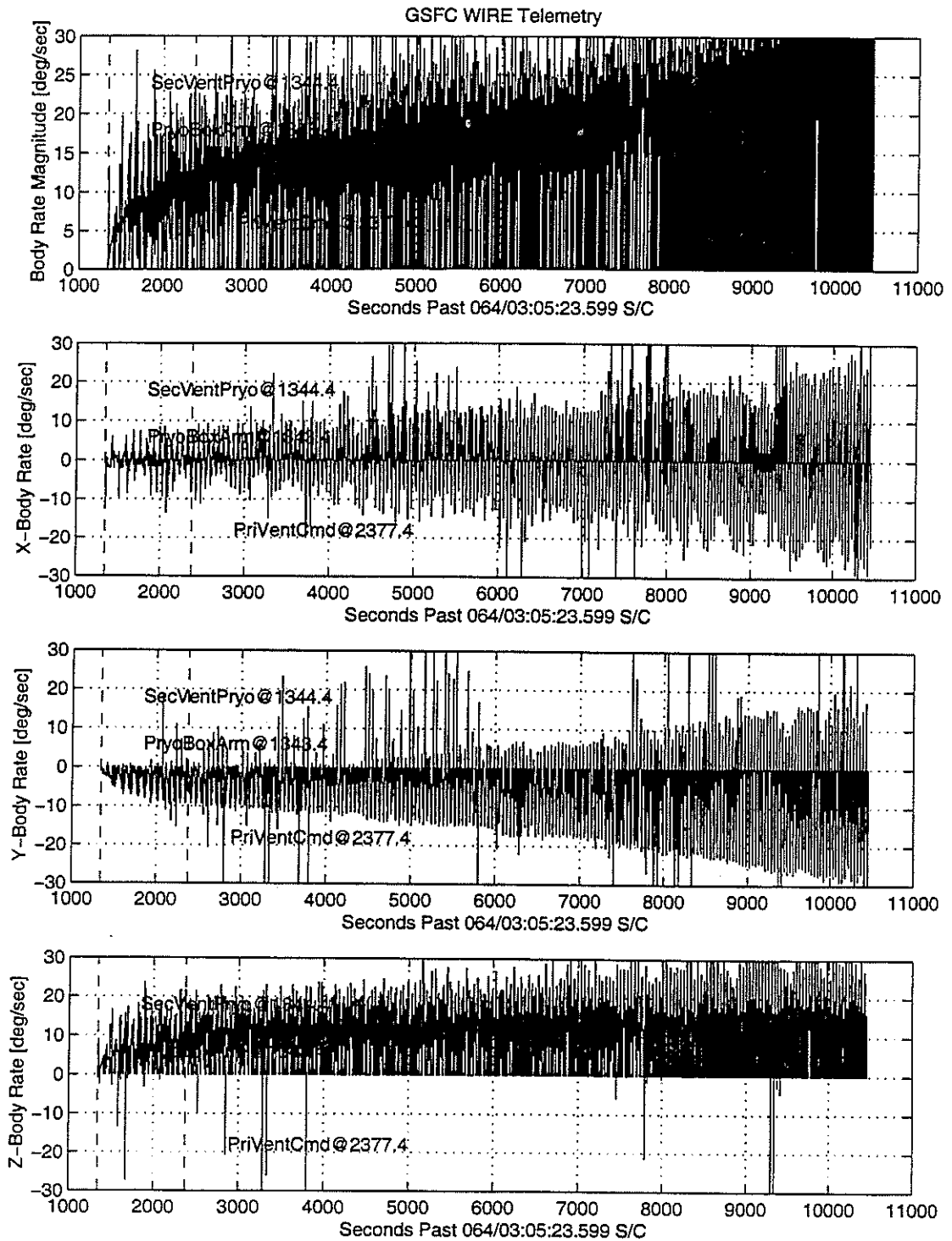
Figure 4.B.7 Magnetic Torque Rods Applied Torques

We see from the figures that a rate discontinuity does take place at the secondary vent pyro firing. This is consistent with the opening of the secondary hydrogen vent at that time. The magnetic torquer data also shows a discontinuity at that time. The torque rods are responding to a sensed change in rate. Experts at GSFC performed a more detailed look at the commanding and telemetry timeline. Their conclusion was that it is likely that the discontinuities seen in the data actually took place *after* pyro electronics box turn-on and *prior* to the command that fired the secondary hydrogen vent. Due to the complexity of the commanding system, telemetry collection and time tagging system, ground station timing and operations, we must trust their expert analysis on this matter. As far as our analysis is concerned, we can only say that we see an event at about the time of pyro electronics box turn-on and secondary hydrogen vent pyro firing.

The rate increases over a period of a few minutes to a level that is large enough to cause the magnetorquers to saturate while opposing the rates. This is expected behavior. What happens next was not expected.

#### Rates and Torques after the "Event"

After the initial rate increase subsided, S/C rates kept increasing but at a substantially lower rate of increase than at the "event". This was not nominal behavior. It was expected that the magnetorquers would once again reduce S/C rates to near zero over about an hour's time span. Instead, S/C rates kept rising. This is evidenced in the derived rate data shown in Figure 4.B.8.

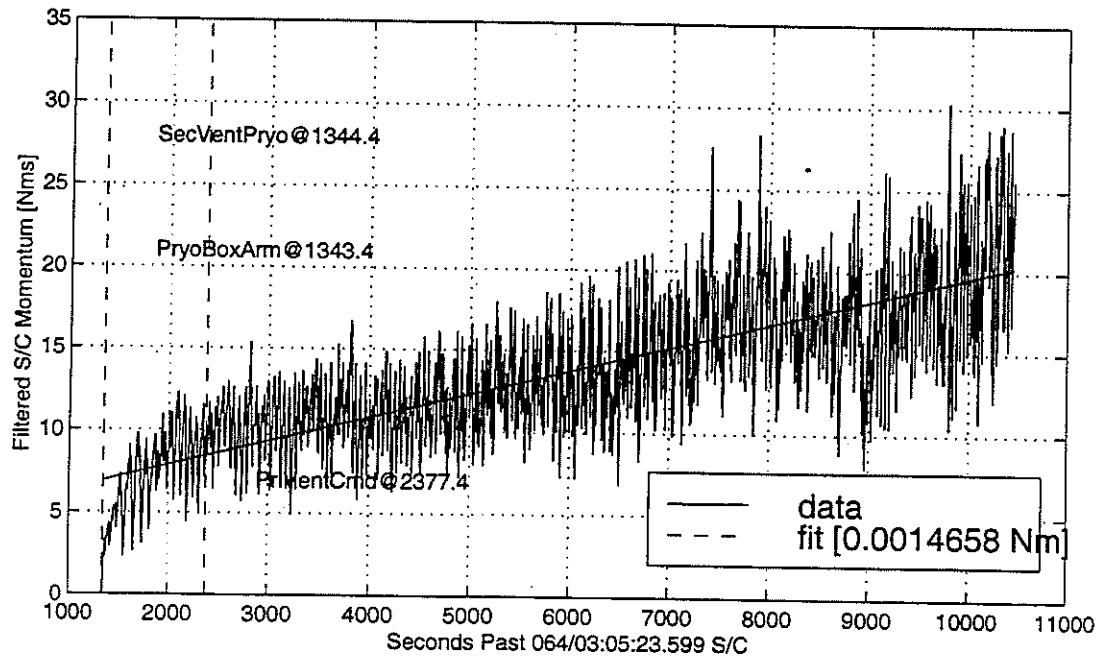
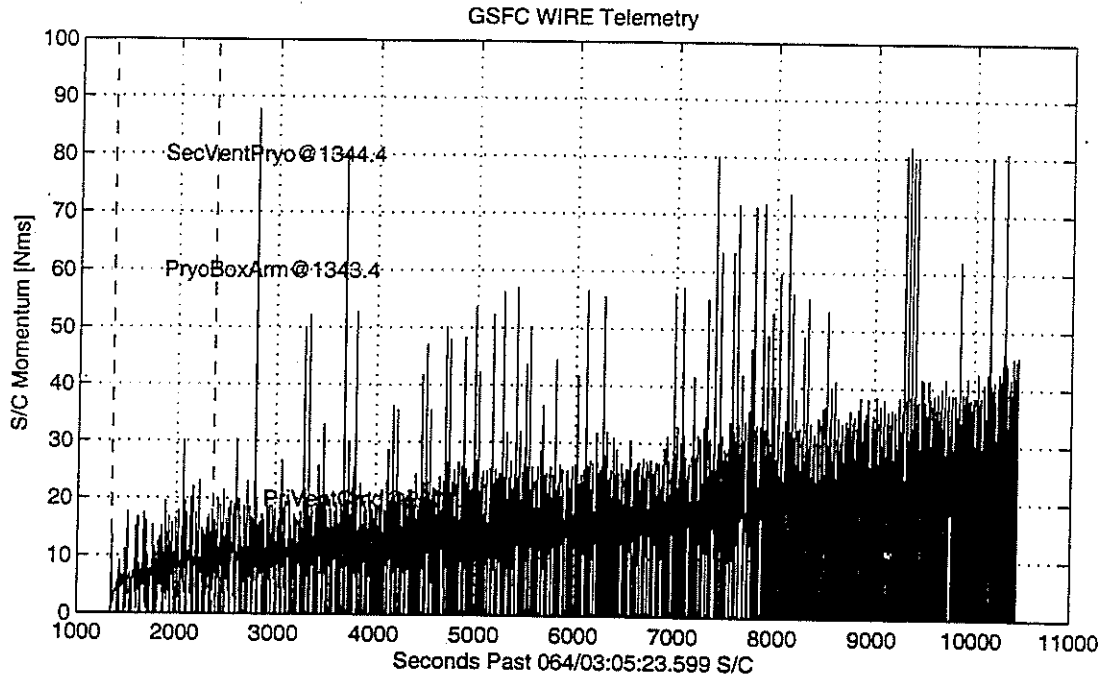


G.A. Macala 30-Apr-1999, 17:01

Figure 4.B.8 GSFC Derived S/C Angular Rates

Note that the derived data is extremely noisy, but the z-axis spin-up is apparent. The S/C momentum (Figure 4.B.9) shows this more clearly via filtering. Also, a straight line fit to the filtered data shows that a net positive torque of about 0.0015 Nm seems to be spinning the S/C up.

Although the flight team at GSFC performed several operational and software changes in an attempt to bring the S/C under control over this time period, the S/C spin-up continued for approximately 15 hours. The final spin rate of the S/C was about 60 rpm.



G.A. Macala 30-Apr-1999, 17:14

Figure 4.B.9 Derived S/C Momentum (Raw and Filtered)

## Simulation Results

For various reasons detailed elsewhere in this report, it seems clear now that the WIRE telescope cover was ejected prematurely. This resulted in a heat load into the cryostat that manifested itself in a much higher cryogen venting rate out of the secondary hydrogen vent. The vent exited to space in a nominal 0 net thrust configuration (T-vent). However, at these higher venting rates, it is speculated that a nominal net thrust will be present, especially if the flow in either direction encountered elements of the S/C (plume impingement). This net thrust was apparently high enough to overwhelm the ACS Magnetorquers and thus resulted in a spin-up of the S/C.

In order to study this possibility, a simulation of some of the relevant S/C dynamics was built, exercised, and tuned to match the flight data.

The total angular momentum for the S/C was written and then differentiated with respect to an inertial reference frame. An auxiliary equation was found by considering the y-wheel and its torque motor along with the y-axis of the S/C as an isolated system. Note that products of inertia were secondary effects for this simple analysis. The following equations of motion resulted.

$$\begin{bmatrix} T_x \\ T_y \\ T_z \\ T_{wheel} \end{bmatrix} = \begin{bmatrix} I_{xx} & 0 & 0 & 0 \\ 0 & I_{yy} + I_{wheel} & 0 & I_{wheel} \\ 0 & 0 & I_{zz} & 0 \\ 0 & I_{wheel} & 0 & I_{wheel} \end{bmatrix} \begin{bmatrix} \dot{\omega}_x \\ \dot{\omega}_y \\ \dot{\omega}_z \\ \dot{\omega}_{wheel} \end{bmatrix} + \begin{bmatrix} (I_{zz} - I_{yy})\omega_z\omega_y - I_{wheel}\omega_z(\omega_y + \omega_{wheel}) \\ (I_{xx} - I_{zz})\omega_z\omega_x \\ (I_{yy} - I_{xx})\omega_x\omega_y + I_{wheel}\omega_x(\omega_y + \omega_{wheel}) \\ 0 \end{bmatrix}$$

The following values were used for the inertias in these equations:

$$I_{xx} = 75kg - m^2$$

$$I_{yy} = 75kg - m^2$$

$$I_{zz} = 35kg - m^2$$

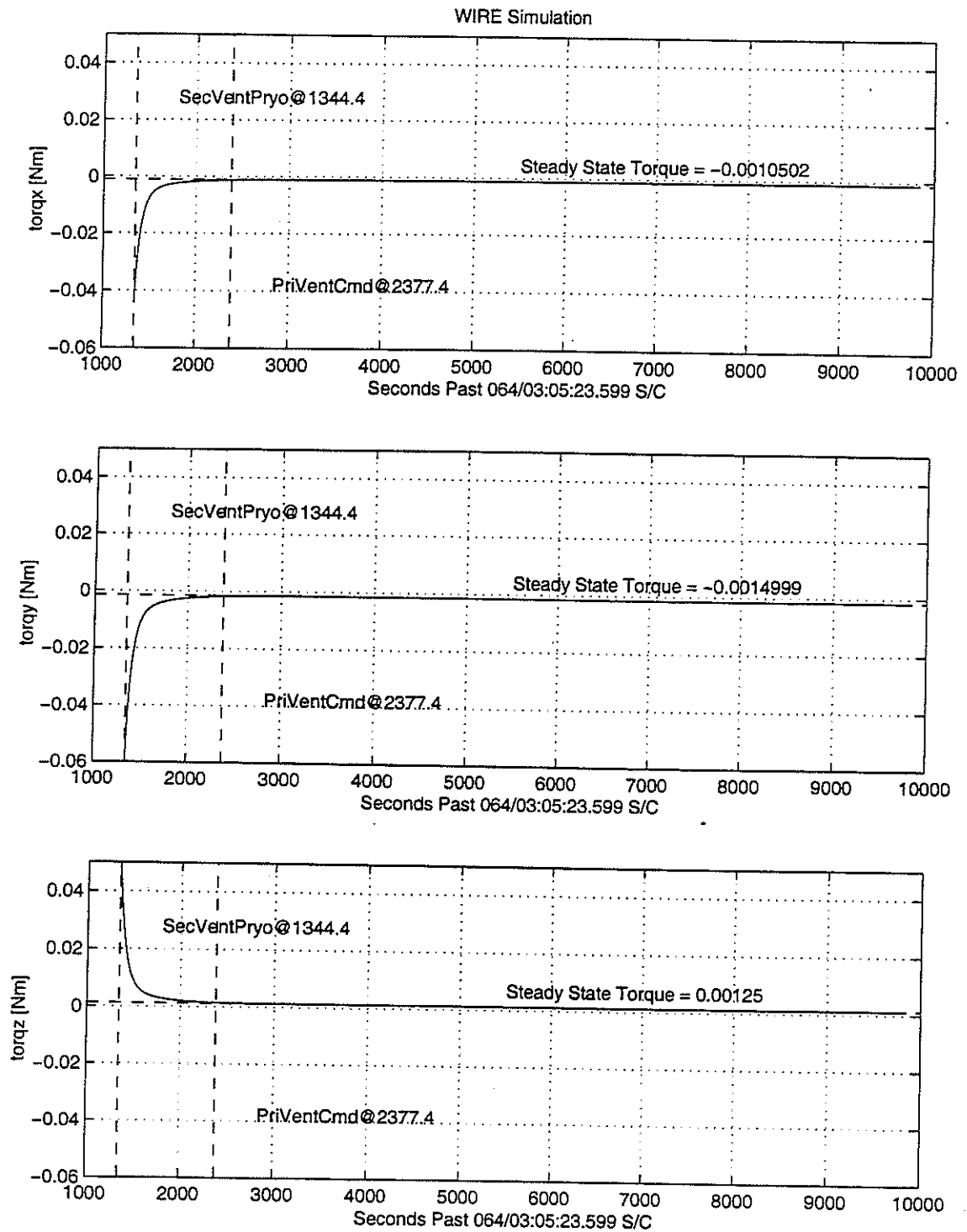
$$I_{wheel} = 0.011kg - m^2$$

An attempt was made to approximate the initial venting torques acting on the S/C by noting the location of the secondary hydrogen vent with respect to the S/C CG. This moment arm was then combined with the thrust direction of the secondary vent and an estimate of total impulse that would result from venting the hydrogen that would have melted during the 3 hours of captive carry and launch. A detailed analysis of this impulse and heat transfer is provided in another section of this report. The steady-state venting torques were modeled in the same manner, except their energy source was considered to be a heat input of about 40 watts (aperture cover off). Again, the details are covered in the Cyrostat/Thermal section of this report.

Unfortunately, when the simulation was exercised with the resulting torques, sign discrepancies resulted. The application of the venting force in either of the T-vents directions at the location of the T-vent resulted in a set of signs for  $\omega_y$  and  $\omega_z$  that were conflicting with the flight telemetry. Because of this, the application point and force direction were simply set to values that resulted in "correct" signs and magnitudes for  $\omega_y$  and  $\omega_z$ .

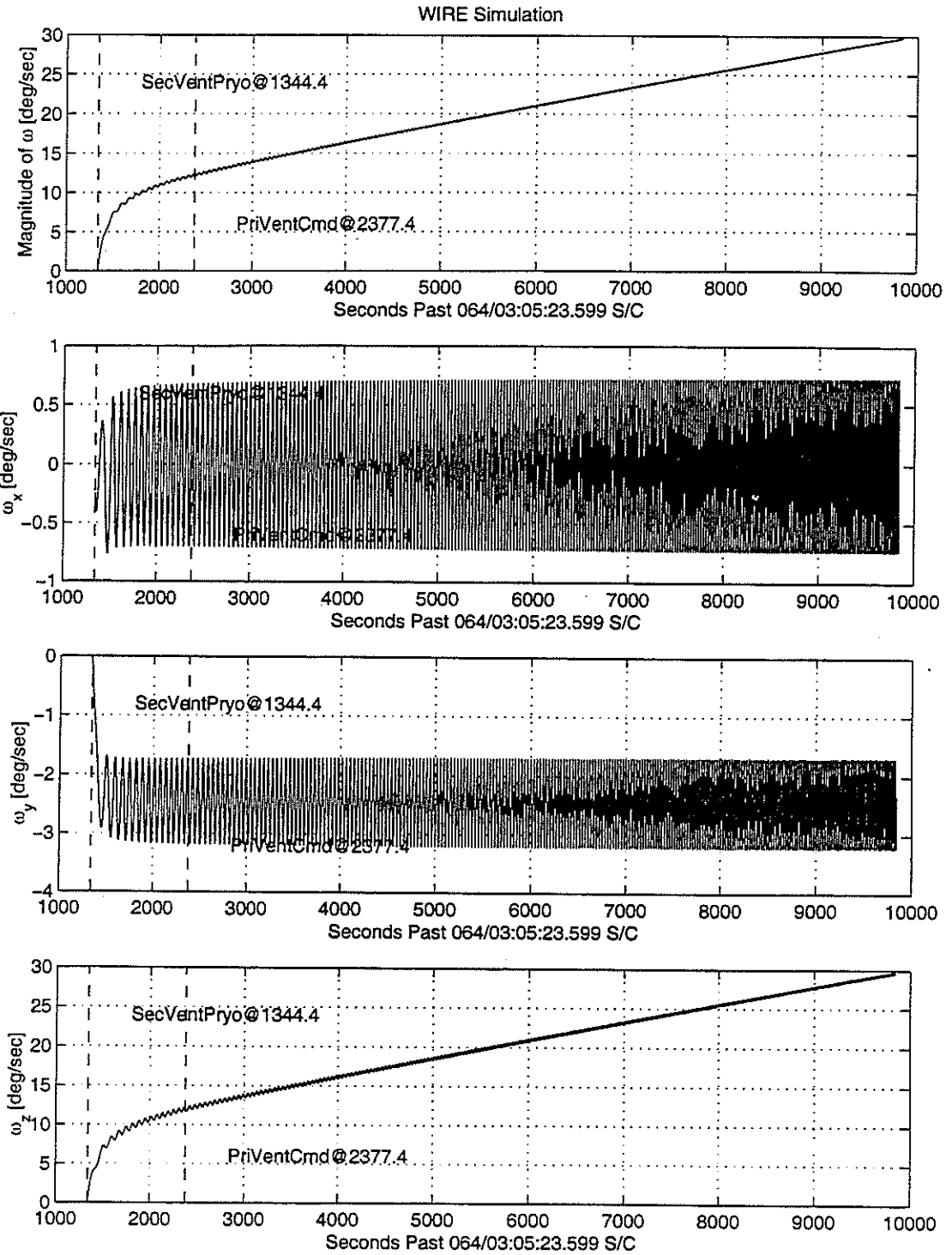
In addition, the initial thrust was found to be more consistent with two decaying exponentials (vent decay and thermal decay) rather than a single decay to a steady-state value. Therefore, two exponential decays were used with the time constants and relative distribution of impulse between the two adjusted to match flight telemetry. The time constants of the exponential decays were 1 minute and 5 minutes.

The final results for the applied torques are shown in Figure 4.B.10. The accompanying simulation rates are shown in Figure 4.B.11.



G.A. Macala 04-May-1999, 10:24

Figure 4.B.10 Simulation Venting Torques



G.A. Macala 04-May-1999, 10:24

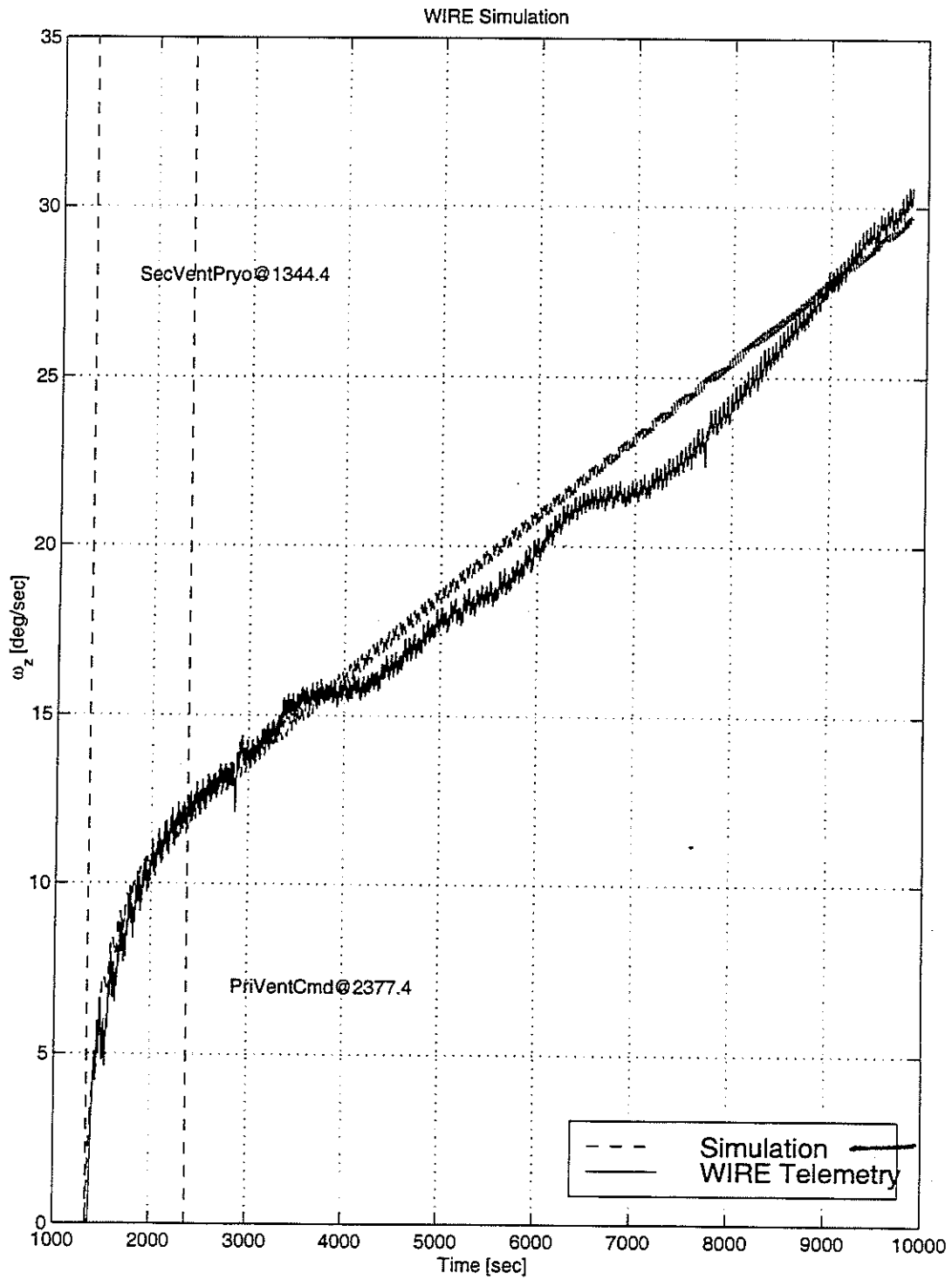
Figure 4.B.11 Simulation S/C Angular Rates

A comparison of the simulated X, Y, Z S/C rates in Figure 4.B.11 with those derived from flight telemetry in Figure 4.B.8 shows general agreement. X-axis rates simply oscillate. Y-axis rates oscillate but also have a negative bias. Z-axis rates quickly climb in the positive direction and then continually climb at a slow rate.

Because the tremendous amount of noise and artifacts present in the derived rate data make comparisons and calculations more difficult, an attempt was made to derive a cleaner set of rate data. A phase-locked loop simulation was used to process the sun body vector data.

The sun body vector data for the X and Y S/C axes consisted of mainly an oscillation that resulted from the X and Y axes sweeping by the sun at S/C spin rate (z-axis rate). The Z-axis body vector data consisted of mainly the nutation or coning of the S/C Z-axis towards and away from the sun. The coning frequency is proportional to the ratio of spin inertia to transverse inertia and the current spin rate. The frequency noted in the Z-axis sun body vector plots did agree well with this formula. It was about  $\frac{1}{2}$  that of the frequency noted (spin frequency) in the transverse axis data.

Although noise and artifacts and other frequencies exist in the transverse axis data, a phase-locked loop can very selectively lock onto an oscillation in a set of data, particularly if the frequency is very dominant in the data. The results of running the X-axis sun body vector data through the phase-locked loop simulation are shown in Figure 4.B.12.



G.A. Macala 04-May-1999, 10:25

Superimposed on the PLL-processed telemetry are the Z-axis rates from the WIRE S/C tuned simulation. Note the excellent agreement.

### Attitude Control/Dynamics Conclusions

The S/C telemetry relevant to the S/C attitude control system operation and the resulting S/C dynamics has been reviewed. A simple S/C dynamics simulation has been exercised and tuned to match flight data. The following conclusions are consistent with the telemetry and observed dynamics, both flight and simulated:

- 1.) S/C attitude control and dynamics appear to be nominal prior to opening the secondary hydrogen vent.
- 2.) S/C dynamics initially appear to be nominal at the opening of the secondary hydrogen vent.
- 3.) S/C dynamics after the initial venting at the opening of the secondary hydrogen vent are *not* nominal and are consistent with a continued venting of the hydrogen at a rate much lower than the initial vent rate.
- 4.) The continued venting of hydrogen resulted in a torque being applied to the S/C that was about twice as large as the Magnetorquers could apply. The result was that the S/C continued to spin-up even though the attitude control system was performing properly.
- 5.) The continued venting of the hydrogen at a rate that would overcome the Magnetorquer's capability is consistent with that which would result from the heat load applied to the S/C cryogen system if the telescope cover came off at roughly the same time as the secondary hydrogen vent opening. However, there is no obvious dynamic signature in the data that could be directly identified as the impulsive ejection of the cover.

One last word about telescope cover ejection dynamics. The cover is nominally ejected at 1 m/sec and has a mass of about 7 kg. This means that an impulse of 7 kg-m/sec would be delivered to the S/C at cover ejection. If the line of force of the cover ejection misses the S/C CG by moment arm  $R$ , then the resulting angular momentum imparted to the S/C would be  $7 R$  kg-m<sup>2</sup>/sec or  $7 R$  Nms.

Given the S/C transverse inertia of about  $75 \text{ kg}\cdot\text{m}^2$ , the S/C angular rate that would result from cover ejection is  $0.093 \text{ R rad/sec}$  or approximately  $0.05 \text{ deg/sec}$  per centimeter that the cover force misses the S/C CG. The CG was spec'd to be within 1 inch of the telescope centerline. Therefore, cover ejection would only induce a few tenths of deg/sec rates on the S/C, much smaller than can be observed at the secondary hydrogen vent opening.

#### 4C. Cryostat/Thermal Analysis

# Cryo/Thermal Analysis of the WIRE Spacecraft Launch Anomaly

R.G. Ross, Jr.

## OBJECTIVE

The first objective of the WIRE cryostat thermal analysis was to thoroughly examine any possible role of the WIRE cryostat in the observed launch anomaly. Possible failure modes examined included:

- Possible excessive heating of the dewar due to early deployment of the aperture cover and subsequent viewing of hot Earth and Solar radiation
- Possible loss of guard vacuum during launch leading to excessive early heating of the dewar
- Possible rupture of the dewar due to launch loads or excessive swelling of the solid hydrogen cryogen during warm-up (as with NICMOS)

The second objective was to analyze the on-orbit cryo venting behavior of the S/C to attempt to confirm the timing and validity of identified candidate failure mechanisms. The key analysis in this area was a comparison of the timing and level of S/C momentum increase due to the excessive hydrogen venting; this was run in collaboration with the S/C ACS study.

## SUMMARY

The cryo/thermal analysis of the WIRE spacecraft launch anomaly found no credible evidence of a dewar-related failure other than early deployment of the cover. Heat rates into the dewar during the early instrumented portion of the flight were nominal, and on-orbit thermal gradients and heating rates are in complete agreement with the nearly 40 watts of solar/Earth heating expected through an open cover, and not in agreement with heating coming from some other external or internal sources.

Second, the greatly accelerated on-orbit cryogen venting rate and resulting spacecraft momentum increase is also in agreement with the premature release of the cover before or at the time of secondary vent opening. However, the level of the blowdown induced torque at the time of secondary venting is higher than expected.

## FAILURE MODE ANALYSIS

As pointed out in the task objectives, three possible failure modes involving the cryostat were examined. These included:

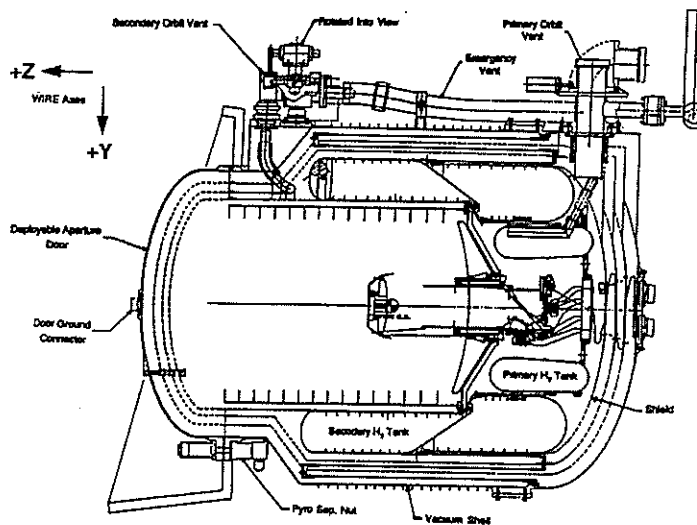


Figure 1. WIRE cryostat.

- Possible loss of guard vacuum during launch leading to excessive early heating of the dewar
- Possible rupture of the dewar due to launch loads or excessive swelling of the solid hydrogen cryogen during warm-up (as with NICMOS)
- Possible excessive heating of the dewar due to early deployment of the aperture cover and subsequent viewing of hot Earth and Solar radiation

### WIRE Cryostat Heating Analysis

Initial emphasis of the analysis centered on the recorded temperature data for the cryogenic instrument components. As shown in Fig. 1 the WIRE cryostat involves two tanks of solid hydrogen: an inner primary tank to maintain the instrument focal plane detectors at a temperature near 7 K, and an outer secondary guard tank to maintain the telescope optics at a temperature around 10 K. Each tank has its own vent in orbit, referred to as the primary and secondary vents; these vents maintain a very low background pressure on the hydrogen so as to achieve the very low temperatures.

A number of temperature sensors are present, both internal to the cryogenic portions of the cryostat, and at various exterior points. The sensors are divided between those connected to the spacecraft data acquisition system, and those connected to the instrument data acquisition system in the Wire Instrument Electronics (WIE); all of the cryogenic temperature sensors are connected to the WIE.

During the launch and early mission, the various temperature sensors were powered on at different times as follows:

- During the L-1011 flight portion of the mission all sensors were on and powered via the ASE in the L-1011
- Upon separation from the L-1011, the WIE box was powered off to conserve battery power and was not powered on until approximately 1 hour after orbit insertion. Thus, no cryogenic data exist from L-1011 separation through the critical period of tank venting and the anomalous heating.
- The spacecraft powered temperature sensors on the exterior of the cryostat are available for the entire launch period

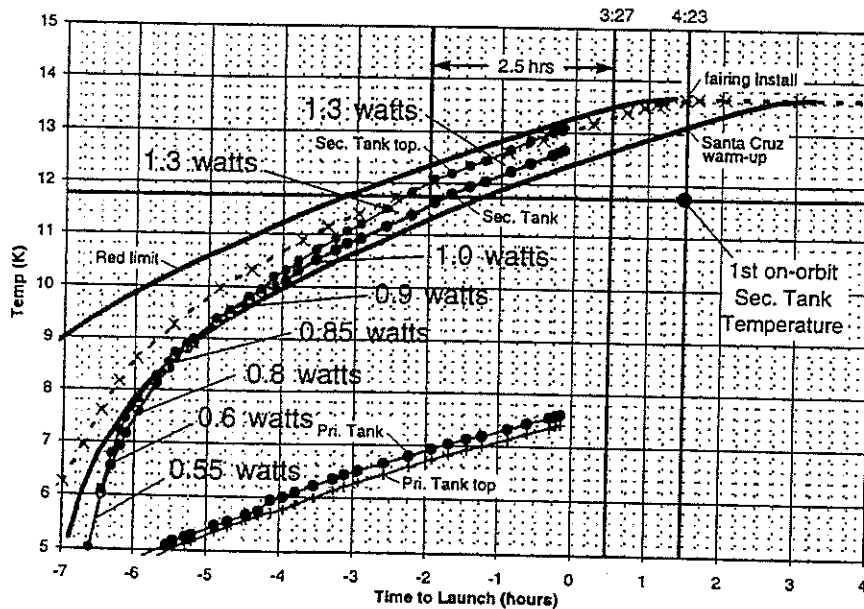


Figure 2. Cryostat tank temperatures and computed heat loads for L-1011 portion of the mission.

**Launch Heating of the Dewar.** Figure 2 displays the recorded temperature of the cryogen tanks during the L-1011 portion of the mission and after the WIE box was turned on approximately one hour after orbit insertion. To assess the possibility of some sort of unexpected heating occurring during launch, the parasitic heat-load into the tanks was computed based on the mass and thermal properties of the hydrogen and the recorded warm-up rate. The computed heat rates are noted on the plot for each 1 K temperature interval. The heating rates are completely nominal.

The heating calculations are also useful to examine the expected cryogen venting upon opening of the vents on-orbit. Upon venting, a sufficient quantity of hydrogen must escape to remove the heat absorbed when the tank temperature was above its final on-orbit temperature of 11.75 K. From Fig. 2, the integrated heating above 11.75 K is seen to be approximately 1.3 watts for 2.5 hours, i.e. 3.25 watt-hrs or  $\sim 12$  kJ.

**On-Orbit Dewar Temperatures.** Figure 3 displays the measured temperature of the cryogen tanks during those on-orbit portions of the mission when the WIE box was turned on. It is apparent from these data that the telescope optical baffle has been heated to nearly 120 K from its expected temperature near 10 K; the secondary mirror has similarly been greatly heated. Heating of the baffle is totally consistent with the cover being off and solar and Earth radiation being incident upon the baffle surfaces. The baffle temperature would not be expected to be elevated above the tank temperature for the case of an external heating source. This strongly discredits the possibility of a guard vacuum leak or other failure leading to the excessive heating.

**On-Orbit Solar and Earth Heating.** To assess the total expected heating of the dewar due to Earth and solar radiation, the spacecraft attitude data were combined with models for the incident Earth and solar radiation level as a function of angle of incidence. Figure 4 displays computations of the instantaneous Earth and solar heating of the open dewar based on the measured spacecraft attitude data from the time of initial ACS powering just after separation from

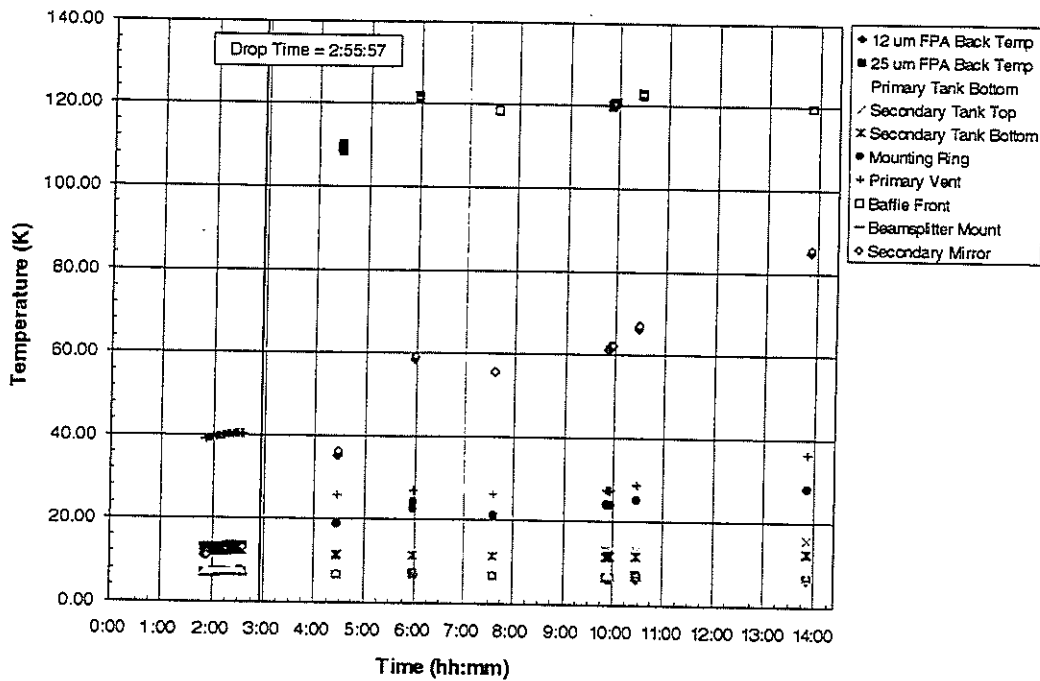


Figure 3. Cryostat temperatures for the on-orbit portion of the mission.

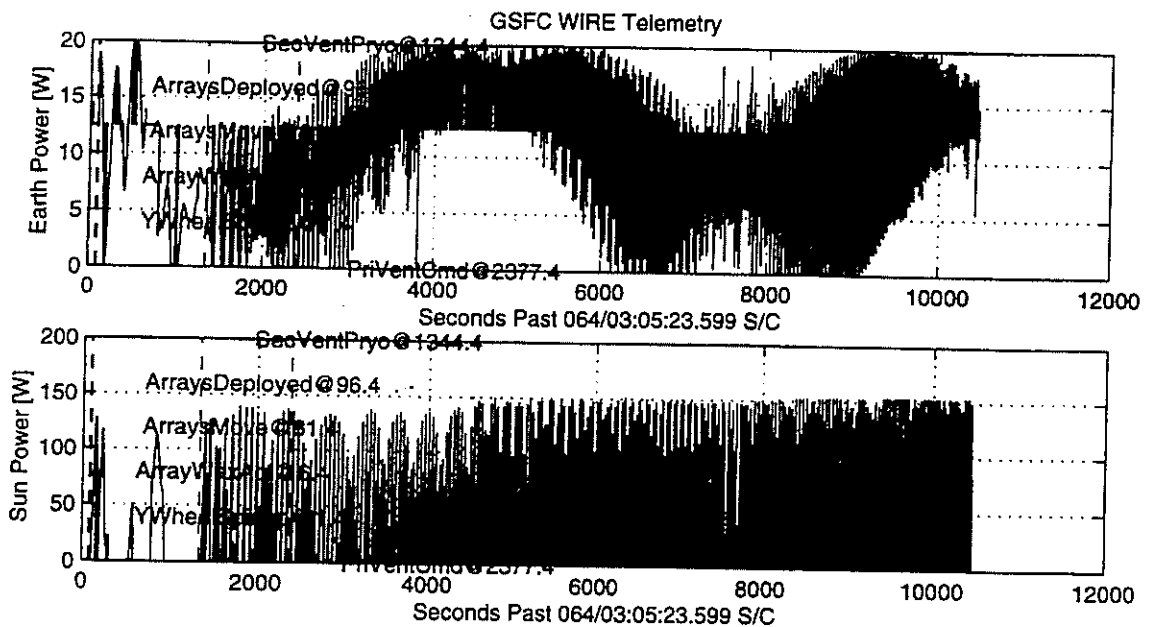


Figure 4. Computed Earth and solar heating of the open dewar based on the measured WIRE spacecraft attitude data for the first 12,000 seconds of the mission.

the launch vehicle. Figure 5 displays the resulting integrated heat loading which is seen to total to about 40 watts. As will be shown later, this heat load is consistent with the observation that the cryogen was totally exhausted at around 15 hours after cover deployment.

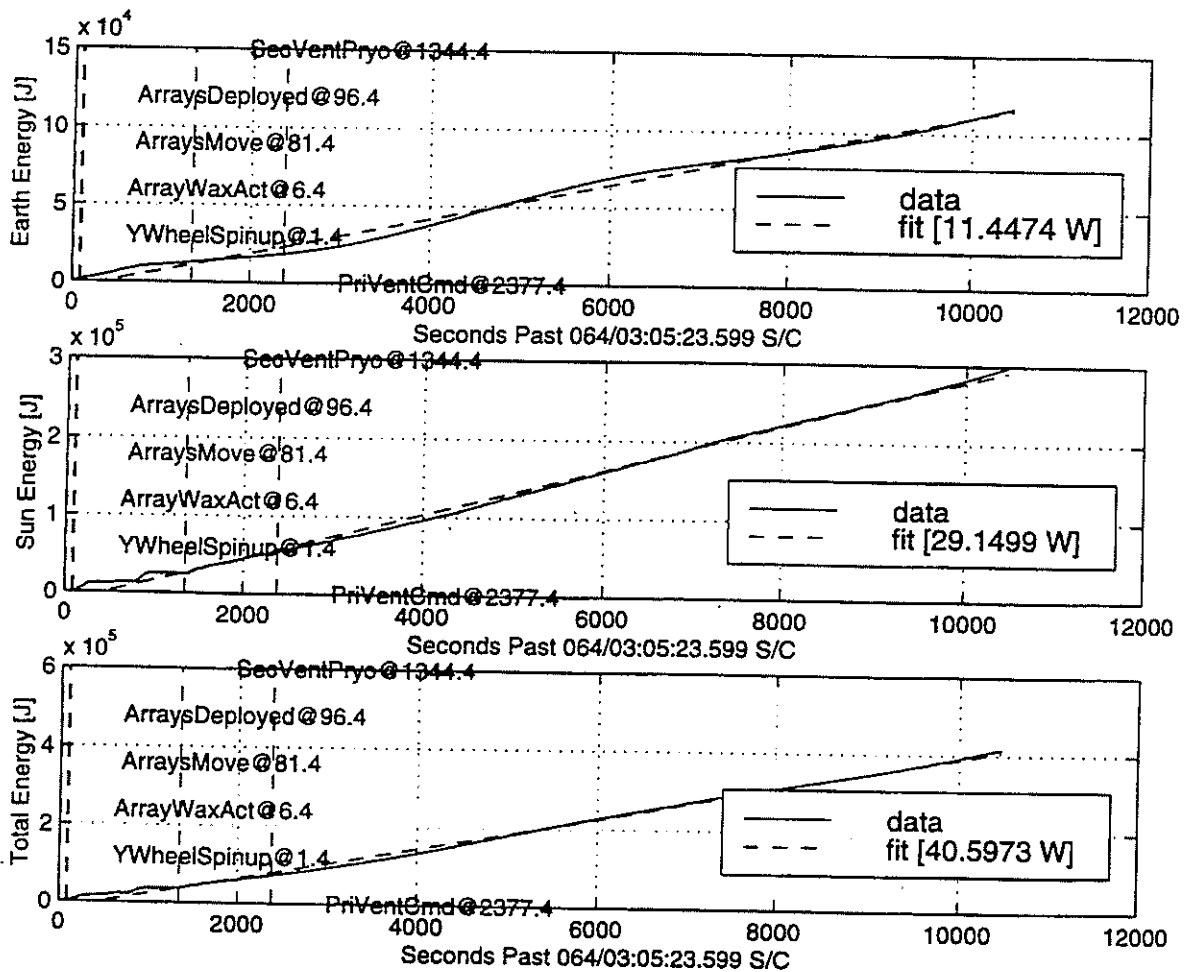


Figure 5. Integrated Earth and solar heating of the open dewar based on the measured WIRE spacecraft attitude data for the first 12,000 seconds of the mission.

## CRYOGEN VENTING ANALYSIS

Given the strength of the evidence arguing an early deployment of the dewar cover as the fundamental failure, a detailed analysis was carried out to compare the observed spacecraft angular rates over time with the momentum kick to be expected from the venting forces. A key objective of the venting analysis was to further define the time when the cover deployed.

### Cryogen Venting Fundamentals

During launch and orbit insertion the cryogen tanks are sealed shut. Thus the external heat soaking into the tanks through the tank insulation causes the cryogen to heat up and the hydrogen pressure to increase toward its triple-point state where the hydrogen begins to melt at constant temperature and pressure. Upon venting, the pressure in the tank is rapidly reduced toward a vacuum level. With this reduced pressure, the heated hydrogen rapidly sublimates and the heat of sublimation rapidly cools the hydrogen remaining in the tank. As the gas travels between the tank and the external vent it is heated by extracting heat from the plumbing walls, and the plumbing walls and connected vapor cooled shields are cooled by the escaping gas. The initial rapid venting process

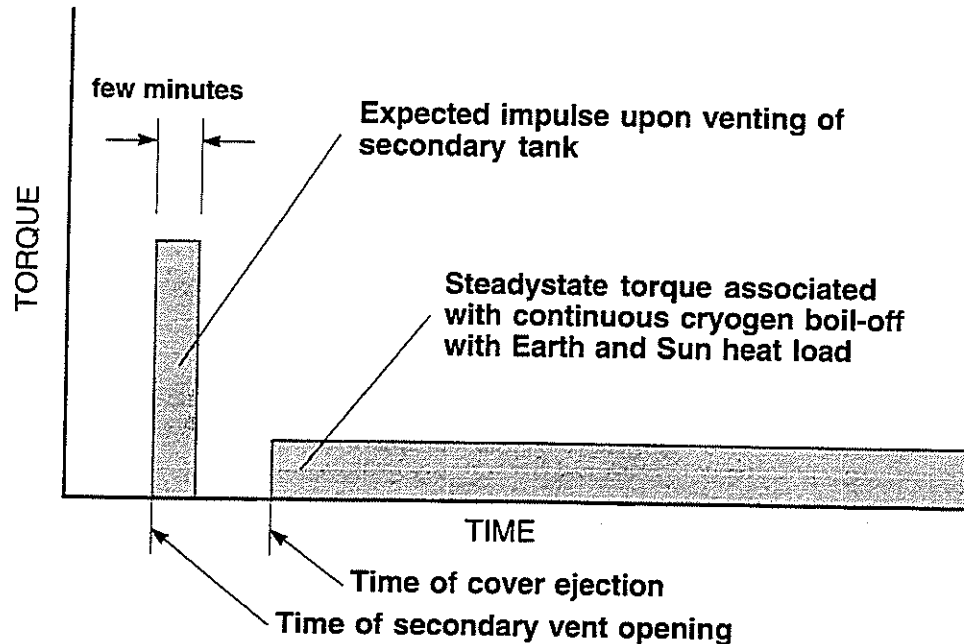


Figure 6. Expected spacecraft torque attributes associated with vent firing and cover deployment.

slows to a low rate as the hydrogen achieves a temperature consistent with the pressure drop in the vent equaling its vapor pressure, and the plumbing reaches a new lower equilibrium temperature consistent with the equilibrium heat inputs and ultimate hydrogen flow rate.

The long-term on-orbit vent rate is driven by the long-term rate of heating into the dewar. In this case the heat of sublimation plus the heat capacity of the heated gas times the mass flow rate will equal the external heating level.

### Cryogen Venting Analysis

Based on the above background, the WIRE venting analysis can be broken down into two distinct parts: 1) analysis of the initial cryogen blowdown following secondary vent opening, and 2) analysis of the steady cryogen sublimation associated with the ~40 watt solar/Earth heat load radiating through the telescope opening into the dewar. Figure 6 highlights the momentum attributes associated with these two events. Notice that initial venting provides an impulse that causes a rapid increase in spacecraft spin rates, whereas long-term venting provides a constant torque leading to a linearly increasing spin rate over time (if there were no counteracting torques from the spacecraft attitude control system). In fact, there is a counteracting torque from the torque rods of the WIRE spacecraft and it is explicitly considered in the presented analysis.

In addition to the input heat load, a critical input to the momentum calculations is the hydrogen exit velocity and its radius arm from the S/C center of gravity. The secondary vent on WIRE exits in a thrust neutralizing "T" that ideally provides two equal and opposite gas jets normal to the Z-axis (see Fig. 1); the radius arm about the Z-axis is approximately 0.45 m. However, in the assembly of the thrust neutralizing "T", a large electrical connector was placed within 2 inches of the "T" and directly in front of one of the gas exit ports. Thus, the extent of thrust neutralization is open to question and not expected to be particularly high.

Lastly, given the vacuum pressure downstream of the vent, the exit velocity of the hydrogen gas will be limited to the sonic velocity of hydrogen at the exit stagnation temperature of the gas. This

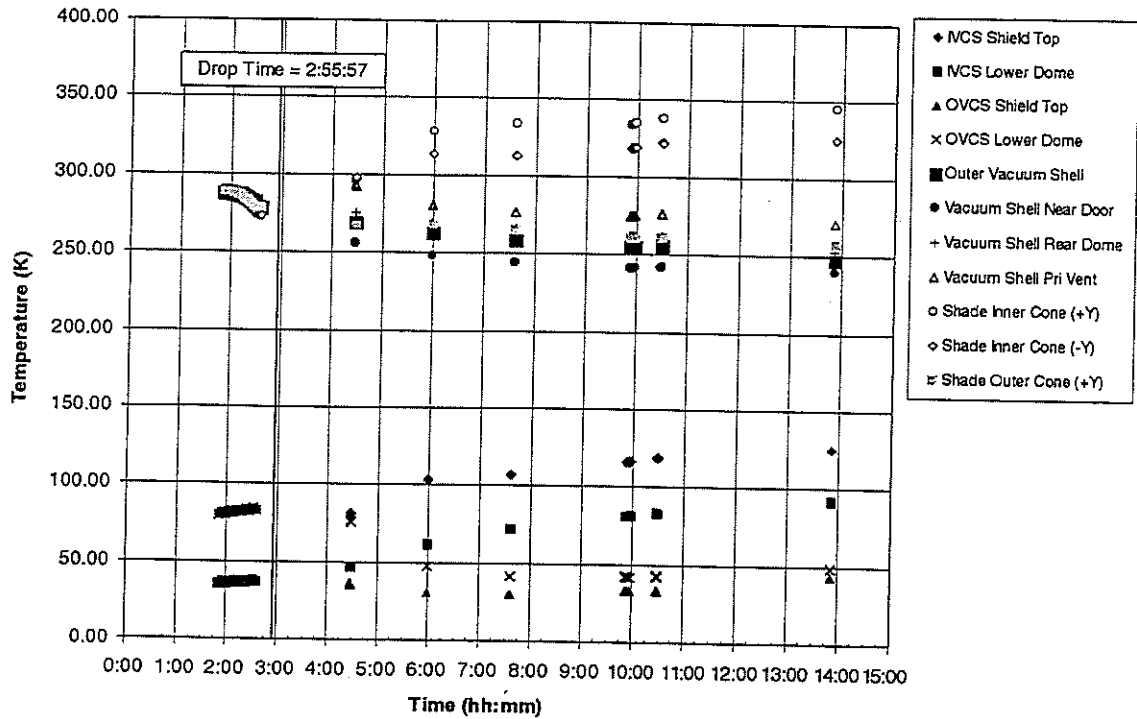


Figure 7. Vapor cooled shield and outer cryostat temperatures for the on-orbit portion of the mission.

exit temperature is quite uncertain, but has been assumed to be 200 K during the initial rapid blowdown, and 50 K after the vent plumbing has cooled to its long-term equilibrium value. These values are guesstimates reflecting the initial (80 K) and final (30 K) temperature of the outer vapor cooled shield as measured in orbit (see Fig. 7). The sonic velocity varies as the square root of the absolute temperature, somewhat tempering the uncertainty in these exit temperatures.

**Steady Venting Analysis.** Because of its more known state, the long-term steady venting analysis associated with the  $\sim 40$ -watt Earth/solar heat load is considered first. Table 1 displays the calculations and findings. This analysis begins by using the 40-watt heat load computed in Figs. 4 and 5 to predict a steady hydrogen sublimation rate of around 0.07 g/s. In this calculation it is assumed that the energy to heat the gas from tank temperature of 13 K to 20 K comes from the 40 watt heating internal to the dewar, and that heating of the gas from 20 K to the gas exit temperature of 50 K comes from separate external heating of the outside of the vacuum shell; the overall sublimation rate of 0.07 g/s agrees reasonably well with the observed dewar end-of-life of around 15 hours. Next, the mass flow rate is combined with the sonic velocity of 585 m/s (associated with an estimated gas exit temperature of 50 K) and a radius arm of 0.45 meters to estimate the thrust-induced torque, assuming no thrust neutralization. The predicted torque is 0.0184 Nm.

In contrast, the momentum data derived from the S/C spin-rate (Fig. 8) imply a net steady torque of around 0.00163 Nm including an estimated 0.0017 Nm torque reduction from the operation of the torque rods. The effect of the torque rods (shown in Fig. 9 for the first 1400 seconds), was estimated using three approaches: 1) the 0.002 Nm slope from Fig. 9, 2) examination of the S/C momentum rate in the post-11,000s timeframe when the torque-rod torque was reversed (this yielded an estimated torque-rod torque of 0.0014 Nm), and 3) by integration of ACS telemetry indicating the instantaneous torque applied by the rods about the S/C Z-axis; the Z-axis torque is a good estimate

Table 1. Calculation of torque due to steady hydrogen sublimation with 40-watt Earth/solar heat load.

Calculation	Method	Result
Total dewar heating due to Earth and Sun viewing	Computed from S/C flight attitude data	10 W from Earth view 30 W from Sun view 40 W Total heating
H <sub>2</sub> mass flow release due to Earth/solar heating into telescope; gas heating above 20K assumed external source	Calculation based on Earth/solar heating rate, heat of sublimation, and heat capacity of gas heated to 20 K.	$\dot{m} = 40 \text{ J/s} / (500 \text{ J/g} + 10 \text{ J/g}\cdot\text{K}\times(20\text{K}-13\text{K}))$ = 0.07 g/s
Bound on angular momentum increase (i.e Torque) from steady venting	Analytical calculation assuming 50 K gas exit temperature, 100% thrust effectiveness, and 0.45 m radius	$T = \dot{m}vr = 0.07\text{g/s}\times 585\text{m/s}\times 0.45\text{m}$ = 18.4 milliNm
Observed angular momentum increase (i.e Torque) from steady venting	Measured rate of flight angular momentum increase plus correction for expected reduction caused by torque rods	$T = T_{\text{spinrate}} + T_{\text{rods}}$ = 1.6 + 1.7 = 3.3 milliNm
Thrust effectiveness	Ratio of observed to computed for 100% thrust eff.	$E = 3.3/18.4 = 18\%$

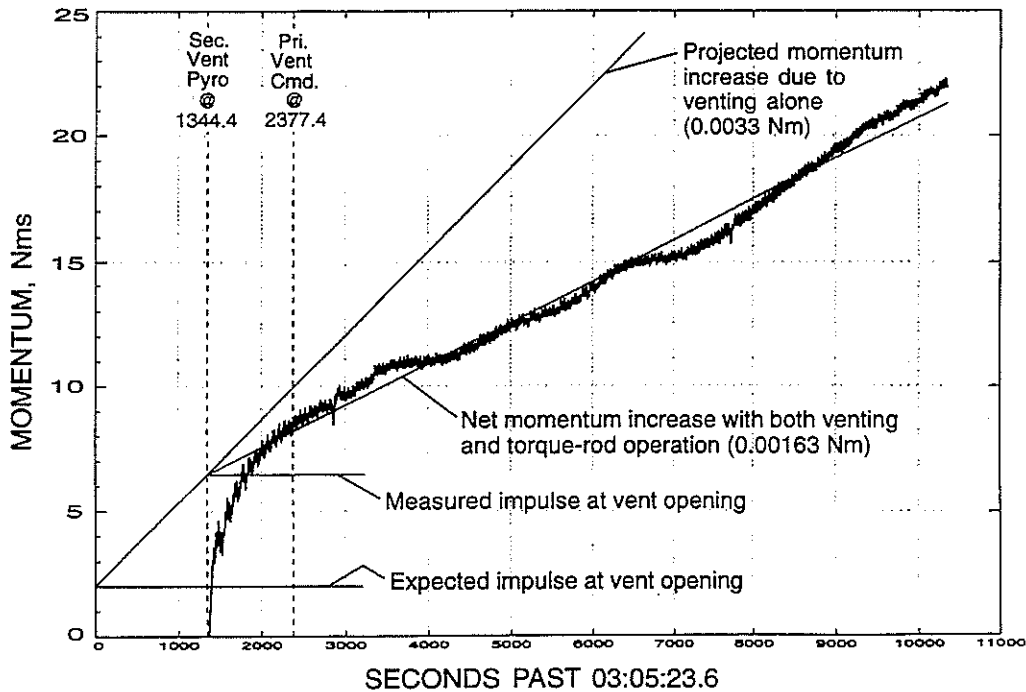


Figure 8. Recorded increase in spacecraft momentum following secondary vent opening.

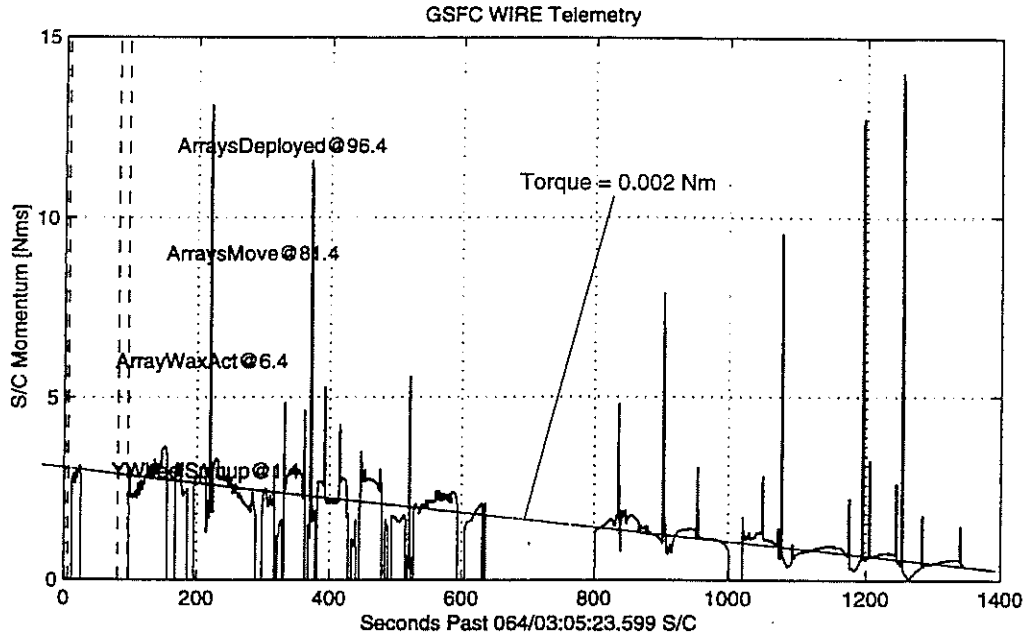


Figure 9. Measured decay in spacecraft momentum due to torque rod operation after L/V separation.

of the effective torque that reduces the S/C momentum, as the momentum is dominated by spin about the Z-axis. The result of this third approach is displayed in Fig. 10, and is in close agreement with the average (0.0017 Nm) of the first two approaches.

In Table 1, the torque-rod influence is approximated using a value of 0.0017 Nm, which gives an estimated S/C torque due to venting of approximately  $0.0016 + 0.0017 = 0.0033$  Nm. This is about 18% of the 0.0184 Nm torque predicted assuming no thrust cancellation. This thrust cancellation of 82% is considered very plausible, so both the analysis and the measured S/C rates are considered to be in good agreement with the cover coming off or being off at the time of secondary vent opening.

**Vent Blowdown Analysis.** To assess whether the cover came off at the time of secondary vent opening, or before, it is useful to examine the size of the momentum impulse that occurred at the time of venting. For the vent blowdown analysis, summarized in Table 2, the radius arm, and level of thrust cancellation were assumed to be the same as in the steady venting analysis presented in Table 1. In this case the mass of hydrogen vented is controlled by the integrated level of heat

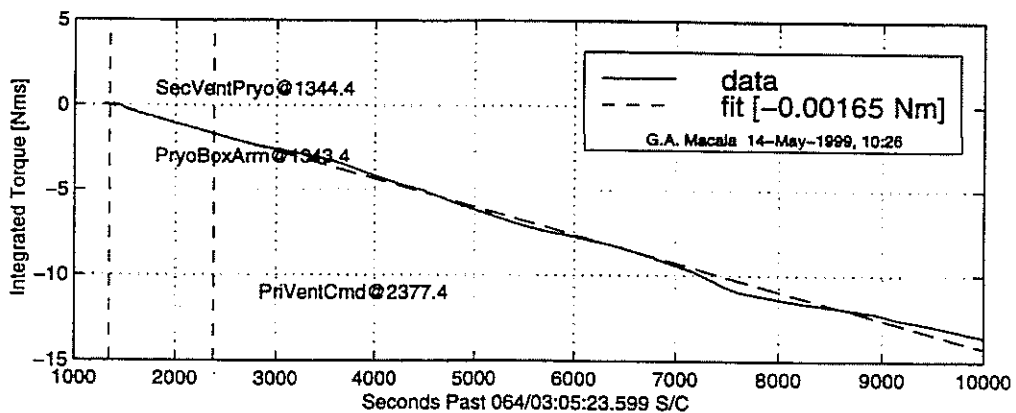


Figure 10. Time integration of ACS torque-rod torque applied about the S/C Z-axis.

**Table 2.** Calculation of the impulse due to initial hydrogen blowdown immediately following opening of the secondary vent.

Calculation	Method	Result
Dewar heat that must be released during venting to return to measured post-vent temperature of 11.75 K	Extrapolated measured warm-up rate during L-1011 flight	1.3 watts heating rate x 2.5 (hours above 11.75 K) ≈ 12 kW (kJ)
Total H <sub>2</sub> mass release during initial venting	Cryo calculation	m = 12 kJ/500 J/g = 24 g
Gas velocity out of vent at time of vent release assuming 200 K gas exit temperature due to heating by plumbing	Tabulated data for the properties of H <sub>2</sub> for a gas temperature of 200 K	Sonic velocity = 1050 m/s
Expected angular momentum increase from initial vent blowdown	Analytical calculation assuming 0.45 m radius and 18% thrust effectiveness	M = 0.18 × mvr = 0.18 × 0.024 kg × 1050 m/s × 0.45 m = 2.0 Nms
Measured angular momentum increase of S/C at time of vent release	Obtained from measured S/C flight spin-rate data at time of venting	M = 6.5 Nms

absorbed into the secondary hydrogen tank prior to venting; this is estimated to be on the order of 12 kJ, assuming the cover remained on until the time of secondary vent firing (see Fig. 2). Given the initial warm temperature of the outer vapor cooled shield and the cryostat outer shell, the gas is considered to be heated to an exit temperature of 200 K for this case; this gives a sonic velocity of 1050 m/s. The gas is then assumed to be cooled over time to the steady exit temperature of 50 K noted in Table 1. Using the same radius arm of 0.45 meters, and thrust efficiency of 18% gives a predicted venting-induced impulse of 2.0 Nms. The observed impulse of 6.5 Nms in Fig. 8 is a factor of three higher than this. However, given the uncertainties in the estimates, the data do not rule out cover separation at the time of secondary vent firing.

A possible explanation for the higher than expected impulse at the time of secondary vent firing is the momentum kick from the separating 7 kg cover, if it separated poorly at this time. However, detailed review of the S/C angular velocity data show no significant instantaneous increase in velocity at the time of vent opening. Instead, the velocity increase is a smooth linear increase over many seconds. This, together with the low expected impulse (< 0.1 Nms) from the cover, which deploys with a 1 m/s velocity vector very close to the S/C center of gravity, strongly discounts the cover separation kick as the reason for the higher than expected impulse.

As a final clarifying step, it is useful to compute what level of hydrogen mass venting and therefore hydrogen heating would have to be present to yield a thrust impulse of 6.5 Nms. This can be done by scaling from the steady venting analysis, thus de-coupling the results from the more poorly determined parameters (thrust direction, radius arm, and neutralizer efficiency). From the steady-venting analysis, a 6.5 Nms impulse requires the application of the estimated 0.0033 Nm torque for about 2000 seconds. Thus, the integrated mass of hydrogen vented should equal 0.07g/s × 2000 s = 140 g. This corresponds to a heating level of 500 J/g × 140 g = 70 kJ. Assuming that the dewar heat leak through the walls remained at the 12 kJ level predicted in Table 2 and Fig. 2, the excess heating is estimated as 70 - 12 = 58 kJ. A possible means of generating this heat is for the cover to have come off at an earlier time. The predicted time would be 58 kJ / 40 watts = 1450 s

prior to secondary vent opening. This corresponds to the timeframe of spacecraft separation from the launch vehicle and initial powering of spacecraft subsystems such as solar arrays and the ACS.

These results are intriguing and worth noting. However, because of the uncertainty in the thrust vector direction and behavior of the venting gas due to the partially blocked thrust neutralizer, this mismatch in the predicted versus measured vent-opening impulse must be viewed with a critical eye and must be interpreted within the total body of evidence. In particular, careful examination of the electrical telemetry found no evidence that the latching relays that provide enabling power to the pyro circuits were energized prior to the 3:27:47 time immediately prior to the secondary vent firing. Thus, no credible opportunity for firing the cover pyros was found to exist prior to the 3:27:47 time of secondary vent opening.

## CONCLUSIONS AND LESSONS LEARNED

The cryo/thermal analysis of the WIRE spacecraft launch anomaly found the greatly accelerated on-orbit cryogen venting rate and resulting spacecraft momentum increase to be in full agreement with the premature release of the cover before or at the time of secondary vent opening. However, the impulse associated with the vent blowdown is somewhat larger than expected at the time of vent opening.

Second, no evidence was found of a dewar-related failure other than early deployment of the cover. Heat rates into the dewar during the early instrumented portion of the flight were nominal, and on-orbit thermal gradients and heating rates are in complete agreement with the nearly 40 watts of solar/Earth heating expected through an open cover, and not in agreement with heating coming from some other external or internal sources.

### Lessons Learned

- The unavailability of definitive cryo temperature data during the critical dewar venting operation hampered early real-time identification of the root problem (premature cover deployment) by the S/C operations personnel. This was caused by having these temperatures only readable through the instrument electronics and having the instrument electronics OFF during the critical dewar-venting time period. For this particular failure, the most definitive parameter was the baffle temperature, which is strongly influenced by the deployment of the cover. Hydrogen tank temperatures are also critical measurements for confirming and understanding the success of the vent opening procedure. However, they too were not powered during the vent-opening event.

- The high vent-thrust levels experienced both at vent opening and with solar/Earth viewing and the limited torque capability of the WIRE S/C attitude control system suggest an overall attitude control system design with marginal robustness. Even without the premature cover ejection, two issues that appear marginal include recovering from the very large vent blowdown impulse within the battery state-of-charge at the time of secondary vent opening, and recovering from a possible future safe-mode condition that included earth viewing. If the cover had not come off or been off at the time of secondary vent opening, the initial blowdown impulse would have been even higher, as the blowdown would have continued until the nominal in-flight predicted hydrogen equilibrium temperature ( $\sim 10$  K) was reached. Future systems should consider designing the thrust neutralizer/ACS to bring these transient venting induced torques well within the capability of the ACS.

#### 4D. Functional Design Verification Analysis

Analysis of the functional verifications summarizes those tests performed at SDL (box level) at GSFC (system level) and at Vandenberg Air Force Base (VAFB).

##### 1.) Testing at SDL

Testing of the electronics at the unit (box) level was performed at SDL using soft-start bench power supplies (with approximately 150 msec rise time) a combination of flight and representative simulator cables, and a squib simulator device that used fixed resistors (one Ohm). Firing events were detected at the squib simulator using LEDs across the one-Ohm resistors that would flash during the pyro event (100 millisecond). No provision for simulation of the burnwire opening was provided. It was unclear that the simulated cabling was built with the same wire and shield treatment as the flight cables. Testing was conducted informally (with minimal formal test plans and test procedures), under the direction of the cognizant engineer. Test results and records were documented in the engineer's notebook.

During development testing, significant (700-800 mA) transients were observed at the squib interface during turn on of the pyro box. A design change was implemented that provided a bias to the squib firing circuits to limit the transients. This design change provided approximately 15 kOhm across the arming relay contacts to ensure bias to the FET pyro drivers. The turn on transients were thus reduced to the level of six to seven mA for a few microseconds, which is not a significant concern for firing real NASA Standard Initiators (NSI) which require over one Amp. to initiate firing. Detailed records of these tests were apparently documented only in engineers' notebooks. These records were not available to the investigation team. As implemented, the design change only biased one side of the drive circuits (A or B) when only one Enable (power-on) relay was closed. This oversight had no apparent contribution to the WIRE anomaly.

At SDL, the configuration of the Spacecraft Power Electronics (SPE) to WIRE Pyro Electronics (WPE) harness was made using a simulator cable. The functions of the SPE were implemented using bench power supplies. Configuration of WPE to Squibs was provided using SDL supplied flight cabling. For convenience, the simulator load box was connected to the SAFE/ARM connector, thus eliminating the harnessing from the SAFE/ARM connector to the squibs (estimated 9-11 ft). One set of real NSIs was fired during testing at SDL. The NSIs were connected to the full complement of WPE to pyro cables. Waveforms were measured to confirm energy delivery and were satisfactory, indicating approximately one millisecond time to fire (normal for the WIRE design). Box level EMI/EMC tests, including conducted susceptibility were performed. Squib simulation for EMC/EMI testing was the SDL load box (one-Ohm fixed resistors). Due to the operation of the SDL load box, short but significant transients would likely not have been observable.

## 2.) Testing at GSFC

Testing of pyro circuits at GSFC generally was conducted using a different pyro simulator box (GSFC provided) that also was plugged into the pyro SAFE/ARM connector. On at least one occasion, the GSFC pyro simulator was connected to the squib connectors at the squib interface. This is the closest test to an end-to-end pyro test that was performed. It does provide evidence that the wiring from the WPE to the squibs was electrically correct and that there were no obvious wiring faults (at least DC or adjacent circuit coupling) that would cause an unintentional device firing due to commanding any other device to fire. It also supports that there were no firing faults that would prevent any pyro device to be fired on command (although that is not in question in the WIRE anomaly). The GSFC pyro simulator is an electronic device with logic that connects a one-Ohm resistance to the pyro circuit 21 msec after the event starts, and leaves the load on the circuit for approximately 60 milliseconds. A real squib would have fired in about one millisecond. The GSFC simulator box had been designed when pyro firing circuits were predominantly relay operated. Since it was undesirable to have a load on the relays during contact transfer

in test (to avoid damage to the contacts) the 21 msec delay permitted the contact transfer to be complete before the load was applied. During testing at GSFC, the pyro simulator box was observed to "glitch" occasionally, when the pyro electronics (WPE) was turned on by spacecraft command. This glitch required the routine manual resetting of the pyro simulator box before testing could continue. No problem report was written. At the time, it was concluded that the glitching was caused by the same low level turn on transients that had been observed at SDL. A potentially significant difference between the SDL tests and the GSFC tests was that on the flight spacecraft, the power turn-on to the WPE is accomplished through a hard relay closure to a battery (NiCd), instead of the current limited soft start (bench power supply) used at SDL.

EMC/EMI tests at the system level did not include any simulation of the squibs although the pyro box may have been powered-on for these tests. Any observed anomalies would only have been detected through event telemetry data. No anomalies were observed.

### 3.) Testing at VAFB

The final assembly testing of pyro circuits was conventional, being primarily designed to confirm expected pyro circuit loop resistances, and verify the connection and integrity of the NSI burnwires after installation. These tests again confirmed that the pyro devices were connected properly, and that there were no wiring faults or phasing errors.

4E. Environmental Design Verification/Qualification Summary

The WIRE instrument qualification test program was reviewed and found acceptable. For example, even though the flight dynamic environment was expected to be an order of magnitude lower (and was), the random vibration levels were kept up at the normal industry workmanship standard of  $>0.04 \text{ g}^2/\text{HZ}$ . The sine burst test was an adequate qualification for static loads during first, second, and third-stage Pegasus burns, L1011/Pegasus separation dynamics, and L1011 aerodynamic yaw dynamic characteristics prior to separation.

Other qualification testing was not reviewed in as much depth as vibration, but did appear to be consistent with normal JPL qualification practices. One possible exception is the lack of a comprehensive set of EMC (Electromagnetic Compatibility) measurements during simulated pyrotechnic firings.

Some key dynamic test versus flight levels and associated margins are below:

Event	Instrument Qualification Testing	Flight Levels	Margin
Pegasus Burn	12.9g	8g	1.6
Static Loads			
Random Vibration	( $\text{g}^2/\text{HZ}$ )	( $\text{g}^2/\text{HZ}$ )	
:			
Captive	$>.04$	.0001 to .001	$>> 10\text{db}$
1 <sup>st</sup> Stage	$>.04$	.0001 to .003	$> 10\text{db}$
2 <sup>nd</sup> Stage	$>.04$	.0001 to .001	$>> 10\text{db}$
3 <sup>rd</sup> Stage	$>.04$	.000001 to .00003	$>100\text{db}$
Separation Dynamics	$\geq 8 \text{ g @} \approx 20\text{HZ}$	$3\text{g @} 10\text{HZ}$	$>2.5$

In summary, the environmental conditions seen by the WIRE instrument were well within qualification levels. The flight random dynamic environment (usually a design driver) was approximately that of take-off and landing inside a modern large commercial aircraft, i.e. a non-issue.

It is concluded that there is no apparent connection between the as-flown environmental conditions and the early release of the instrument cryostat cover.

4F. Mechanical Devices - Pyro Mechanical Hardware Analysis

The mechanical hardware analysis covered two major areas - the cover and hold-down design, and the release nut design.

1.) Cover and Hold-Down Design

The cover used in this design must be very robust based on its weight and passing the system spacecraft environment test, thereby eliminating structural design failure. The release nut is certainly of a size large enough to fasten the cover using three 3/8" diameter bolts each capable of holding in excess of 15,000 pounds (JPL has flown spacecraft with primary separation system bolts loaded to this range of preload without problems). There was no independent review done of material dependent strength or other properties of the cover release. A note from Scott Schick, dated April 23, 1999, documented a bolt heat-treat anomaly (reduce bolt strength by 50%) but would have no effect on fit or function.

2.) Release Nut Design

The release nut had heritage to other applications that OEA shows as developing an operating reliability of .999922 based on firing 29,505 units in many space applications. It is likely that test and qualification adds many more units that are not included in the database. Credible failures were considered and assessed that could contribute early release using hardware drawings and spacecraft build logs.

The following shows credible failures:

1. Bolt too Long

- Changes load path in the nut
- The internal stack in the nut that would carry torqueing load would feel mushy
- Most likely failure would be failure to actuate

2. Failure to Torque Bolt

- Installation monitoring would detect
- Possible no preload of cover seal

- Loose bolt would rattle and possibly come out
  - Unlikely at all three places
3. Segments Misaligned at Assembly
- Bolt would bind when torqued
  - Configuration would preclude segment movement during assembly
  - Unlikely if torque is monitored during assembly
4. Piston Moved Prior to Assembly
- Bolt could not be torqued at assembly
  - Inspection log would show problem
  - Assembly would have a bad feel to it prior to torquing

The SDL assembly records evaluated by JPL did not reveal any problems during installation.

In spite of the possible failures listed, it seems very unlikely that hardware problems would be of the same type at all three release nut locations involved without some warning to a trained mechanic.

It is concluded that it is highly unlikely that a release nut mechanical failure was involved in the mission failure as a result of this review.

#### 5. Cause Disposition Summary

Based on data analysis in (4), a large majority of fish-bone diagram items and functional failure causes shown in the summary matrix were dispositioned. Disposition of all eighteen (18) possible causes is summarized below:

##### 5A. Broken Bolts at Cover Attachment

This scenario requires multiple faults in bolts having significant design margin for this application. In addition, this fault scenario is inconsistent with the observed orbital position of the cover.

5B. Pressure-Induced Cover Ejection

The design incorporates burst disks that would have vented the telescope well before pressures sufficient to jettison the cover would have been reached. In addition, such an explosive ejection likely would have caused physical damage to parts of the telescope that have been verified operating in post anomaly evaluation.

5C. Shock/Dynamic loads

Dynamic loads from the launch system have been verified as well within expected values. Loads verification testing was performed at levels well above those observed during the mission.

5D. Incorrect Prelaunch State

Since the pyro related activities related to the anomaly for WIRE were all ground-commanded, the only credible prelaunch state anomaly scenario would be a permanent short of the arming relay contacts in the pyro electronics box. This would make the anomalous cover ejection more likely by removing one inhibit to firing any pyro device. Ground tests on engineering model hardware have demonstrated that the arming relay short is not a necessary precondition to the anomaly.

5E. Cover Squibs Fired Prelaunch

If the cover squibs were fired before launch, the cover would have been retained by the internal vacuum in the telescope system until an altitude of approximately 75,000 to 100,000 ft. Since the cover has been observed in orbit with the spacecraft at approximately 540 km, it is unlikely that a cover that would be free from the spacecraft at 100,000 ft. would end up in such a high orbit.

5F. Onboard Sequencing Errors

The pyro events of interest in the anomaly were ground-commanded. Command/Telemetry verification does not indicate any unexpected command execution. Verification of the software load shows no evidence of any pyro firing sequences on the spacecraft other than those that were intentionally provided for activation at a later time. None of the onboard sequences included commands to cause cover ejection.

5G. Ground-Commanding Errors

The secondary cryogen tank orbit vent pyro appears to have fired when the pyro electronics was turned on which is approximately three seconds before this event was commanded. Any condition sufficient to cause this would be sufficient to also cause the cover eject pyro to fire which is consistent with flight data. All telemetry indicates correct commands were transmitted to turn on the pyro electronics and to fire the secondary orbit vent pyro. Command transmission bit errors are also unlikely due to adherence to CCSDS standards for commanding.

5H. Spacecraft-Launch Vehicle Separation Electrical Transient

The spacecraft power to the pyro electronics is off during launch vehicle separation. Telemetry indications that the pyro electronics were in the off state prior to the command to turn it on as well as the use of latching relays for the power-on function make a transient turn-on unlikely. Direct coupling of a transient to the cover separation pyro would require concurrent faults in multiple, independent circuits that were not powered.

5I. Miswiring of Harnesses, Pyro Electronics

The wiring from the pyro electronics to the cover pyro devices is independent for each squib. Multiple wiring faults are required to cause energy delivery to all three squibs. Pyro functional testing and loop resistance measurements during installation demonstrated correct wiring of the pyro devices.

5J. SAFE/ARM Connector Miswire/Mismatch

Multiple faults in the wiring of the SAFE/ARM connector would be required to cause cover eject. Mismatch/miswire of the SAFE/ARM connector would most likely cause a failure-to-operate fault than the observed fault since the connector pins are not adjacent.

5K. Component SEU, Radiation, Latchup

Transient latchup of the FPGA could potentially exacerbate the effect of the observed turn-on induced firing of the secondary vent pyro. Although this scenario is not required to explain the anomaly, it could have been a contributor. Because the anomaly is well correlated with the power turn-on event by flight data, analysis and subsequent ground test, SEU and radiation effects are not likely contributors.

5L. Control Computer Fault

The only significant control computer fault scenario involves inadvertent, premature turn-on of the pyro electronics box. This, coupled with the demonstrated turn-on transient or coupled with a second inadvertent command fault from the computer would be required to eject the cover. Since latching relays are used for power-on, a third control computer fault to turn off the pyro box would have been required to leave the pyro box in the state that was verified at the time the ground command to turn it on was sent. No onboard sequences were loaded that contained cover ejection commands.

5M. Component Contamination or Debris

The field effect transistors (FET) used to control the squibs have a history of internal debris-shorts. This scenario, however, would require debris shorts to exist simultaneously in three FETs. There is no indication that other circuit components that would be single point failure causes in relation to the cover eject have contamination or debris related failure tendencies.

5N. Pyro Electro-Magnetic Interference Induced Crosstalk

It is unlikely that the firing of the secondary tank orbit vent pyro would cause the cover eject pyro to fire since it would require energy transfer to three separate circuits. Pyro wiring used complied with NASA requirements for shielding, bonding and freedom from wire splices.

5O. Pyro Firing Electrical Sneak Path

Electrical sneak paths due to the effects of transients in one (intentional) squib circuit could have potentially caused a transient latching of the control electronics and triggered additional pyro firings. There is no clear flight evidence that this scenario is a contributor in this case, due to the observed pyro box turn-on transient effects. But the flight telemetry sampling was probably not fast enough to detect a sneak path firing.

5P. Incorrect Flight Software Load

Since ground commands were used to turn on the pyro box and the flight software load was verified as correct, as well as the fact that there were no cover eject commands resident in any onboard sequence, make an incorrect flight software load an unlikely contributor to the anomaly.

5Q. Pyro Lot Defects

Pyro lot defects are not a likely cause of the anomaly since a minimum of three faulty pyro devices would have been required. Firing at less than the one amp-one watt limit is also unlikely since the observed turn-on transient effect produces sufficient energy to expend in-specification NSIs.

5R. Pyro Box Turn-On Transient

A turn-on transient in the pyro box is probably the likely failure scenario for the premature cover ejection event. Rationale: attitude rate change expected for

secondary tank orbit vent opening is correlated to pyro box turn-on time rather than the subsequent pyro command; attitude rate changes consistent with cover deployed heating were initiated at approximately the time of the pyro box turn-on event. Because pyro turn-on transients are thought to be the most likely failure cause, an intensive analysis and test effort was pursued.

#### 6. Intensive Electronics-Focused Investigation Effort

As discussed in Paragraphs 4. and 5., after comprehensive, systematic review of the WIRE development/test data, the prelaunch/flight data and the NORAD tracking data, it is concluded that no credible evidence exists to support or suggest that mechanical, thermal, environmental software, flight sequence or operational faults caused or contributed to the premature release of the telescope cover. Based on this conclusion, the most likely explanation is that cover release was caused by spurious electrical transient signals generated at initial power turn-on of the pyro electronics in the WIRE instrument. The pyro electronics unit was turned on, as planned, by ground command about 2 to 3 seconds PRIOR to the ground-commanded secondary vent pyro firing. The second pyro electronics power-on commands were sent, as planned, by the ground one second later. Paragraphs 6A., 6B., and 6C. provide focused investigation regarding the credibility of an electronic transient cause.

#### 6A. PYRO Electronics Functional Description

The pyro electronic box is internally block redundant and contains the necessary circuitry to arm and activate three WIRE events - secondary venting (2NSIs), cover release (6NSIs) and primary venting (2 wax actuators). Each pyro electronics unit simultaneously activates half of the NSIs and wax actuators initiated on command from the spacecraft's central computer, e.g., "A" side fires one NSI and "B" side fires one NSI for the secondary vent event (See Figure 5). Each side is implemented with a +5 volt power supply (derived from the spacecraft's +28 volt battery), ACTEL (1020) FPGAs/logic circuitry and other circuitry for arming, firing control and monitoring. Note that after arming occurs, all circuits are enabled for firing. The pyro arming function is activated

by closing redundant relay contacts; the firing is activated by FETs and the firing event is detected by the pyro monitor circuit. The pyro firing monitoring circuit is a voltage sensor and not a current sensor, so pyro firing is inferred. The monitor circuit indicates a pyro firing event when the input voltage is at least 13.6 volts for at least 500 microseconds. Hence, given the spacecraft's present pyro squib configuration (fired-open circuit), the monitor circuits response to fire commands if sent now would detect a firing event even though no current flows.

## 6B. Transient Models

To determine the credibility of the electrical transient model, detailed circuit analyses were performed: (1) to characterize the end-to-end transient power turn-on response of the pyro electronics, particularly the FPGAs, and logic and (2) to characterize the end-to-end transient response interactions when squibs are fired.

### 6.B.1. Transient Scenario One

#### 1.) JPL Analysis

Analysis showed that after initial application of power or a Power-on-Reset (POR), there is a time period, under ideal no-fault operation, of about 25 msec when the ACTEL (1020) FPGA circuit states are unpredictable because the +5 volt power supply is still ramping up from zero to 5 volts (See Attachment 1). The arming relay contacts are guaranteed to close in 15 msec and likely close in less than 10 msec. Further analysis showed turn-on transients are sufficient to produce spurious signals to latchup the FPGA/logic to a state that can issue fire commands for 50-100 milliseconds. Furthermore, under a known, possible, single-fault condition (shorted 15 microfarad capacitor) in the power supply, the time period may be as long as 200 milliseconds. During the +5 volt ramp-up time, spurious arming and firing signals can be issued to one or all of the functions including the arm relay and any of the firing circuits. The likelihood of logic all going to high state is at least 50-50 depending, e.g., on the specific device, noise environment. It is noted that squib firing data taken from other JPL

projects shows that NSI squibs can be fired between 100-500 microseconds depending on the circuit firing current, e.g., with 20 and 7 Amps, respectively. Squib firing data from Langley showed that a current of 5 Amps will fire a squib in about 1 msec. In the WIRE application, squib firing probably can occur in about 1 msec.

2.) GSFC Analysis

See Attachment 3.

6.B.2. Transient Scenario Two

During a pyro firing, it is possible that pyro firing transients generated by an intended firing may have caused other pyros to fire, sympathetically. Pyro firing transient data taken from other projects shows that when squibs fire, a transient (~100 - 500  $\mu$ sec) ionization-induced electrical path is formed between the squib body and spacecraft chassis. This path momentarily creates a short circuit across the +28 volt spacecraft battery (the battery circuit return is tied to spacecraft chassis). This "shorted" condition can result in significant transients in the logic return causing the FPGA to issue spurious fire signals (See Figure 5A).

Analysis shows that the voltage swings in logic return exceed 1 volt per microsecond which is above the  $dV/dt$  maximum specification for the gate array (See Attachment 2). At these high voltage slew rates, the gate array can latch up causing all outputs to be pulled high. The condition that causes the latch can be created in just a few nanoseconds. In extreme cases, the latch can be permanent, but it can be cleared in as little as 100 milliseconds. This is more than sufficient time to cause sympathetic firing of the remaining pyros.

6C. Ground/Flight Confirmation Tests

Ground tests, using commercial equivalent ACTEL 1020 FPGA hardware were performed to confirm the transient analyses. Additional tests were performed at GSFC using flight-like parts in a controlled thermal environment.

### 6.C.1. SDL Tests

Tests were performed on the Engineering Test Unit (ETU) with a "hard" relay closure for turn-on. These tests demonstrated that the outputs of the pyro circuit logic do cause inadvertent arming and firing of pyro during the time period when the logic is initializing, and well before the initialization was complete (See Figure 6). Since the transient firing occurs at power on and manifests itself in a short (approximately two-millisecond) pulse, the potential for observing the event using either the GSFC or SDL pyro simulators is deemed small. This, combined with the idiosyncrasy of the system to glitch the GSFC simulator due to a presumed small transient at turn-on, may have masked the existence of a serious fault condition. Fuses (1/4 Amp) were installed for these tests but did not blow. Since the duration of the transient was approximately 2 milliseconds, and the current is limited to approximately 6 Amp per fuse by the circuitry, there is approximately 336 milli-Joule available per squib whereas the selected fuse requires approximately 500 milli-Joule to blow. The 336 milli-Joule is large, however, in relation to the approximately 150 milli-Joule required to fire an NSI. The transient firing was not detected by the pyro telemetry because this telemetry was cleared as part of the power-on reset process that completes after the anomalous firing occurs.

The tests performed at SDL also uncovered that the large transient firing anomaly only occurs at first turn-on of the WPE. It was empirically determined that the anomaly would only repeat if the WPE were left powered off for a period in excess of approximately 90 minutes to permit the electrical charges in the FPGA to dissipate. Attempts to reproduce the anomaly by immediately recycling power to the box were unsuccessful even after many cycles. An on-orbit test on the flight spacecraft to investigate the anomaly was unsuccessful for the same reason. This feature of the anomaly makes it additionally unlikely that the anomaly would have been detected by immediate investigation of the turn-on "glitch" mentioned earlier. Since there was no way of knowing that the WPE required a long powered-off period, so detection of the anomaly during test would have been lucky at best.

## 6.C.2. GSFC Tests

See Attachment 3.

## 7. Conclusions

As a result of the comprehensive systematic data analyses, it is concluded that premature cover ejection was due to faulty pyro electronics design which permitted Sun/Earth heating of the telescope causing solid hydrogen "boil-off" and subsequent loss of mission. A major contribution to the WIRE failure was the failure of the JPL development/management team to penetrate the electronic design of the pyro electronics box. It is the JPL Anomaly Team's assessment that a peer review, held by the appropriately knowledgeable people would have identified the turn-on characteristics.

## 8. Lessons Learned/Proposed Actions

Based on troubleshooting analyses and test data, it is highly likely that all the pyros were fired at pyro electronics power turn-on. Hence, the cover most likely was ejected at turn-on by either transient scenario (1) or a combination of transient scenario (1) and (2). The following paragraphs provide a set of lessons learned and identify actions that can be taken to preclude future similar occurrences.

### Lessons Learned/Proposed Actions

Several lessons learned/proposed actions are presented as a result of this investigation. The lessons learned/proposed actions are categorized into three functional areas: - design approach/philosophy, design review and design verification approach.

### 8A. Design Approach/Philosophy

#### Finding One

The pyro design did not appropriately consider electronic transients effects known to occur at power turn-on of electronics.

Lesson Learned and Recommended Action:

- a) Perform electronics power turn-on characterization tests, particularly for applications involving irreversible events. In some applications, power turn-off characterization may also be important and should be considered.

b) Independent, separate pyro inhibits should be considered for mission critical events, particularly if all pyro functions can be simultaneously armed and enabled. Hence, activation of a pyro event would require two separate independent actions -- one separate action to enable the inhibit and another to fire the pyros. This approach would preclude spurious transient pyro firings during turn-on and preclude sympathetic firings induced by sneak path and/or crosstalk/magnetic field interactions that may occur in cabling.

### Finding Two

No design requirement existed for explicit, real-time telemetry of important, irreversible functions. If available, ground contingency commanding may have been possible (but unlikely) to save the mission.

### Lesson Learned and Recommended Action:

a) Cover ejection, cover removal or deployable events should have positive unambiguous telemetry indications augmented, if desired, by other indicators such as temperature measurements.

b) A pyro monitor firing circuit should measure the most reliable indication of a pyro firing. A current monitor rather than a voltage monitor would be a more reliable indicator.

### Finding Three

Fault containment was not adequately considered.

### Lesson Learned and Recommended Action:

In the WIRE case where formal FMEAs were not done, it is prudent to design so that a fault could not propagate, particularly if the fault can cause catastrophic or irreversible effects.

#### Finding Four

Consideration of vent-produced torques received little/no analysis for a worst-case venting scenario.

Because the expected nominal vent rate from the secondary tank was low, the WIRE team spent little effort on the design of the secondary vent exit. A simple T at the exit of the vent would adequately balance the thrust from a nominal flow rate, and the exit was placed as close as possible to the exit point on the cryostat shell to minimize the pressure (and therefore temperature) inside the secondary tank. Unfortunately, the team never analyzed the effect of this exit design during a worst-case venting scenario. As it turned out, the excessive heat load from the earth and sun and the corresponding high vent rate created more torque than the attitude control system could handle, so the spacecraft spin rate increased, causing more exposure to earth and sun loads. If the vent exit were closer to the spacecraft center of mass, or if one side of the T did not point directly at a connector, perhaps the total torque produced by the escaping hydrogen gas would have been less than the torque produced by the attitude control system. In this case, the spacecraft may have been brought under control before the hydrogen was completely expended. But the mission may still have been lost due to the exposure of the telescope optics to the extreme sun and earth heat loads.

Of greater concern is the fact that the expected hydrogen flow immediately after the opening of the secondary vent produced a torque which was substantially greater than the maximum torque specified in the WIRE System Requirements Document (INS.REQ.GEN.8 in WIRE-SPEC-003). This initial opening torque had an effect similar to the initial tip-off from the launch vehicle, inducing spacecraft body rates on the order of 4 degrees per second. Had a slightly off-nominal separation from the launch vehicle occurred, this initial opening torque from the cryostat would have added enough spin to the system to possibly prevent the spacecraft from acquiring the sun before it had depleted its battery reserves. An action item from the instrument pre-ship review (PSR) directly addressed whether or not the

instrument met INS.REQ.GEN.8, and the team reported at the spacecraft PSR that it did, but analysis now shows that it did not - by two orders of magnitude.

Lesson Learned and Recommended Action:

The design configuration and location/mounting of external vent hardware should consider the possibility of a worst-case venting scenario. The configuration should be implemented to prevent mission loss or major degradation.

8B. Design Reviews

Finding One

Detailed Peer Review was done on the WIE electronics only. Detailed peer reviews of the PYRO electronics box and its interfaces with the spacecraft were not done.

Lesson Learned and Recommended Action:

- a) Detailed, independent technical peer reviews are essential. Furthermore, it is essential that peer reviews be done to assess the integrity of the system design, including an evaluation of system/mission consequences of the detailed design and implementation.
- b) Peer reviews should be encouraged by Project Management and held as often as necessary.
- c) Peer reviews should consider the heritage capability and limitations of the support equipment planned to be used for testing the flight design.
- d) Project review board members should consistently penetrate the system and subsystem functional design and implementation to expose risk areas, particularly where multiple/complex interfaces exist.

## 8C. Design Verification Approach

### Finding One

No end-to-end test was performed in full flight configuration with flight sequence.

#### Lesson Learned and Recommended Action:

Testing of pyro circuits should be performed at least once in a flight configuration with the actual flight sequence ("Test what you fly and fly what you test.") where the transient effects of the complete system can be observed using a circuit interruption device, if necessary, (perhaps a fuse, if appropriate) to simulate the operation of a real NSI. Use of an interrupting device ensures that any transient energy still in the system at the time of squib firing is dissipated in a safe way. Device detection design should be such that stray currents well below the one-Amp-no-fire limit will be observable.

The measurement of input/output transients at turn-on and in operation is strongly recommended as a component for all system level interfaces. It is particularly indicated for pyro circuits where the ramifications of faults are generally severe and irreversible. The observation of a glitch at the GSFC pyro simulator box during turn-on of the WPE was, in retrospect, significant. Had the pyro device simulator been able to measure the real magnitude of the transient at initial turn-on, the fault in the design might have been detected in test.

### Finding Two

Testing to find anomalous behavior.

#### Lesson Learned and Recommended Action:

Design engineers, being very familiar with their design, may discount the existence of faults if they believe they have considered and accommodated them. It is important to have independent verification that the design is free of latent functional defects. While testing to verify correct functional behavior is essential, some testing should be considered to reveal anomalous behavior, particularly for mission critical items.



# WIRE MRR

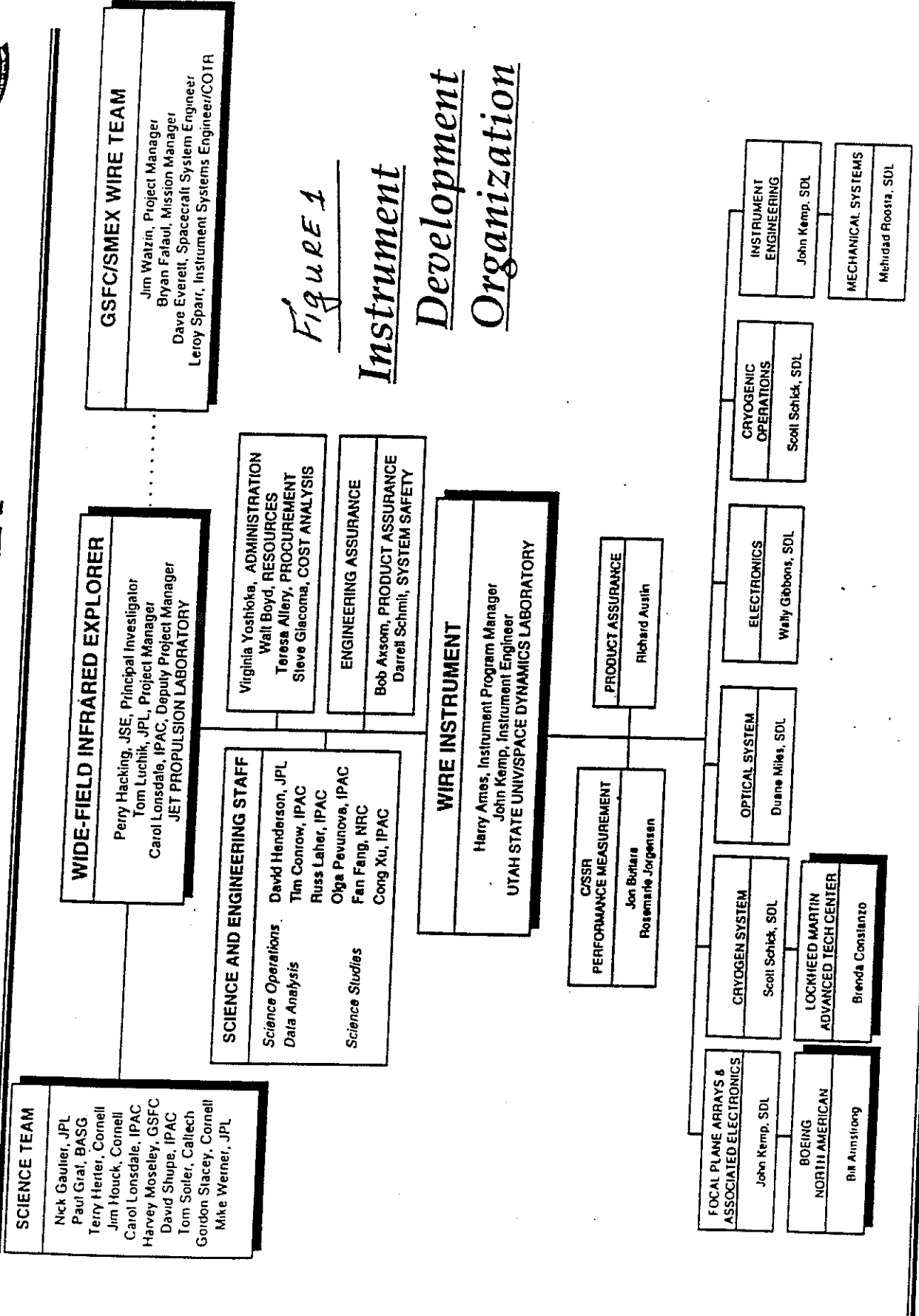
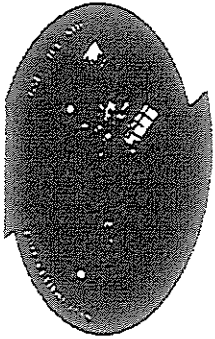


Figure 1

## Instrument Development Organization



# Spacecraft Overview

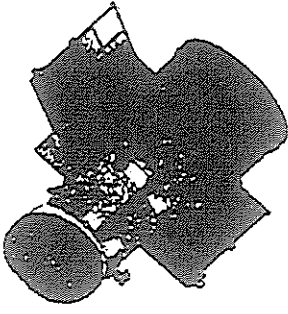
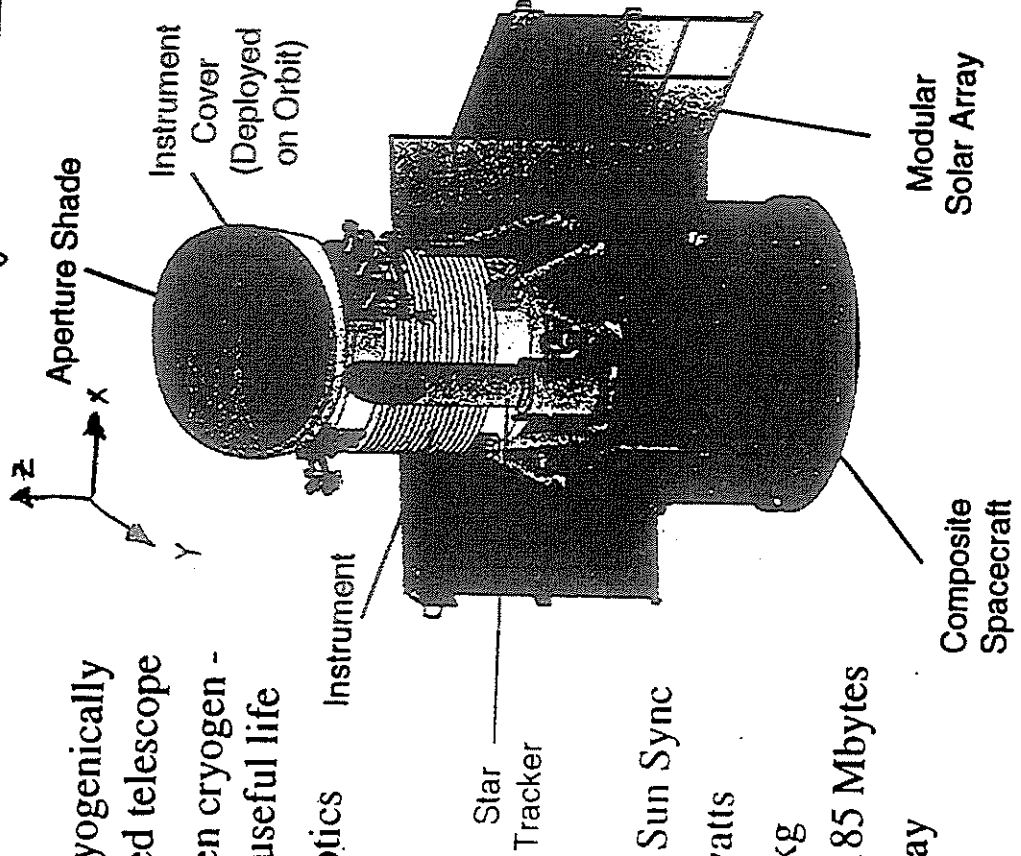


Figure 2

## Instrument:

- Dual stage cryogenically cooled infrared telescope
- Solid hydrogen cryogen - 4 to 6 month useful life
- Cassegrain optics



## On-Orbit:

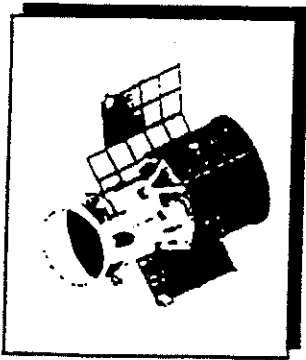
- 540 x 540 km Sun Sync
- Power: 135 watts
- Weight: 259 kg
- Daily TLM: 185 Mbytes
- 2 downlinks/day

## Spacecraft (developed in-house at GSFC):

- 3-axis stabilized fine pointer
- Autonomous on-orbit operations
- IPAC provided target observation plan
- Avionics identical to TRACE
- SMEX•Lite modular solar arrays
- All composite spacecraft bus
- Software system TRACE/SWAS pedigree
- ITOS ground system same as TRACE and SWAS

## Launch Vehicle Orbital Pegasus XL:

- Readiness date September 15, 1998
- Current launch scheduled for February 26, 1999



# WIRE Flight Operations and Readiness Review

---

## Spacecraft Systems Overview

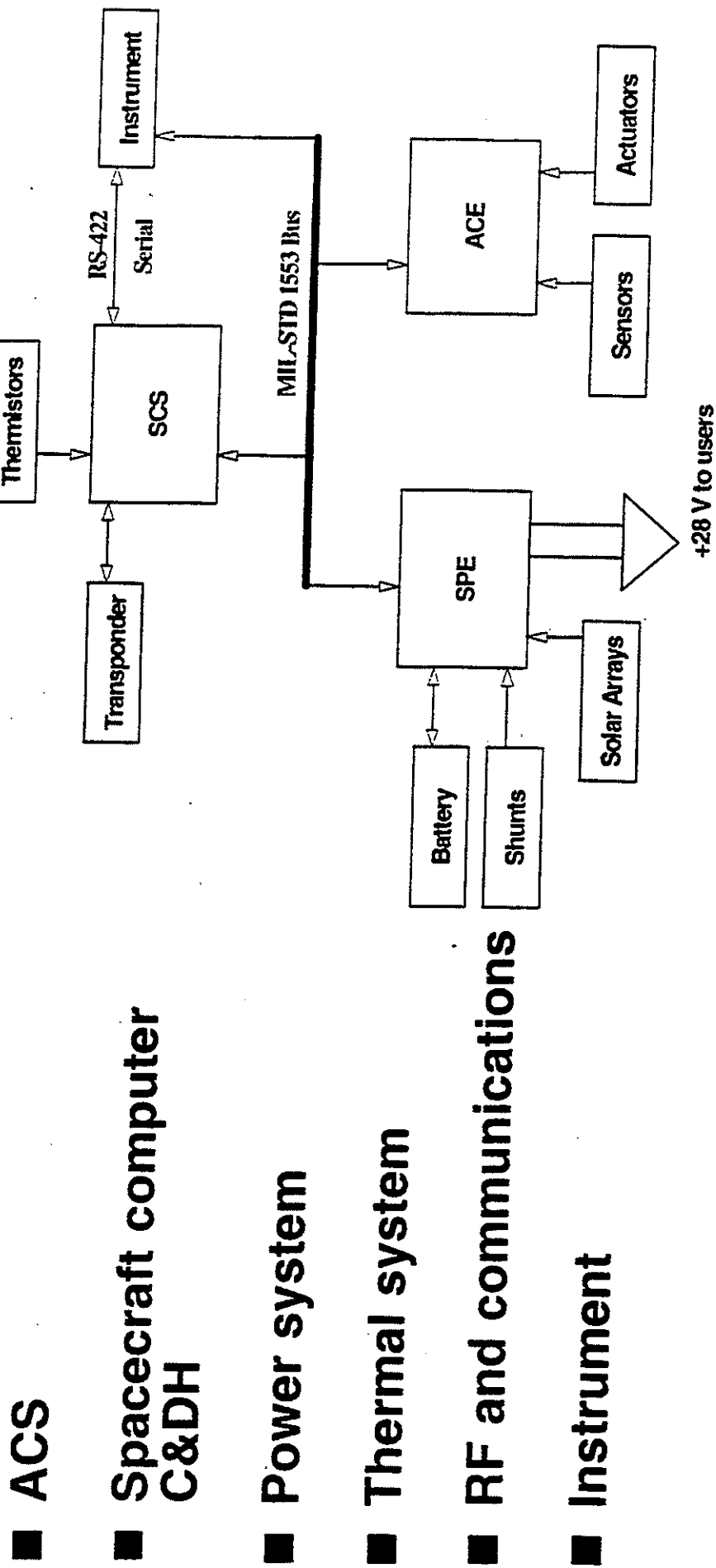
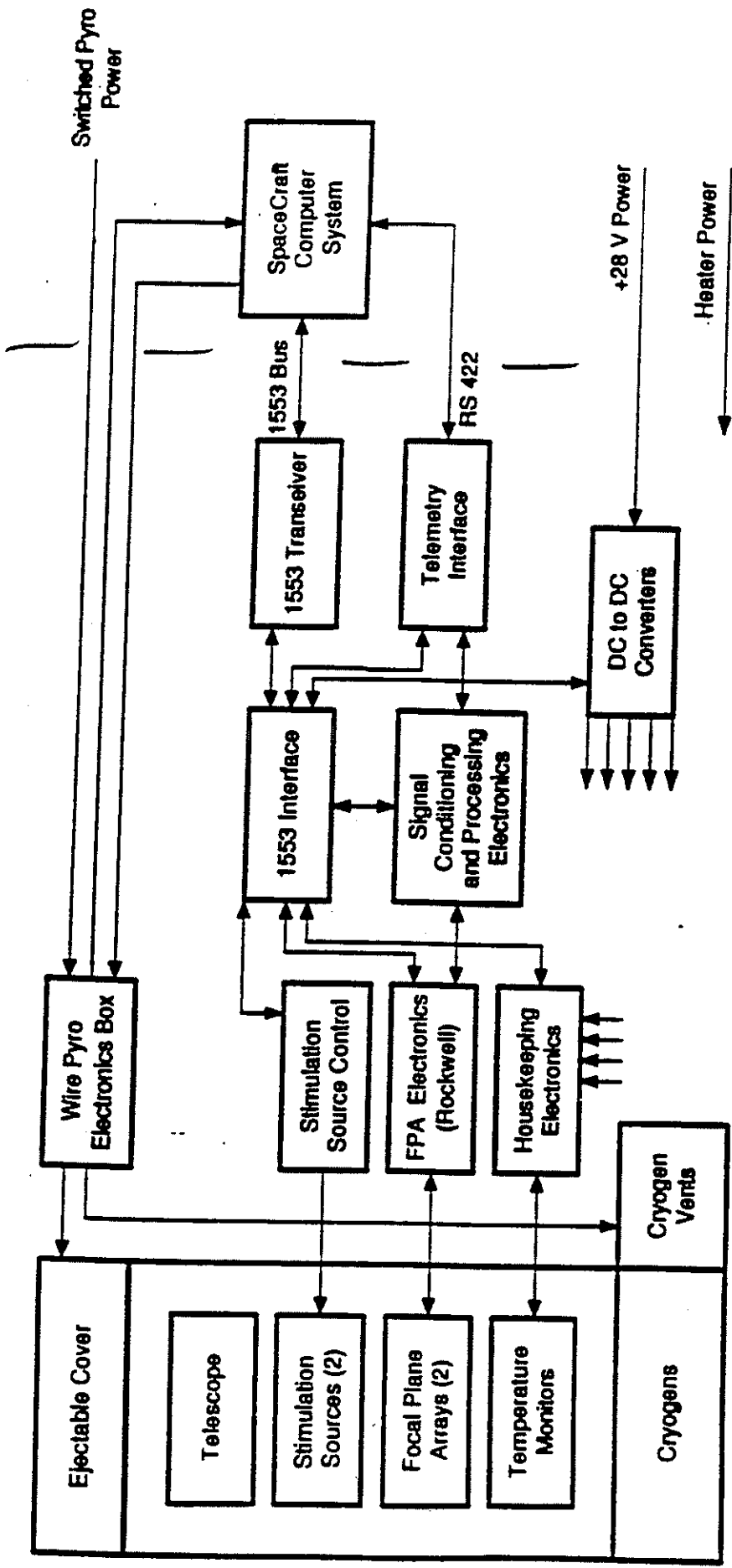


Figure 3



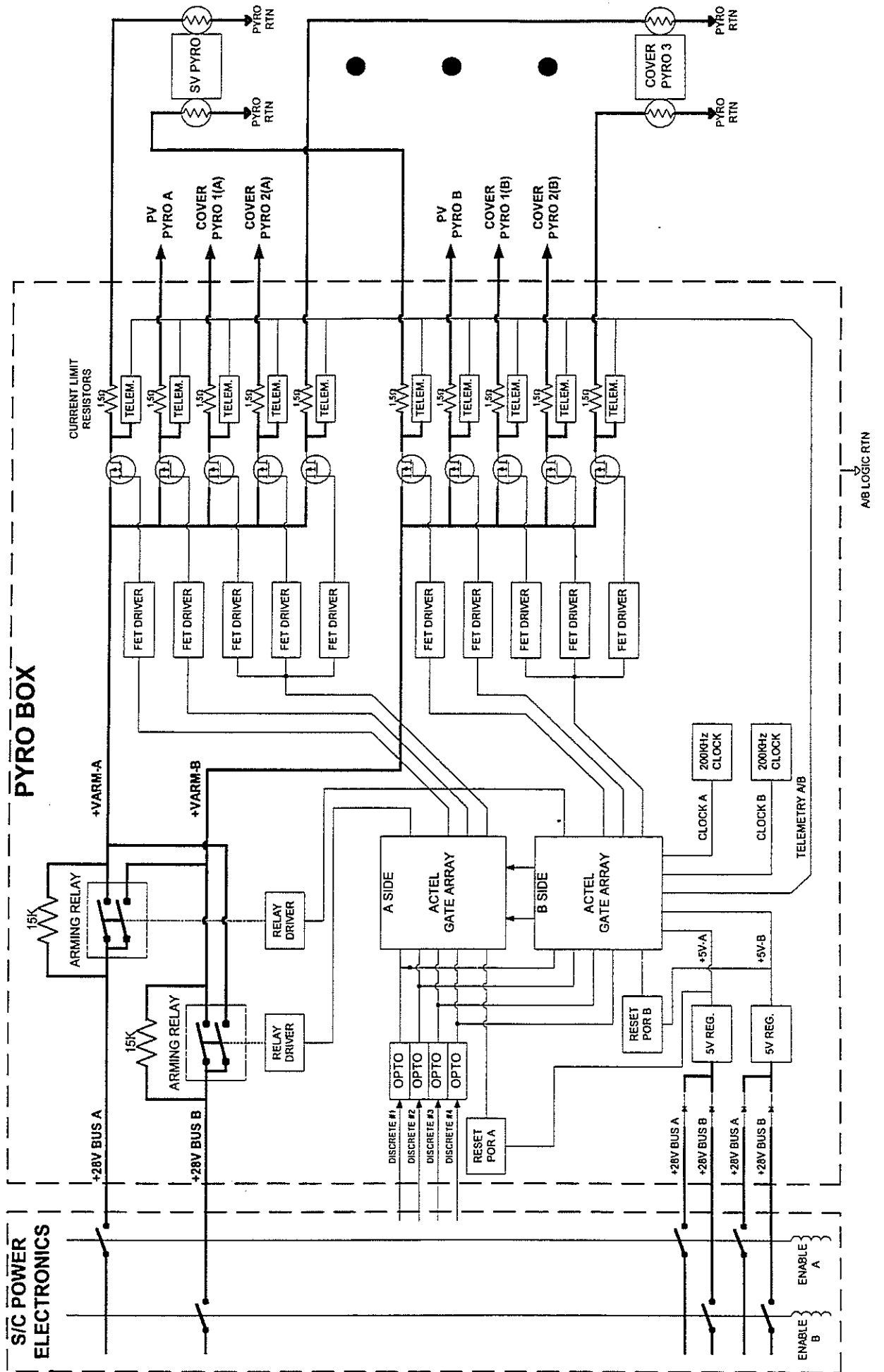
S/C

3/5/98

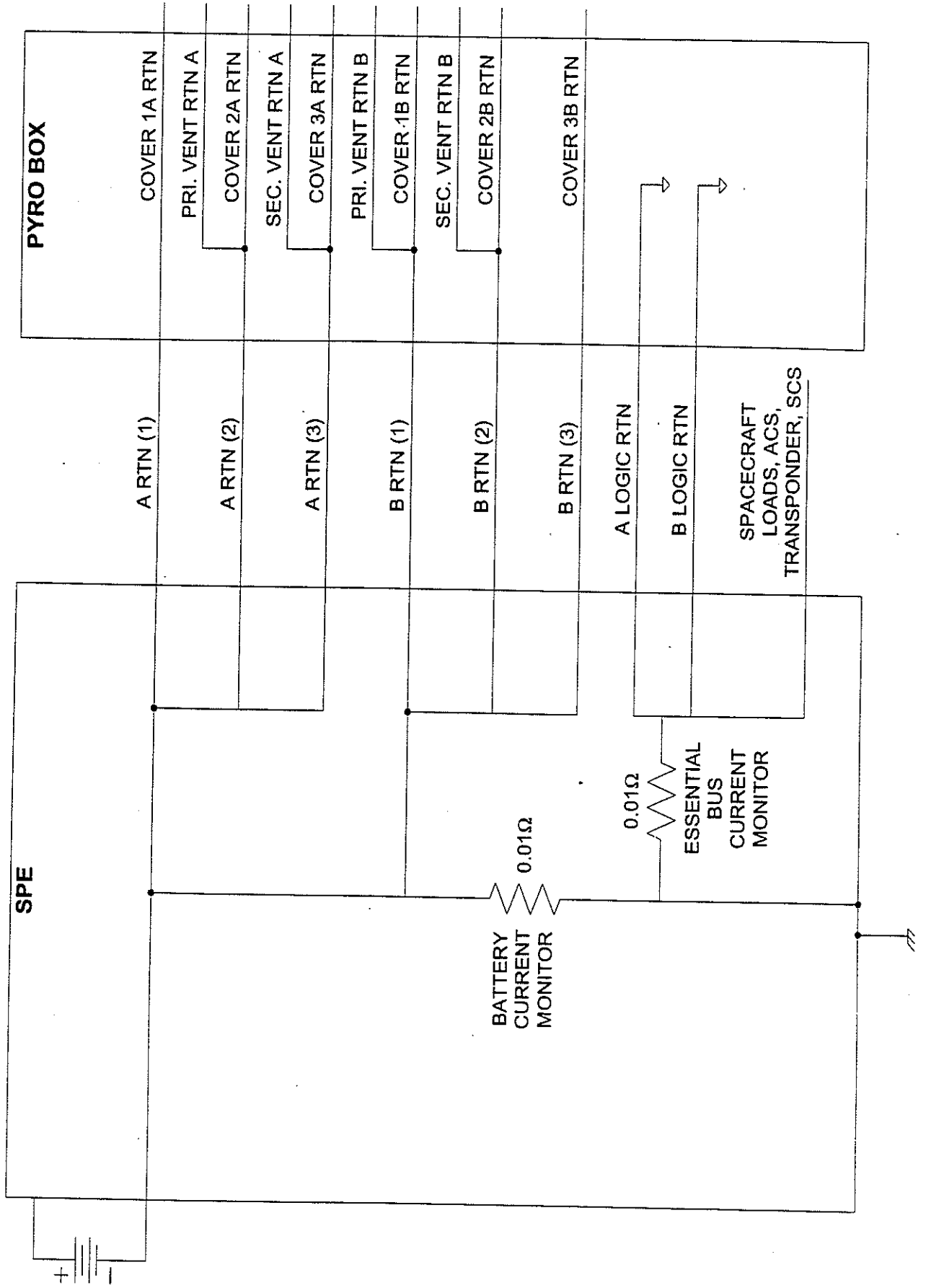
Figure 4 WIRE Instrument Block Diagram



# FIGURE 5: WIRE PYRO BOX CIRCUIT BLOCK DIAGRAM



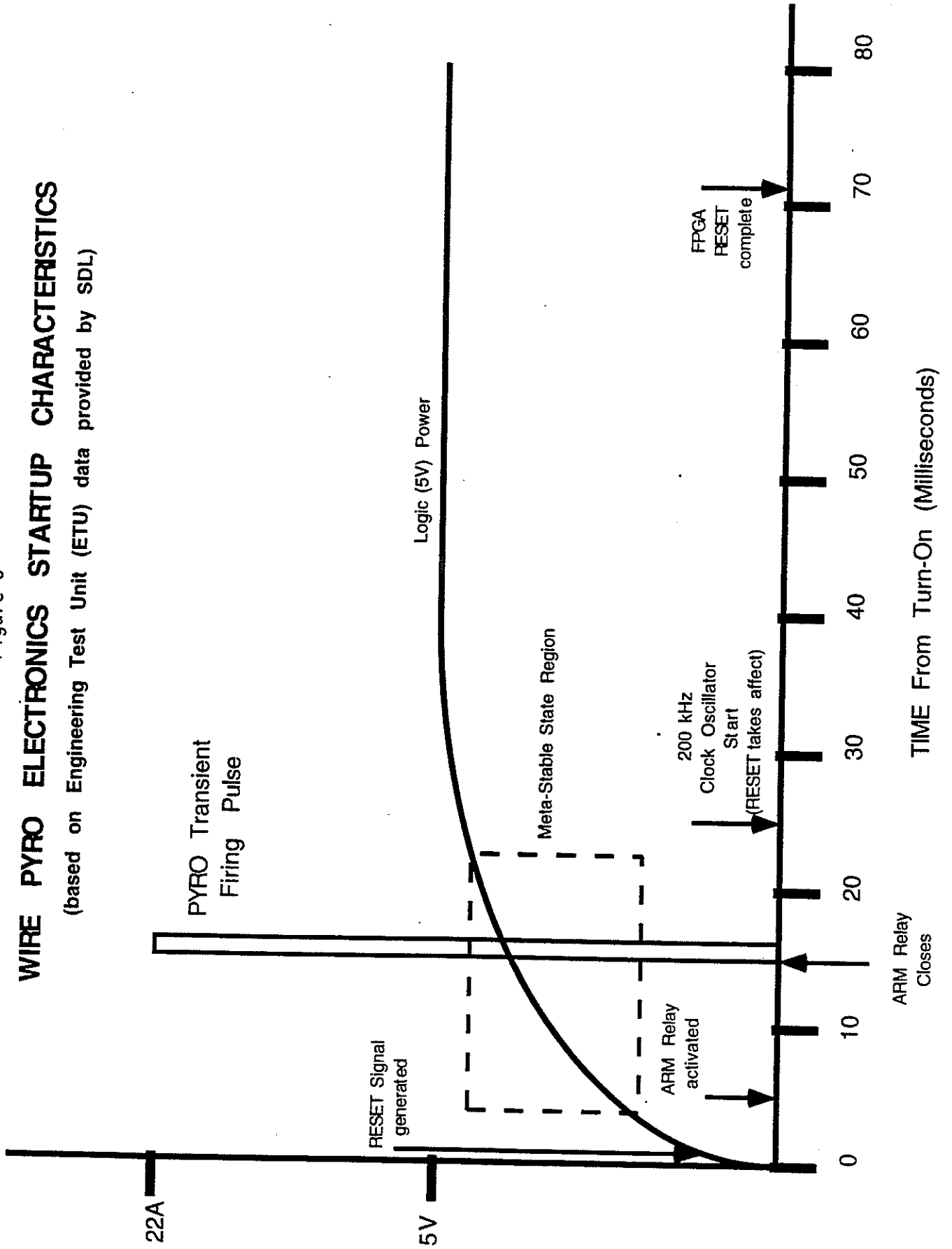
# 5A. SPE to PYRO BOX RETURNS



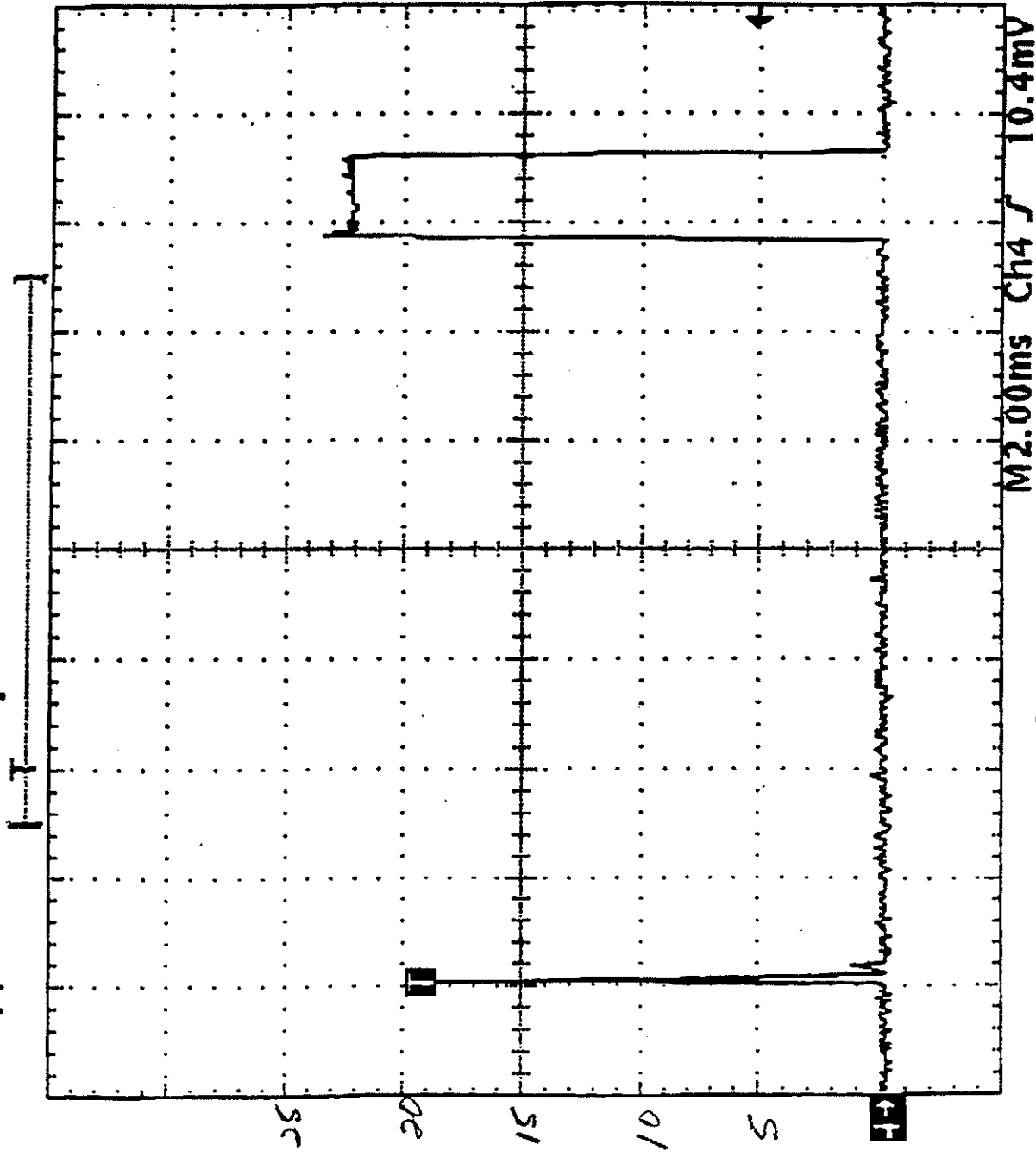
# WIRE PYRO ELECTRONICS STARTUP CHARACTERISTICS

(based on Engineering Test Unit (ETU) data provided by SDL)

Figure 6



Tek Stopped: 3 Acquisitions



5A/DIV  
A SIDE POWER  
INPUT - ETH  
PYRO BOX

26 APR 1999  
14:21:57

Figure 7 ETH TRANSIENT

TABLE I  
WIRE Launch-Day Timeline  
David Everett  
May 4, 1999

Time (UT)	Event	Source
99-063-22:54	Cryostat temperature monitoring starts at LPO station on L-1011	Notes from launch day
99-063-22:58	Spacecraft Powered	Notes from launch day
99-063-23:13	Instrument Powered--additional cryostat temperatures available	Notes from launch day
99-064-01:56	Orbital Carrier Aircraft Takeoff	Notes from launch day
~99-064-02:37	Instrument turned off, LPO provides only cryostat temperature monitoring	Launch day procedure, memory
99-064-02:54	Cryostat temperatures: PriTop 7.45 K, PriBot 7.64 K, SecTop 13.14 K, SecBot 12.71 K	Notes from launch day, read by LPO
99-064-02:55:49	Secondary tank bottom temperature is 12.72 K	Notes from launch day, read by LPO
99-064-02:55:57	Drop	Notes from launch day
99-064-02:56:02	Stage 1 ignition	Pegasus accel data plus drop time
99-064-02:57:07	Stage 1 burnout	Pegasus accel data plus drop time
99-064-02:57:28	Stage 2 ignition	Pegasus accel data plus drop time
99-064-02:58:06	Fairing separation	Pegasus accel data plus drop time
99-064-02:58:37	Stage 2 burnout	Pegasus accel data plus drop time
99-064-03:02:58	Re-point of Pegasus in preparation for 3 <sup>rd</sup> stage burn	Pegasus accel data plus drop time
99-064-03:03:09	Stage 3 ignition	Pegasus accel data plus drop time
99-064-03:04:17	Stage 3 burnout	Pegasus accel data plus drop time
99-064-03:05:18	Payload separation	Notes from launch day
99-064-03:05:20	Spacecraft separation as sensed by the spacecraft	packet 10, IOPEGSEP
99-064-03:05:22	Attitude control electronics (ACE) box powered, b-dot starts rate damping	Tom Correll estimate from next event
99-064-03:05:23.6	First ACS data available	packet 29
99-064-03:05:26.4	Y-wheel begins spin-up	estimate from next event
99-064-03:05:30.6	First non-zero indication of y-wheel speed	packet 29
99-064-03:06:21.0	Y-wheel spin-up complete	packet 29
99-064-03:05:30	Solar array wax actuators begin to heat	packet 10, IOSADEPLOY
99-064-03:06:50	Solar array potentiometers still at zero	packet 10, IOSAPOT
99-064-03:06:52	Beginning of solar array deployment in CSS data	packet 29
99-064-03:06:55	Solar array potentiometer shows movement	packet 10, IOSAPOT
99-064-03:06:59	End of solar array deployment in CSS data	packet 29
99-064-03:07:00	Solar arrays are fully deployed	packet 10, IOSAPOT
99-064-03:16:20	Blockage of sun (+Z CSS)	packet 29
99-064-03:16:44	End of blockage	packet 29
99-064-03:17:58.0	Blockage of sun (+Z CSS)	packet 29
99-064-03:18:38	Approximate end of blockage	packet 29

99-064-03:26:10	First McMurdo pass begins	
99-064-03:27:07	/SNOOP command sent	ground system event
99-064-03:27:08.5	Barker time for SNOOP	packet 1
99-064-03:27:08.7	FARM B counter increments for SNOOP	transfer frame time
99-064-03:27:20	/SNOOP not in bypass sent	ground system event
99-064-03:27:21.3	Barker time for /SNOOP	packet 1
99-064-03:27:22	Command verification for /SNOOP	ground system event
99-064-03:27:42	/PSACEPWR ON	ground system event
99-064-03:27:42	/PSDSSPWR ON	ground system event
99-064-03:27:42	/PSEARTHSENS ON	ground system event
99-064-03:27:43.5	FARM B counter inc for /PSACEPWR ON	transfer frame time
99-064-03:27:44.7	FARM B counter inc for /PSDSSPWR ON	transfer frame time
99-064-03:27:45	/PSPYROA ON	ground system event
99-064-03:27:45.3	FARM B counter inc for /PSEARTHSENS ON	transfer frame time
99-064-03:27:45.6	All pyro box telemetry shows box is off	packet 10
99-064-03:27:46	/PSPYROB ON	ground system event
99-064-03:27:46.3	Barker time of a command (/PSPYROA)	packet 1
99-064-03:27:46.5	FARM B counter inc for /PSPYROA ON	transfer frame time
99-064-03:27:47	/IPYRO ARM	ground system event
99-064-03:27:47.2	Pyro bus A "ON" and B "OFF" in telemetry	packet 11, PSPYRO
99-064-03:27:47.5	Sharp increase in spacecraft body rates	packet 29
99-064-03:27:47.8	FARM B counter inc for /PSPYROB ON	transfer frame time
99-064-03:27:48	/ISECVENT DEPLOY	ground system event
99-064-03:27:48.2	Pyro bus B shows "ON" in telemetry	packet 11, PSPYRO
99-064-03:27:49.0	FARM B counter inc for /IPYRO ARM	transfer frame time
99-064-03:27:49.2	Essential bus shows 100 mA rise in current due to pyro box arming relay	packet 11, PSESSCURR minus PSACECURR
99-064-03:27:49.5	Barker time of a command (/ISECVENT)	packet 1
99-064-03:27:49.6	FARM B counter inc for /ISECVENT DEPLOY	transfer frame time
99-064-03:27:50.2	Essential bus shows 70 mA rise in current due to pyro box arming relay (previous sample caught current in the middle of its increase, this is the rest of the increase)	packet 11, PSESSCURR minus PSACECURR
99-064-03:27:50.6	Telemetry indicates secondary vent fire voltage exceeded threshold (last sample 5 sec before)	packet 10, ISECPYROMON
99-064-03:27:52	/ISECVENT RESET ground command	ground system event
99-064-03:27:53	/IPYRO RESET ground command	ground system event
99-064-03:27:53	/PSMASTERHRM ENABLE	ground system event
99-064-03:27:53	/PSTHERMACT1 ON	ground system event
99-064-03:27:53	/PSTHERMACT2 ON	ground system event
99-064-03:27:53.9	FARM B counter inc for /ISECVENT RESET	transfer frame time
99-064-03:27:54	/SCRTSENABLE RTSNUM=15	ground system event
99-064-03:27:54	/SCRTSSTART RTSNUM=15	ground system event
99-064-03:27:54	/PSSCSR VHTR ON	ground system event
99-064-03:27:54	/PSSCOPHTR ON	ground system event
99-064-03:27:54.5	FARM B counter inc for /IPYRO RESET	transfer frame time

99-064-03:27:55.6	IPYRO and ISECVENT both show RESET state	packet 10
99-064-03:27:55.7	FARM B counter inc for /PSMASTERHRM	transfer frame time
99-064-03:27:56.9	FARM B counter inc for /PSTHERMACT1 ON	transfer frame time
99-064-03:27:57.5	FARM B counter inc for /PSTHERMACT2 ON	transfer frame time
99-064-03:27:58.8	FARM B counter inc for /SCRSENABLE	transfer frame time
99-064-03:27:59.2	Essential bus shows 170 mA drop in current, indicating pyro arm times out and relay opens	packet 11, PSESSCURR minus PSACECURR
99-064-03:27:59.4	FARM B counter inc for /SCRSSSTART	transfer frame time
99-064-03:27:59.4	Event: Can't start RTS #15, in use	event log (spacecraft time in evt)
99-064-03:28:00.6	FARM B counter inc for /PSSCSR VHTR ON	transfer frame time
99-064-03:28:01.3	Barker time for /PSSCOPHTR ON	packet 1
99-064-03:28:01.8	FARM B counter inc for /PSSCOPHTR ON	transfer frame time
99-064-03:33:10	+X DSS data point off by 2.5 degrees, could be sampling problem	packet 29
99-064-03:35:07	First McMurdo pass ends	

99-064-03:45:42.2	Essential bus shows 160 mA increase in current, indicating pyro arm command via on-board sequence	packet 11, PSESSCURR minus PSACECURR
99-064-03:45:43	Secondary vent DEPLOY command via on-board sequence	based on time of arm indication and separation RTS
99-064-03:45:44	Primary vent DEPLOY command via on-board sequence	based on time of arm indication and separation RTS
99-064-03:45:45	Secondary vent RESET command via on-board sequence	based on time of arm indication and separation RTS
99-064-03:45:45.6	Primary vent open command shows up in 0.2 Hz telemetry, ISECVENT reads RESET	packet 10, IPRIVENT
99-064-03:47:05.6	Primary vent opens	packet 10, IPRIVNTSTATE
99-064-03:47:20.6	Telemetry indicates that the on-board sequence has stopped primary vent deployment	packet 10, IPRIVENT
99-064-03:47:27.2	Essential bus shows 200 mA drop in current, indicating pyro arm times out and relay opens	packet 11, PSESSCURR minus PSACECURR
99-064-03:52:55.4	The first of 12 missing data points in packet 29	packet 29
99-064-04:09:52	First NORAD tracking data for 3 <sup>rd</sup> stage	NORAD tracking data
99-064-04:15:05	First NORAD tracking data for debris (cover)	NORAD tracking data
99-064-04:17:14	First NORAD tracking data for spacecraft	NORAD tracking data
99-064-04:23:09	First Poker Flat pass begins	
99-064-04:23:40.6	Solar array deployment actuators powered off	packet 10, IOSADEPLOY
	WIE box turned on to check cryostat temperatures	
	WIE box turned off to save power	
99-064-04:29:13	First Poker Flat pass ends	
99-064-05:03:00	beginning of solar array potentiometer noise	packet 10, IOSAPOT
99-064-05:07:00	end of solar array potentiometer noise	packet 10, IOSAPOT
99-064-06:02:22	Exit analog acquisition	packet 29
99-064-09:54:26	Command verification for /PSPYROA ON	ground event log
99-064-09:54:30	Command verification for /PSPYROB ON	ground event log
99-064-09:54:30.6	telemetry indicates one pyro bus is on	packet 10, IPYROARMV
99-064-09:54:35.6	telemetry indicates both pyro busses are on	packet 10, IPYROARMV
99-064-09:56:48	Command verification for start of cover deploy sequence	ground event log
99-064-09:57:00.6	Cover pyro telemetry indicates OPEN for the first time	packet 10, IACVAPYROMON, IACVBPYROMON
99-064-10:29:23.21	Essential bus shows ACE box is on	packet 11, PSESSCURR
99-064-10:29:23.25	Barker time of ACE off command	packet 1
99-064-10:29:23.39	ACE telemetry still reads OK (box is on)	packet 29
99-064-10:29:23.48	ACE box telemetry goes to static state	packet 29
99-064-10:29:24.20	First indication of ACE power off in essential bus current	packet 11, PSESSCURR

# WIRE Anomaly Cause Summary Matrix

06 MAY 99

Cause Scenario	Disposition Approach										CRED 0-10	
	Fit Data	Gnd Test Data	Ckt Analysis	Design Verif	Func. Qual	Env Qual	Parts Qual	Design Verif	Func. Qual	Env Qual		
Broken Bolts @ cover attachment	Cover ephemeris			Single Point Failure eval								0
Pressure induced cover ejection				burst disks								1
Shock / Dynamic Loads	Launch Loads											0
Incorrect prelaunch state	Prelaunch configuration	Arm relay contact status		Single Point Failure eval								4
Cover squibs fired prelaunch	Cover ephemeris											0
On-board sequence errors	Command/Tlm verification											0
Ground commanding error	Command/Tlm verification											0
S/C-LV sep elect transient				Sep interface isolation								0
Miswiring (Harness, Box, etc.)		pyro phasing/ install testing		Single Point Failure eval								0
Safe/Arm conn. Wiring/mismatch		pyro phasing/ install testing		Single Point Failure eval								0
PYRO Box turn on transient	Attitude rate timing/thermal	ETU testing to reproduce	Start up (POR) evaluation	FMEA								9
Part SEU/RAD/Latchup			transient analysis	FMEA								7
Control Computer fault			FMEA/SPF evaluation	FMEA/SPF evaluation								1
Part internal contam/debris			SPF vulnerability	FMEA/SPF evaluation						review of any alerts		2
Pyro EMI induced xtalk			Model harness characteristics	harness design								3
Pyro fire elect sneak path	knowledge of tlm/cmd time		Ckt/Harness effects	harness design								7
Incorrect flight S/W load	load verification			Operations plan evaluation								0
Pyro Lot Defects	CMD telemetry			Single Point Failure eval						Lot Acceptance data review		0

CRED = Credibility Rating:  
 0-3 = Unlikely  
 4-6 = Possible but not likely  
 7-10 = Likely

APPENDIX A  
Timing of the WIRE Vent Opening  
David Everett May 6, 1999

The time of the cover deployment is a critical clue to the cause of the Wide-Field Infrared Explorer (WIRE) flight anomaly. If the cover came off around the time of spacecraft separation, the likely causes would be mechanical, while cover deployment around the time of the secondary vent opening would indicate a problem with the pyrotechnic (pyro) electronics. The following detailed look at the opening of the secondary vent demonstrates an anomaly which clearly indicates a problem with the pyro electronics and a probable time of cover deployment.

WIRE uses the Consultative Committee for Space Data Systems (CCSDS) command and telemetry standards (see [http://ccsds.org/blue\\_books.html](http://ccsds.org/blue_books.html) for complete documentation). The command protocol used is COP-1 (CCSDS 202.1-B-1: Telecommand Part 2.1 -- Command Operation Procedures). During the time of interest, commands were sent from the ground in bypass mode, so the FARM B counter will increment by one for each command sent. The FARM B counter is a two bit counter, so it increments from 0 to 3, then returns to 0. The FARM B count is downlinked from the spacecraft as part of the command link control word (CLCW) in each transfer frame. The data rate at the time of interest was 23.4375 kbps, and a transfer frame is 14,320 bits long, so one frame reaches the ground every 0.61 seconds, providing a FARM B count update. The ground system buffers commands so that there is more than 0.61 seconds between commands, so the FARM B counter will provide unambiguous identification and timing of individual commands with 0.61-second resolution. Each transfer frame is tagged with the time the frame was completed and ready for downlink, and any CLCW update is inserted just before the frame completion.

The WIRE spacecraft computer contains hardware which latches the time the last bit of a command start sequence is received by the spacecraft. The time is called the barker time of the command. This hardware is used to determine the offset of the spacecraft clock. The spacecraft clock is a hardware mission elapsed timer (MET) with a software offset added. To adjust the spacecraft clock, the ground system latches the time a command is sent, and the operator compares that time to the barker time and computes a new software offset to the hardware MET. The barker time provides 61  $\mu$ s of resolution, but the barker time is downlinked to the ground only once every five seconds, so if more than one command is sent in five seconds, we do not receive the barker time for each command. Using the FARM B counter and the corresponding transfer frame time, we can determine which command's receipt was recorded by the barker time.

Figure 1 shows the commands during the beginning of the first pass. Individual commands are written vertically above the corresponding transition in the FARM B counter. When two or more consecutive transfer frames contain the same FARM B count, the FARM B plot is a horizontal line. At 3:27:46.3, the barker time for /PSPYROA is latched, and the FARM B counter increments in the next transfer frame at 3:27:46.5. This command is the pyro enable command which first powers the pyro box. The /PSPYROB command enables the B side power. The /PYRO ARM command arms the pyro bus in the pyro box, and the /ISECVENT DEPLOY command turns on the

transistors which allow current to flow to the pyros controlling the secondary vent. The barker time of the /ISECVENT command was 3:27:49.5.

Figure 2 adds a plot of the current associated with the pyro arm relay coil. The plot is a scaled version of the difference between the essential bus current and the attitude control electronics (ACE) current. Since the attitude control system was active during this time period, plotting the difference gives a clearer indication of other activity on the essential bus. When the pyro box closes the non-latching arm relay, about 170 mA of additional current shows up on the essential bus, exactly what is expected. The essential bus telemetry is sampled once per second. The sample at 3:27:49.2 is the first indication of the arm condition, and this matches well with the timing of the /IPYRO ARM command, which causes a FARM B increment at 3:27:49.0. The current drops back at 3:27:59.2, ten seconds after the arm, exactly as designed. So far, all of the telemetry fits with what was expected.

Figure 3 adds the B-dot information from the attitude control system. The ACE analog safhold card has hardware circuits which produce a signal that is proportional to the rate of change of the magnetic field read by the spacecraft magnetometer. This B-dot signal is a measure of the spacecraft body spin rate and direction. It is clear from the plot that the B-dot signal suddenly changes at 3:27:47.0. By the next sample at 3:27:47.5, the sharp increase in body rates is obvious. The only activity which could cause this sudden change in the spacecraft attitude is the venting of cryogen caused by the secondary vent opening.

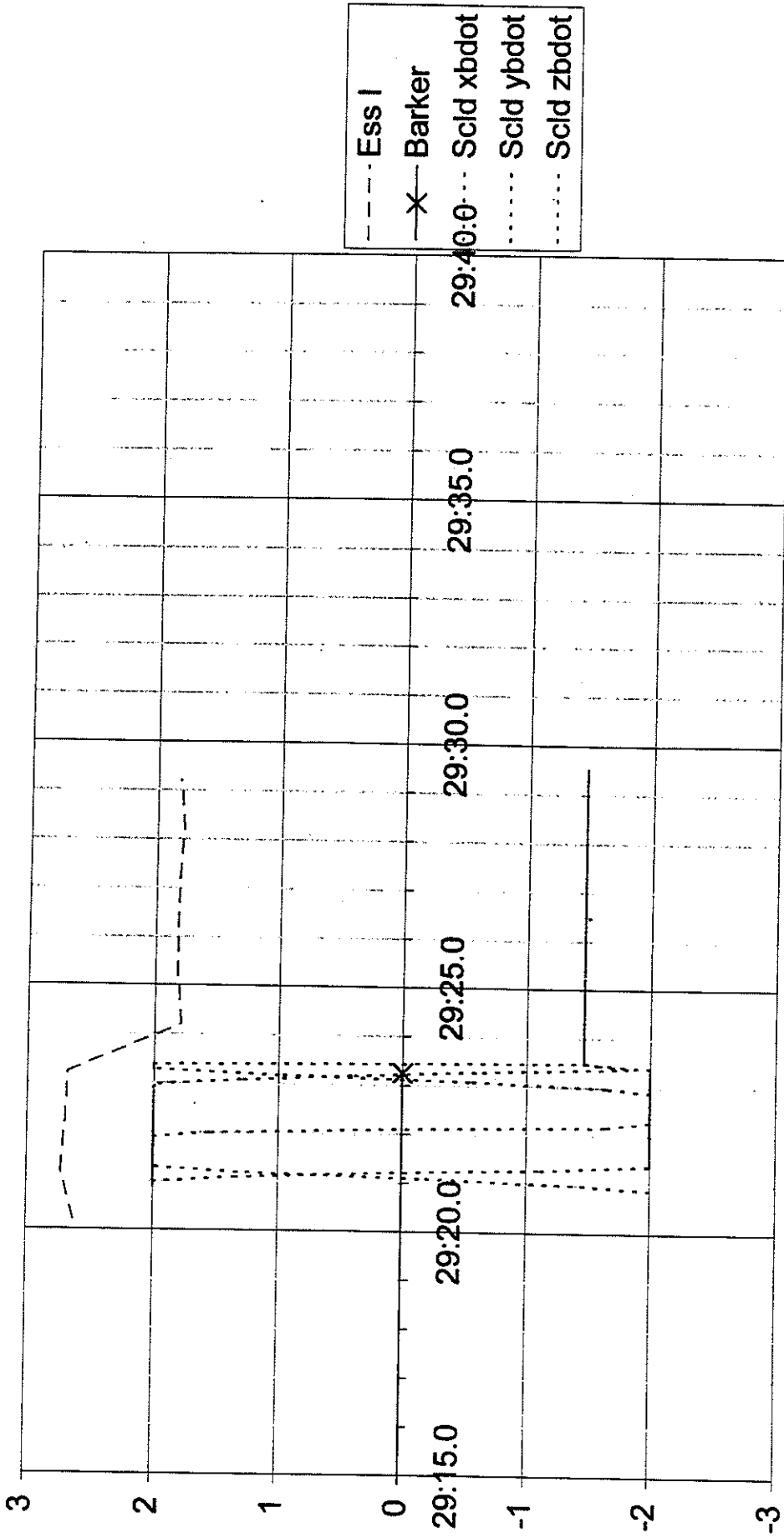
As a double-check of the B-dot data, Figure 4 shows the rate of change of the sun angle, as measured by the digital sun sensor. This telemetry does not respond as quickly as the hardware B-dot, because the rate of change is calculated on the ground from the 2 Hz telemetry. But the answer is the same—the spacecraft body rates increased **before** the command was sent to open the secondary vent. Notice also that there is **no** change immediately **after** the /ISECVENT DEPLOY command, the vent was already open.

As a verification of the accuracy of the time tagging, I analyzed telemetry from the power-down of the ACE box, which occurred at 99-064-10:29:23 (see Figure 5). The barker time of the command is 10:29:23.25. The ACE B-dot telemetry first reads a static value at 10:29:23.48. At 10:29:24.20, the essential bus current shows the drop due to the ACE box no longer drawing current. All of the timing is exactly as expected.

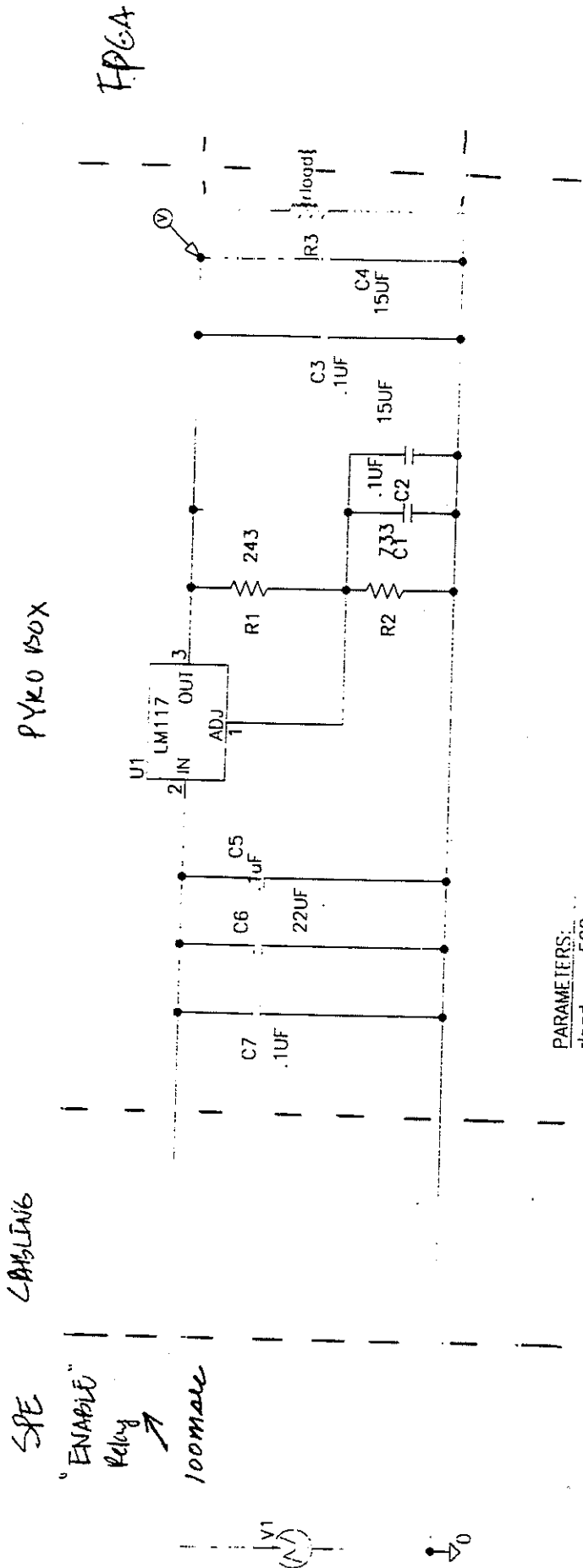
This analysis, especially Figure 3, clearly shows an increase in spacecraft body rates after the pyro box was powered, but before the arm and fire commands were sent. **The powering of the pyro box caused pyros to fire.** This analysis does not indicate whether the cover pyros also fired at this time, but any event which can fire a secondary vent pyro just by powering the box could have easily fired the cover pyros, since the circuit designs are the same.

Attached documents include "First Pass Timing Plots.xls" and "WIRE Launch Timeline.doc".

# WIRE ACE Off Timing



Time



ANALYSIS ATTACHMENT 1 - IDEAL CASE (NO CABLING)

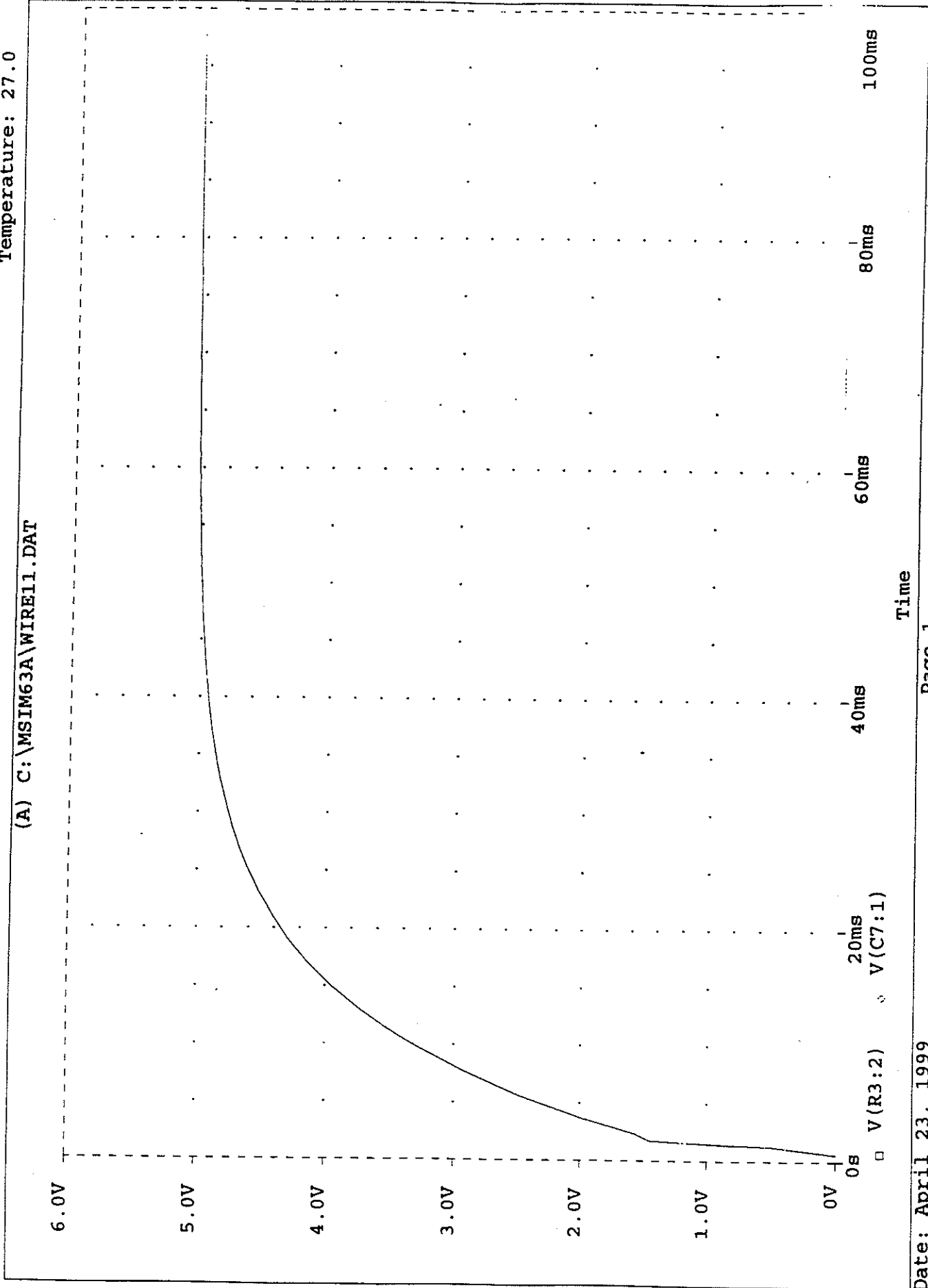
TN - 1

\* C:\msim63A\wire11.sch

Temperature: 27.0

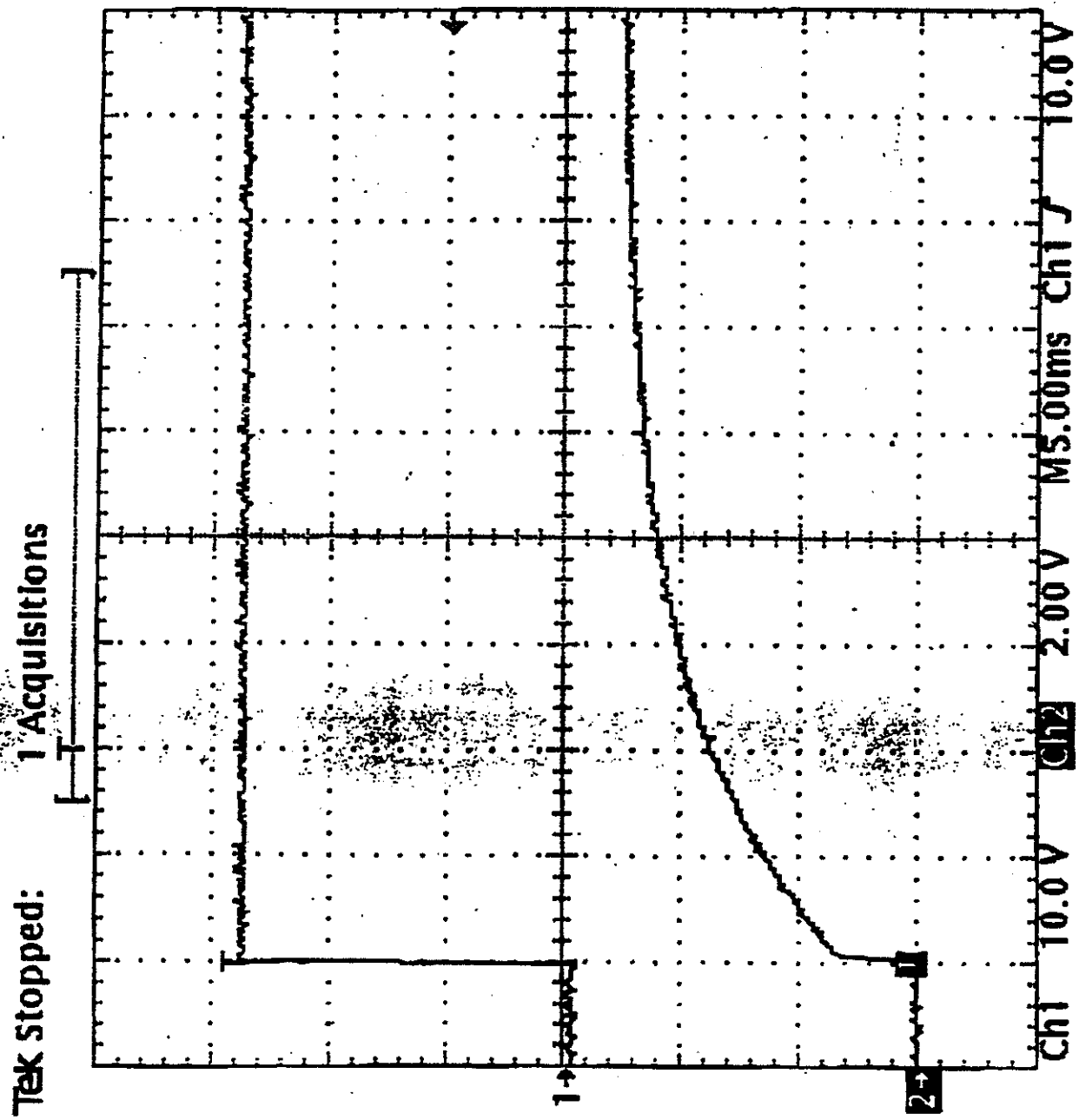
Date/Time run: 04/23/99 10:44:48

(A) C:\MSIM63A\WIRE11.DAT



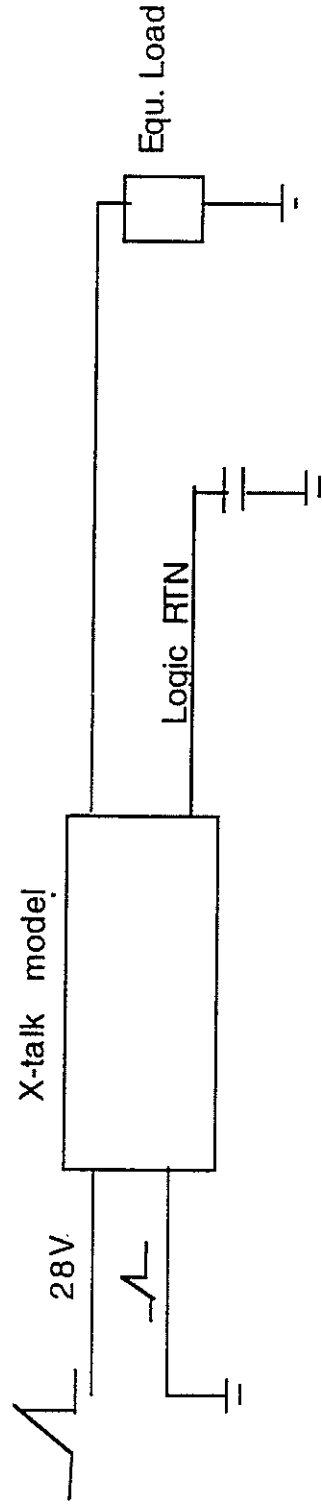
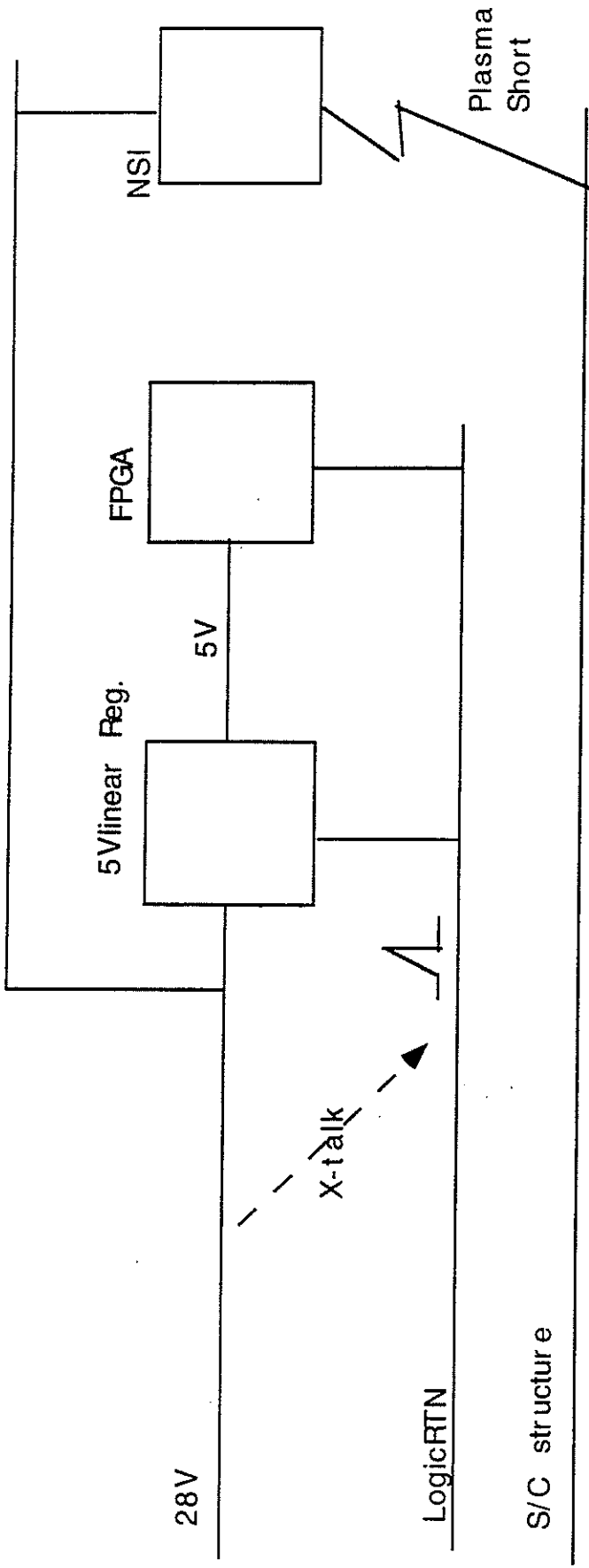
+5 Risetime test  
ETU PYRO BOX

23 Apr 1999  
11:05:02



ETU TEST

A

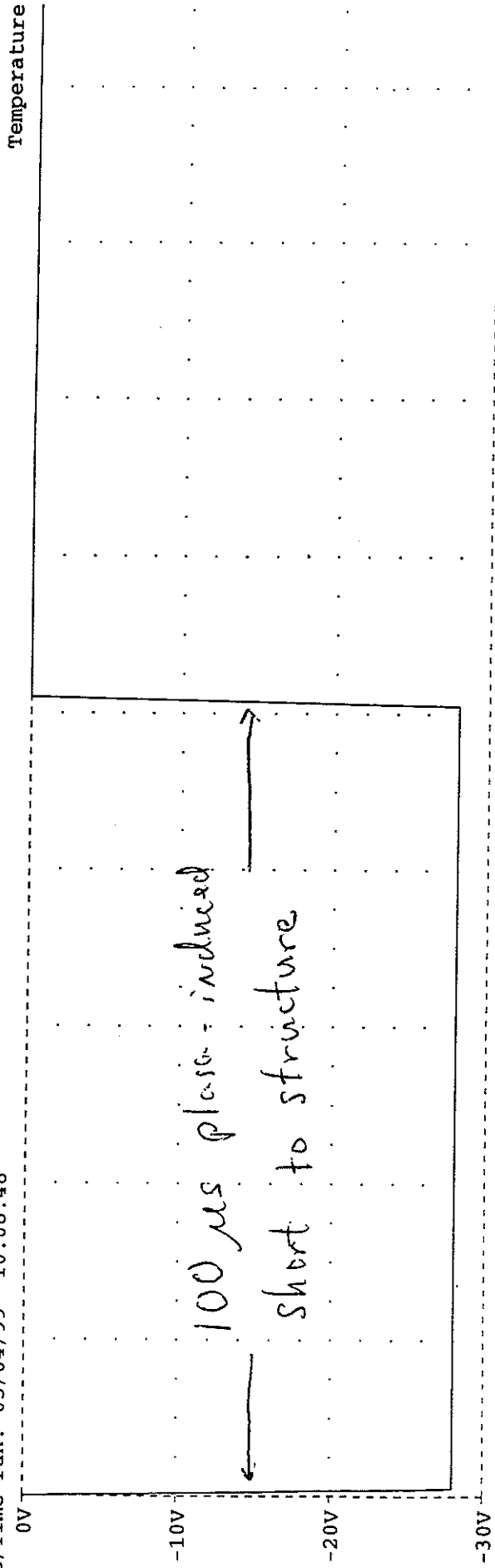


SPICE Model

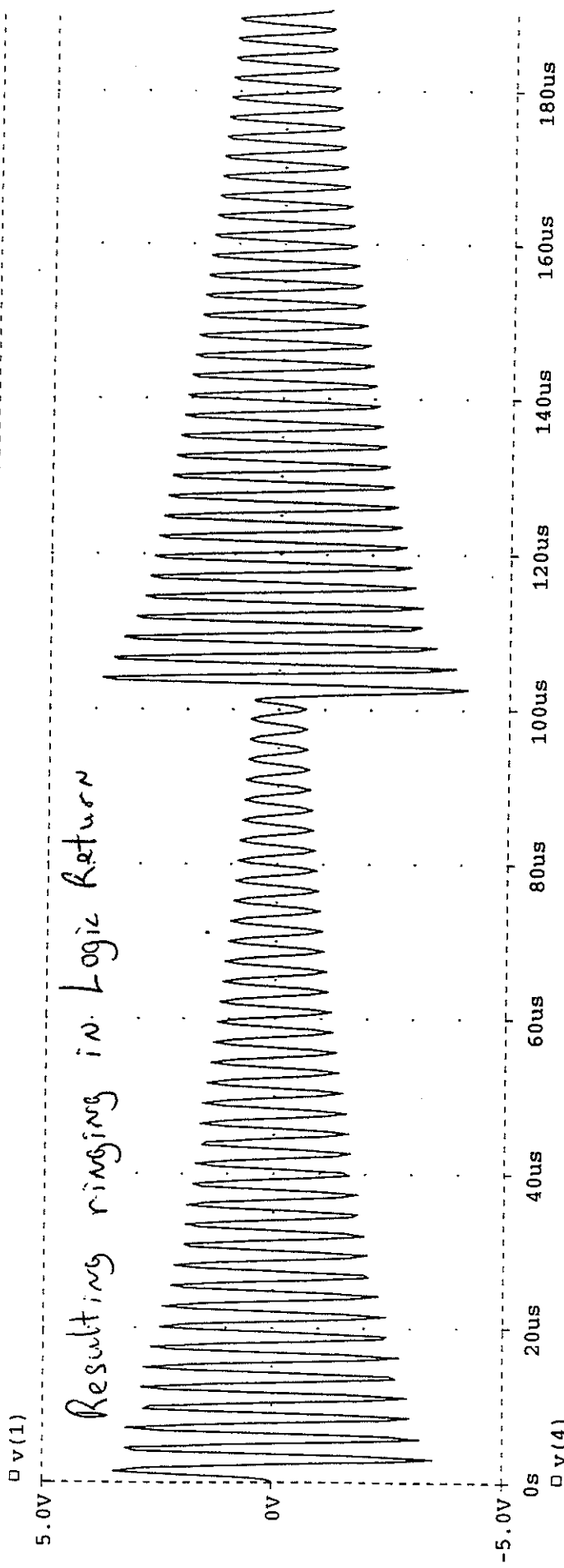
Analysis ATTACHMENT 2: Model for cross-talk induced ringing in Logic Return  
 Leading to sympathetic firing

Date/time run: 05/04/99 10:08:48

wire



Resulting ringing in Logic Return



T: E/1-1-99

# ATTACHMENT 3

## Startup Design and Analysis Note

This application note is based on a article published in the March, 1997 edition of EEE Links [[http://rk.gsfc.nasa.gov/home\\_page/Papers/eee\\_links/9703\\_eee.htm](http://rk.gsfc.nasa.gov/home_page/Papers/eee_links/9703_eee.htm)]. This note is being published to improve the visibility of this subject, as we continue to see problems surface in designs, as well as to add additional information to the previously published note for design engineers.

The original application note focused on designing systems with no single point failures using Actel Field Programmable Gate Arrays (FPGAs) for critical applications. Included in that note were the basic principles of operation of the Actel FPGA and a discussion of potential single-point failures. The note also discussed the issue of startup transients for that class of device. It is unfortunate that we continue to see some design problems using these devices. This note will focus on the startup properties of certain electronic components, in general, and current Actel FPGAs, in particular. Devices that are "power-on friendly" are currently being developed by Actel, as a variant of the new SX series of FPGAs.

In the ideal world, electronic components would behave much differently than they do in the real world. The chain, of course, starts with the power supply. Ideally, the voltage will immediately rise to a stable  $V_{CC}$  level; of course, it does not. Aside from practical design considerations, inrush current limits of certain capacitors must be observed and the power supply's output may be intentionally slew rate limited to prevent a large current spike on the system power bus. In any event, power supply rise time may range from less than 1 msec to 100 msec or more.

For digital logic, a "popular methodology" is to have fully synchronous designs. Again, in the ideal world, the clock oscillator will start immediately upon the application of power, with well-formed edges, rail-to-rail swings, no dropouts, and a stable frequency. However, crystal oscillators do not start instantaneously. From Horowitz and Hill's The Art of Electronics, 2nd Edition:

... However, because of its high-resonant  $Q$ , a crystal oscillator cannot start up instantaneously, and an oscillator in the megahertz range typically takes 5-20 ms to start up; a 32 kHz oscillator can take up to a *second* ( $Q = 10^5$ ). ...

A few different oscillator models have recently been tested and their characteristics varied widely. Some oscillators would output garbage with increasing amplitude as the power supply rises and it starts; some would start rather quickly; a space-flight qualified oscillator took a significantly longer time to start. When the unit starts to oscillate, dropped pulses and varying pulse widths were observed. Additionally, for the flight model oscillator (200 kHz), the start time was not specified on the data sheet. Measurements showed that for that oscillator, start time was a linear function of power supply rise time, when measured with  $t_{RISE}$  varying from 1 msec to 200 msec, the limits of our tests. So, for critical subsystems, the specifications of the oscillator on startup must be known and the system environment, including power supply rise time, must be compliant with the test conditions on the oscillator's data sheet to guarantee in-spec performance. Following this, the time constant of the power on reset circuit can be determined, ensuring that the system is in a safe state when the oscillator starts and is stable. Additionally, the logic design must go to a safe state assuming that either no clock is present or that an out-of-control clock is present during the startup transient. A fully synchronous logic design cannot perform that function.

Startup Design and Analysis Note

200 kHz

+5V

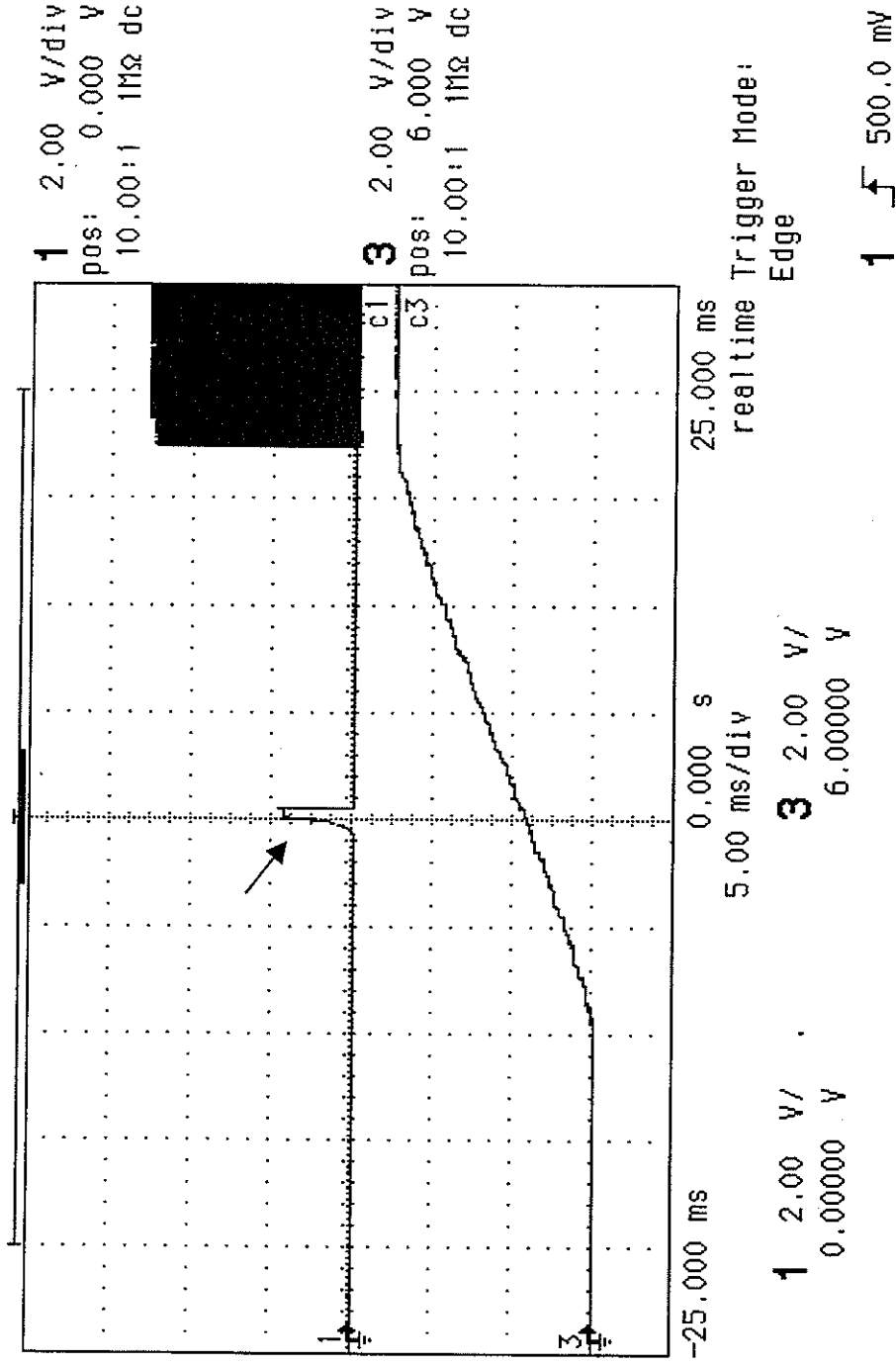


Figure 1. Start time of a space qualified 200 kHz oscillator. The rise time of the power supply is 20 msec and the horizontal scale is 5 msec per division. Start time from the application of power is approximately 27 msec.

Startup Design and Analysis Note

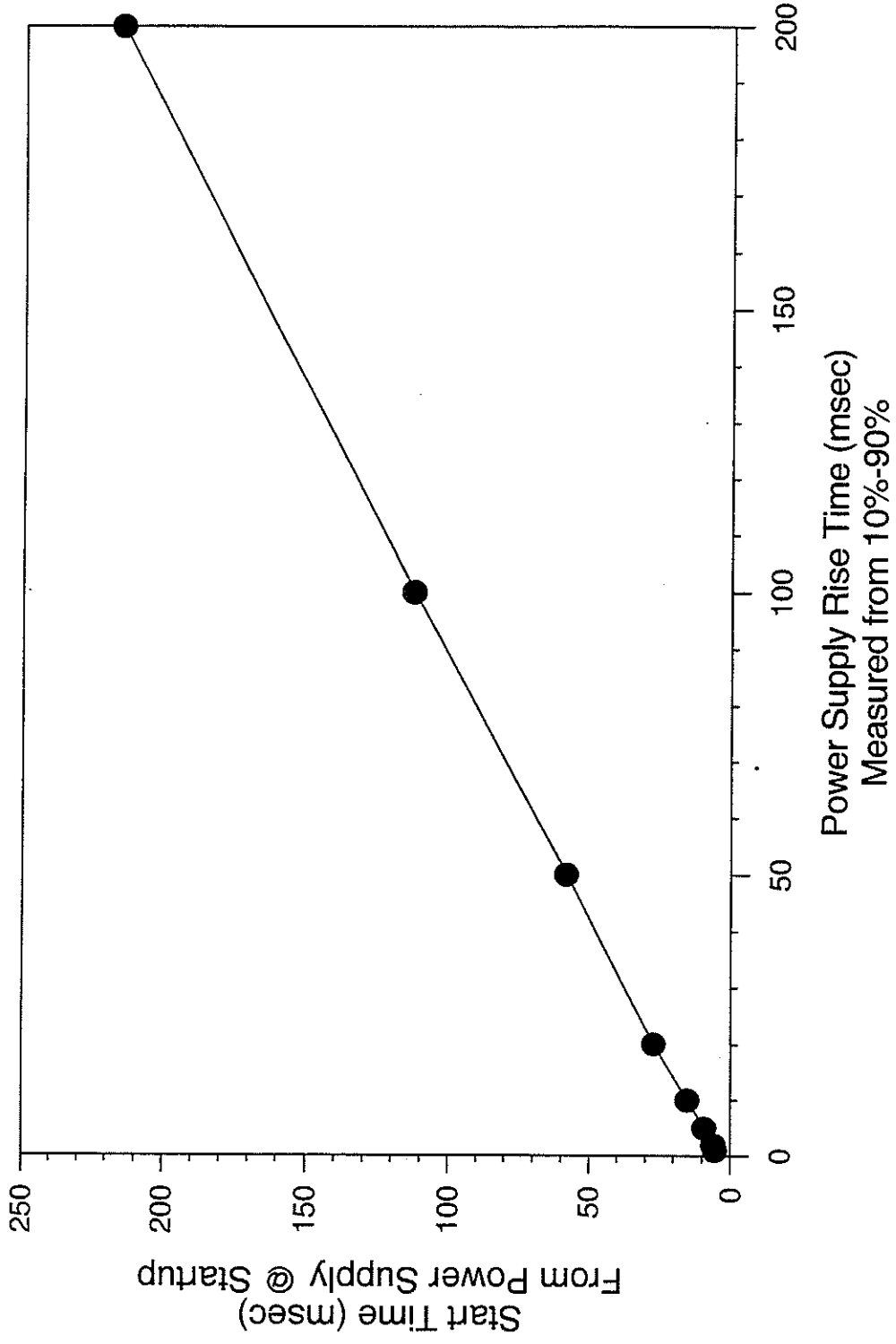


Figure 2. Summary of start time of a space-qualified 200 kHz oscillator as a function of power supply rise time at 10°C.

## Startup Design and Analysis Note

For programmable logic devices, depending upon the type, the startup characteristics of the power supply can affect the behavior of some programmable devices. Devices with internal Power On Reset (POR) circuits such as some FPGAs and configuration memories may require that a minimum slew rate on the power supply be met as well as a monotonic increase in the supply voltage. The UTMC PAL requires that no voltage is present on the device before power up [see <http://rk.gsfc.nasa.gov/richcontent/pals/PalPowerUp.htm>] or the device may be placed into a test mode. Current Actel FPGAs [as of this writing, May 1999] may have inputs that behave as outputs or outputs that do not follow their truth table during startup. The behavior of the Actel devices will be the topic of this rest of this application note. However, in any technology, including SRAM-based FPGAs and some JTAG circuits, the configuration of the device during the startup transient must be taken into account to provide a safe design for critical systems.

Charge pumps are used in Actel FPGAs to bias the transistors (high voltage n-channel FETs) that isolate modules of the logic and I/O cells during programming and connect them in normal operation. The pump produces a voltage higher than  $V_{CC}$  to ensure that the FETs are fully on and can pass a logic '1'. Since the pump takes a finite time to ramp up and turn on the FETs, the device may not behave properly until the pump is up and the system is stable. This amount of time is a function of the device model, its particular lot and unit, radiation degradation and annealing time, and slew rate of the power supply, among other factors.

Additionally, test results show that the startup characteristics are also a function of the device's recent history. In particular, the amount of time since the device was last powered down can affect the startup transient. In a laboratory test supporting a recent space-flight failure investigation, a set of devices (three units each of A1020B and A1020) "glitched" after a cold start and the flip-flops of interest powered up to '1's. After only a brief shutdown, glitches were not observed and the flip-flops powered up to the opposite state. A complete characterization of this *memory effect* is difficult at best and is not considered practical.

This behavior is in contrast to full digital CMOS devices, which generally have I/O pins that behave well and follow their truth tables at quite a low voltage. Currently, some Actel FPGA I/O modules that have been programmed as inputs may behave temporarily as outputs that are in the logical '1' state and may temporarily source current into the drivers connected to them. Device outputs are also not guaranteed to follow their truth tables and may source current at startup, although they "logically" should be sinking current to produce a logic '0', as is frequently used in power-on reset circuits. The time period for the startup transient depends on the power supply slew rate and other factors, including radiation exposure and annealing.

The figure below shows the power-up characteristics of a flight spare FPGA. In this picture, two of the outputs are shown to first spike high and then latch into the high state; subsequently a clock pulse would correctly clear the flip-flop. Following power cycles would not re-produce this behavior and both outputs would remain low with no glitches. After hours in the powered-off state, the glitches would return and the outputs would latch high. Interestingly, after a power on-off cycle, the voltage was ramped at the very low rate of just under 1 volt/sec. This produced both glitches and the outputs were latched high (waveforms not shown).

Startup Design and Analysis Note

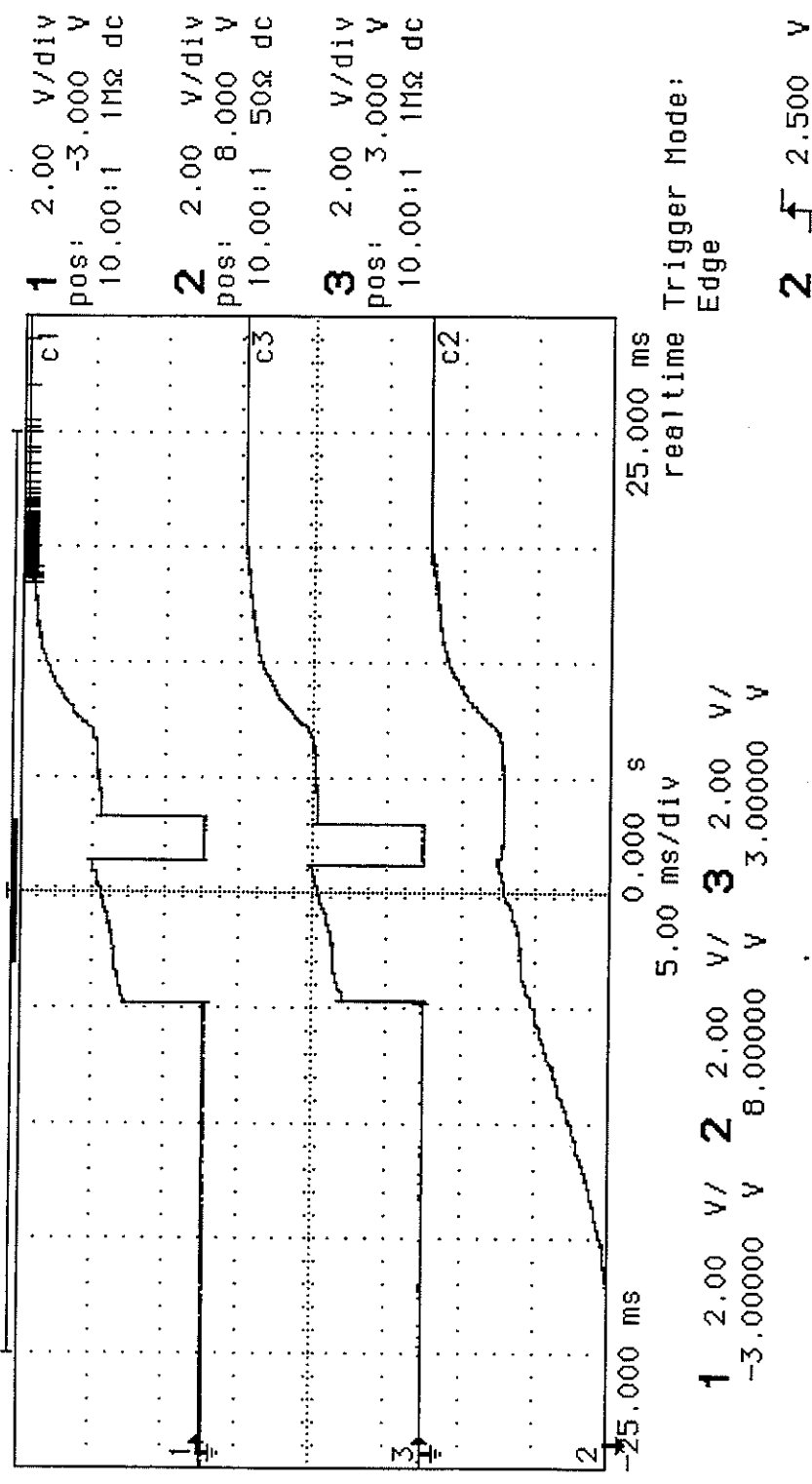


Figure 3. Power-on transient of a space-qualified A1020 (2.0  $\mu$ m). The power supply rise time was approximately 20 msec. Horizontal scale is 5 msec per division and vertical scale is 24 hours off; it would not repeat after rapid power on-off cycles.

## Startup Design and Analysis Note

Actel FPGAs, as do some other manufacturer's devices, need time to 'start' and care must be exercised for any critical spacecraft function implemented with FPGAs (or other components such as oscillators). This is a real problem and analysis of system startup is critical. In particular, here are some examples of system level failures:

- A motor controller FPGA powered up with all outputs high, resulting in high currents, ultimately blowing the fuses in the power supply.
- An instrument controller FPGA powered up in an illegal configuration, forcing latching relays into an undesired state.
- A pyrotechnic controller FPGA had only a synchronous reset function and did not gate the outputs of the device during the power-on transient. A combination of these effects resulted in pyrotechnic devices firing at an inappropriate time.

Any design that directly connects the inputs or outputs of currently available Actel FPGAs to critical spacecraft controls could result in hardware that malfunctions on **power-up without any failure of the FPGA**. Some precautions that may be taken include:

1. Do not attach an FPGA input to the analog part of a power-on reset circuit.
2. Buffer and isolate the FPGA outputs from any critical spacecraft controls that require proper operation during the startup transient.
3. Provide appropriate error detection/correction/fail-safe and isolation schemes for applications that require tolerance to single point failures. For certain reliability levels, this may require putting redundant functions in separate IC packages, as is frequently done with discrete device designs.

Two relevant Actel application notes have been put on-line at our www site and may be accessed by the following links:

[http://rk.gsfc.nasa.gov/richcontent/fpga\\_content/DesignNotes/BoardLevelConsiderationsForActelFPGAs.pdf](http://rk.gsfc.nasa.gov/richcontent/fpga_content/DesignNotes/BoardLevelConsiderationsForActelFPGAs.pdf)

[http://rk.gsfc.nasa.gov/richcontent/fpga\\_content/DesignNotes/PowerOnReset.pdf](http://rk.gsfc.nasa.gov/richcontent/fpga_content/DesignNotes/PowerOnReset.pdf)